

Aus der Klinik für Neurologie mit Experimenteller Neurologie  
der Medizinischen Fakultät Charité – Universitätsmedizin Berlin

## **Dissertation**

**Spreading depression as an endogenous antiseizure mechanism:  
The interplay on the borderland between migraine and epilepsy**

**Spreading depression als endogener antiepileptischer Mechanismus:  
Das Zusammenspiel in der Grenzzone zwischen Migräne und Epilepsie**

zur Erlangung des akademischen Grades  
Medical Doctor – Doctor of Philosophy (M.D./Ph.D.)

vorgelegt der Medizinischen Fakultät der  
Charité – Universitätsmedizin Berlin

von

Isra Tamim

aus Berlin

Datum der Promotion: 23.03.2024



*Für meine Eltern.*

# Table of Contents

## “Spreading depression as an endogenous antiseizure mechanism: The interplay on the borderland between migraine and epilepsy.”

<b>Preface</b> .....	<b>I</b>
<b>1 Abbreviations</b> .....	<b>8</b>
<b>2 Abstract</b> .....	<b>10</b>
2.1 English.....	10
2.2 Deutsch.....	12
<b>3 Introduction</b> .....	<b>14</b>
<b>4 State of research</b> .....	<b>19</b>
4.1 Aura phenomenology: SD as the pathophysiological correlate of migraine aura.....	19
4.2 Symptoms in the borderland: Post-ictal headache and visual disturbance.....	20
4.3 Visual hypersensitivity, stress, and hyperexcitability: triggers in migraine and epilepsy.....	21
4.4 Excessive neural activity as a treatment target in migraine and epilepsy.....	22
4.5 Genetic underpinnings of migraine and epilepsy.....	23
<b>5 Objectives and significance of the work</b> .....	<b>25</b>
<b>6 Methods</b> .....	<b>26</b>
6.1 Animals, housing, and husbandry.....	26
6.2 Surgical procedures.....	27
6.3 Pharmacological interventions.....	28
6.4 Cortical electrophysiological recordings.....	31
6.5 Hippocampal electrophysiological recordings.....	32
6.6 Data processing.....	32
6.7 Intrinsic optical signal (IOS) imaging.....	33
6.8 CBV measurement.....	34
6.9 Rigor and statistical analysis.....	34

<b>7</b>	<b>Results</b> .....	36
7.1	Seizures trigger SD.....	36
7.2	Power intensity and spatial extent influence the incidence of SD in the event of a seizure.....	40
7.3	SDs suppress seizure intensity and spread.....	42
<b>8</b>	<b>Discussion</b> .....	48
8.1	Clinical applications: Human microseizures as the trigger of SD in migraine brains.....	48
8.2	The antiseizure effect of SD in other models.....	51
8.3	Potential beneficial effects of SD.....	52
8.4	SD and seizures after brain injury: post-traumatic epilepsy and migraine.....	54
<b>9</b>	<b>Conclusion</b> .....	57
<b>10</b>	<b>References</b> .....	58
<b>11</b>	<b>Eidesstattliche Versicherung</b> .....	80
<b>12</b>	<b>Anteilserklärung an der erfolgten Publikation im Top-Journal</b> .....	83
<b>13</b>	<b>Journal Summary List</b> .....	84
<b>14</b>	<b>Print copy of publication</b> .....	85
<b>15</b>	<b>Curriculum Vitae</b> .....	112
<b>16</b>	<b>Publikationsliste</b> .....	115
<b>17</b>	<b>Acknowledgements/Danksagung</b> .....	116



## Preface

This dissertation's methods and results sections were previously published as **Tamim, I., Chung, D.Y., de Moraes, A.L., Loonen, I.C.M., Qin, T., Misra, A., Schlunk, F., Endres, M., Schiff, S.J., Ayata, C. Spreading depression as an innate antiseizure mechanism. *Nat. Commun.* **12**, 2206 (2021).**

<https://doi.org/10.1038/s41467-021-22464-x>. Contents are cited where applicable.

The contents of the introduction and research state section of this dissertation have been, in part, extensively researched in an unpublished academic essay of the author during module 23, “scientific working.” The contents are cited where applicable as **Tamim, I., Seizures versus Cortical Spreading Depolarization – Implications for Migraine with Aura and Epilepsy. Charité Universitätsmedizin Berlin, supervisor: Prof. Dr. Jens P. Dreier (2020).**

## 1. Abbreviations:

<b>AED</b>	Antiepileptic drugs
<b>ANOVA</b>	Analysis of variance
<b>AMPA</b>	$\alpha$ -amino-3-hydroxy-5-methyl-4-isoxazolepropionic acid
<b>ATPase</b>	Adenosine 5'-TriPhosphatase
<b>ATP1A2</b>	ATPase Na <sup>+</sup> /K <sup>+</sup> Transporting Subunit Alpha 2
<b>BIC</b>	1(S),9(R)-(-)-bicuculline methiodide
<b>BOLD</b>	Brain oxygen level-dependent
<b>CA</b>	Cornu ammonis
<b>CACNA1A</b>	Calcium Voltage-Gated Channel Subunit Alpha1 A
<b>CBF</b>	Cerebral blood flow
<b>CBV</b>	Cerebral blood volume
<b>ChR2</b>	Channelrhodopsin-2
<b>DC</b>	Direct current
<b>ECoG</b>	Electrocorticogram
<b>EEG</b>	Electroencephalogram
<b>FFT</b>	Fast Fourier transform
<b>FHM</b>	Familial hemiplegic migraine
<b>fMRI</b>	Functional magnetic resonance imaging
<b>GABA<sub>A</sub>R</b>	$\gamma$ -aminobutyric acid type A receptor
<b>GABA</b>	$\gamma$ -aminobutyric acid
<b>IICA</b>	Ictal-interictal continuum abnormalities
<b>IOS</b>	Intrinsic optical imaging
<b>KA</b>	Kainic acid
<b>LFP</b>	Local field potential



<b>LOI</b>	Line of interest
<b>MRI</b>	Magnetic resonance imaging
<b>NMDA</b>	N-Methyl-D-aspartic acid
<b>PG</b>	Penicillin G
<b>PRRT2</b>	Proline-rich transmembrane protein 2
<b>PD</b>	Power density
<b>ROI</b>	Region of interest
<b>SCNA1</b>	Sodium voltage-gated channel alpha subunit 1
<b>SD</b>	Spreading depolarization or Spreading depression*
<b>TTX</b>	Tetrodotoxin
<b>4-AP</b>	4-Aminopyridine

\* See p.16 for a detailed explanation of the correct use of both terms

## 2. Abstract

*Tamim, I., Chung, D.Y., de Moraes, A.L., Loonen, I.C.M., Qin, T., Misra, A., Schlunk, F., Endres, M., Schiff, S.J., Ayata, C. Spreading depression as an innate antiseizure mechanism. Nat. Commun. 12, 2206 (2021).*

<https://doi.org/10.1038/s41467-021-22464-x>.

The abstracts were adapted and revised from this publication to summarize the contents of the dissertation.

### 2.1 English Abstract

**Background:** Migraine and epilepsy are comorbid neurological diseases that have an intriguing relationship as similar genetic mutations and external stimuli trigger both conditions. While the resemblance of their clinical presentation can thus make a diagnosis difficult, the same prophylactic drugs, in turn, decrease attack frequency in both migraine and epilepsy.

Spreading depression/depolarization (SD) and epileptic seizures represent their pathophysiological correlates and are triggered by hyperexcitability. Cortical SD describes an abrupt mass depolarization that creeps along the hemisphere and silences electrical activity for several minutes. In contrast, epileptic seizures rapidly recruit adjacent tissue into a hyperexcitable state.

**Objectives:** To investigate whether epileptic seizures trigger SD, what determines the occurrence of SDs, and to what extent SD contributes to suppression and limitation of seizures.

**Methods:** Four chemoconvulsants were used to induce focal neocortical and generalized seizures in an *in vivo* mouse model. Wildtype CD1 mice (n = 165), familial hemiplegic migraine mutant (n = 14) and transgenic mice (n = 18) were used. Seizure intensity and spread were quantified by an electrocorticogram, while generalized seizures were examined via intrahippocampal recordings. SDs were simultaneously detected via a slow direct current shift and Intrinsic Optical Imaging (IOS) in the cortex and hippocampus. Cerebral blood volume was used as a surrogate of seizure activity

## Abstract

and measured via IOS. The effects of spontaneous, chemically, and optogenetically induced SDs were examined.

**Results:** Focal neocortical and generalized seizures triggered multiple SDs. Severe seizure intensity and generalization were related to SD occurrence. Tetrodotoxin confirmed seizures as the only trigger of SD. SDs exerted an antiseizure effect, thereby inhibiting seizure intensity and limiting its spread. Chemically and optogenetically induced SDs showed a similar antiseizure effect. A single SD was capable of limiting the recurrence of seizures. The results could be reproduced in all mice strains. Pretreatment of the cortex with an SD 5 and 30 minutes before applying the chemoconvulsant prevented seizure development. Vice versa, the blockage of SDs with MK-801 resulted in greater expansion of the seizures.

**Conclusions:** SD might function as an endogenous defense mechanism to diminish the occurrence of epileptic activity. Following the seizure suppression, SD manifests as a migraine aura. The data supports the understanding of migraine and epilepsy as related disorders linked by cortical hyperexcitability that either result in SD or seizures. It allows for a nuanced view of SD's role in neurological disease and facilitates the identification of new therapy concepts for migraine and epilepsy.

## 2.2 Deutscher Abstract

**Hintergrund:** Migräne und Epilepsie sind komorbide neurologische Erkrankungen, die in einer engen Beziehung stehen, da sie durch die gleichen externen Einflüsse sowie genetischen Mutationen getriggert werden. Während ihre ähnliche klinische Präsentation eine Diagnose erschweren kann, reduziert die gleiche Medikation wiederum die Episodenfrequenz in beiden Erkrankungen.

Die Netzwerk-Phänomene Spreading Depression/Depolarization (SD) und epileptische Anfälle stellen hier die pathophysiologischen Korrelate dar und stehen in einer engen wechselseitigen Beziehung: Beide Phänomene werden durch eine Hypererregbarkeit des Kortex getriggert. SD liegt einer abrupten und intensiven Massendepolarisation zugrunde, breitet sich langsam im Kortex aus und supprimiert dort für einige Minuten hirnelektrische Aktivität. Im Gegensatz dazu rekrutieren epileptische Anfälle mit ihrer schnellen Ausbreitung benachbartes Hirngewebe in einen übererregten Zustand.

**Zielsetzung:** Es soll untersucht werden, inwieweit epileptische Anfälle SDs triggern, welche Charakteristika SD-induzierende Anfälle aufweisen und inwieweit SDs zur Abschwächung und Limitierung von Anfällen beitragen.

**Methoden:** Vier pharmakologische Anfällsmodelle wurden genutzt, um fokale neokortikale Anfälle und generalisierte Anfälle zu erzeugen. Es wurden Wildtyp- (n=165), transgene (n=18) und FHM1-Mäuse (n=14) genutzt. Ein Elektrokortikogramm wurde abgeleitet, um die Intensität und Expansion der epileptischen Anfälle zu erfassen. Systemisch induzierte Anfälle wurden über elektrophysiologische Messungen im Hippocampus beurteilt. Das Auftreten von SDs wurde simultan über die langsame Gleichstrompotenzialänderung im Kortex und Hippocampus, sowie über Intrinsic Optical Imaging (IOS) registriert. Das zerebrale Blutvolumen als metabolisches Korrelat einer gesteigerten neuronalen Aktivität wurde ebenfalls über IOS beurteilt. Es wurden Effekte spontaner, chemisch und optogenetisch induzierter SDs quantifiziert.

**Ergebnisse:** Fokale neokortikale und generalisierte Anfälle triggerten multiple SDs. Das Auftreten spontaner SDs korrelierte mit einer schwerwiegenderen Anfallsintensität und -generalisation. SDs übten einen antiepileptischen Effekt auf den Anfall aus und schwächten sowohl Intensität als auch eine Generalisation. Chemisch und optogenetisch induzierte SDs zeigten einen ebenso potenten antiepileptischen

Effekt. Eine einzelne SD konnte ein Wiederauftreten des Anfalls verhindern. Die Ergebnisse konnten in allen Maus-Stämmen reproduziert werden. Eine Vorbehandlung des Kortex mit einer einzelnen SD fünf bzw. 30 Minuten vor Applikation der epileptogenen Substanz verhinderte die Bildung eines Anfalls. Eine Inhibition von SDs mit MK-801 führte umgekehrt zu einer ausgedehnteren Generalisation.

**Schlussfolgerung:** SD als endogener antiepileptischer Mechanismus kann epileptische Anfälle ausbremsen, um dann klinisch als Aura in Erscheinung zu treten. Die Daten festigen die These, dass Migräne und Epilepsie zwei sich überschneidende Erkrankungen darstellen, bei denen die Übererregbarkeit des Kortex entweder eine SD oder Anfälle triggert. Dies erlaubt einen nuancierten Blick auf das Phänomen SD in neurologischen Erkrankungen und erleichtert die Identifikation neuer Therapie-Strategien bei Migräne und Epilepsie.

### 3. Introduction\*

*“Some surprise may be felt that migraine is given a place in the borderland of epilepsy, but the position is justified by many relations, and among them by the fact that the two maladies are sometimes mistaken, and more often their distinction is difficult.”*

WILLIAM R. GOWERS, 1907 [1]

**T**ransient brain dysfunctions are often related to electrical, vascular, and metabolic activity alterations in neuronal networks, and various types of network phenomena in the brain can contribute to the development of specific neurological syndromes. Each of these network phenomena is characterized by its own molecular and electrophysiological signature, which has specific consequences for brain tissue and neuronal functionality [2].

Spreading depolarization (SD) and epileptic seizures are two network phenomena that co-occur in numerous neurological diseases: migraine with aura, epilepsy, subarachnoid and intracerebral hemorrhage, and traumatic brain injury [3].

During SD, neurons and glial cells depolarize and initiate a wave of electrical excitation that spreads across the affected hemisphere. Interestingly, the network phenomenon occurs in many species (e.g., insects, vertebrates), thereby indicating its conservation during evolution [4]. As decades of research have demonstrated, SD is the pathophysiological mechanism that underlies migraine aura. More recently, it was discovered that SD is most likely linked to the stimulation of the trigeminovascular system, resulting in pain due to headaches [5].

Epileptic seizures comprise a disruptive brain function caused by the hyperexcitability and hypersynchronous activity of neuronal clusters. Although SD and seizures co-occur in many neurological disorders, the significance of their interplay in migraine and epilepsy is still unknown. However, both disorders share one essential commonality that distinguishes them from other brain conditions, namely that they are characterized by recurring symptoms of paroxysmal onset [6].

---

\* Parts of this section have been extensively researched in an unpublished academic essay by the author, and were revised and adapted from **Tamin, I.**, *Seizures versus Cortical Spreading Depolarization – Implications for Migraine with Aura and Epilepsy*. Charité Universitätsmedizin Berlin.

## Introduction

Affected patients typically do not show any residual neurological deficits and remain symptom-free between attacks, wherefore both migraine and epilepsy are considered *chronic episodic* disorders [3]. Both are prevalent disorders, with migraine affecting about 19% of females and 10% of males worldwide [7].

Chronic migraine frequently causes disability in young patients, therefore imposing a high burden on society as it shows a prevalence of 2% in the general population [8, 9].

Although epilepsy is less common than migraine, it still ranks among the most prevalent neurological disorders, with a reported overall prevalence ranging from 0.5–0.8% [10]. Modern epidemiological studies established comorbidity between migraine and epilepsy that is independent of the seizure pattern, etiology, age at disease onset, or family history of epilepsy [11]. Individuals with epilepsy show a roughly two-fold increase in migraine prevalence over that of the general population [12]. Congruently, epilepsy is much more common in migraine patients, with a reported median prevalence of 5.9% [13]. Interestingly, studies report that the prevalence of epilepsy is 3.2 fold higher in children with migraines compared to children suffering from tension-type headaches [14].

Subsequently, physicians have long suspected the comorbidity of both disorders. In 1873, E. Leveing attempted to unravel the mechanisms underlying a migraine attack. He described the condition immediately before the aura as an “unstable equilibrium and gradually accumulating tension,” resembling seizures. The attack itself might serve as a “storm by which this condition is dispersed and the equilibrium for the time restored” [15]. Later, “intermediate” cases were reported by W. Gowers, who suggested that migraine is a disorder “on the borderland to epilepsy (...) near it but not of it” [1, 3]. In the 1940s, scientific thinking was dominated by the concept of migraine aura as a condition of vascular dysregulation. Migraine aura, a transient sensory disturbance (e.g., scintillating scotoma, photophobia, phonophobia), usually occurs 10–60 min before or during a migraine headache. The term “migraine aura” must be differentiated strictly from the “prodrome aura” that precedes a clinically overt seizure [16] and represents focal aware seizures (i.e., partial simple seizures) [3].

In 1963, H.G. Wolff suggested that vasoconstriction of cranial vessels would severely reduce cerebral blood flow (CBF). He further argued that hypoperfusion causes the

typical negative symptoms during aura (e.g., scotoma) [17], which often lead to migraine being referred to as a “stroke mimic”. Intra- and extracranial vessels would presumably respond to oligemia with vasodilatation, thereby leading to inflammation and corresponding perivascular edema. As a result, pain-sensory fibers of meningeal blood vessels are mechanically activated, resulting in a headache. However, with technological advances in imaging tools, further research could not verify a correlation between cerebral blood flow and migraine symptoms. While CBF variations do occur during migraine attacks, the increase or reduction of blood flow is not linked to headache intensity [18, 19]. Compelling new evidence has linked heightened cortical excitability and responsivity to SD, thereby providing further knowledge on migraine pathophysiology [3].

SD causes large transmembrane ion fluxes and movements of water molecules that substantially alter ion homeostasis and neurotransmitter signaling. In otherwise healthy brain tissue, it ultimately resolves itself and only lasts for approximately one minute [20]. The almost complete depolarization of brain cells hinders the development of new action potentials, which results in a propagating wave of cortical electrical silence (termed “spreading depression”) [21]. Several mechanisms exist that contribute to the reestablishment of the ion homeostasis after such an episode, including the  $\text{Na}^+\text{-K}^+\text{-ATPase}$ , intracellular  $\text{Ca}^{2+}$ -buffering, and the astrocytic reuptake system. However, restoring the massive molecular shifts is highly energy- and  $\text{O}_2$ -dependent and therefore impaired in metabolically compromised tissue (e.g., subarachnoid hemorrhage, ischemic stroke) where SD implies tissue deterioration. In the adequately supplied migraine brain, SD probably represents a benign event, and recovery typically occurs within minutes [22]. SD progresses at a rate of millimeters/minute [23], presumably through intercellular synchronous activation of direct gap-junctional neuron-to-neuron communication [24]. Its speed of propagation is thus a lot slower than that of epileptic seizures [3].

Notably, spreading depression requires depression of spontaneous electrical activity, which is often absent in the peri-infarct or injured brain. Under normoxic conditions (e.g., in the migraine brain), spreading depolarization is accompanied by spreading depression [20, 23]. In other words, in the adequately supplied tissue, spreading depression is an epiphenomenon of spreading depolarization. As this dissertation mainly focuses on the uninjured brain, spreading depolarization and depression are both referred to as SD since the borders between both are blurred in this context.



## Introduction

Furthermore, the term spreading depression emphasizes the effect on brain activity in the context of seizures. In cases where spreading depolarization is not followed by spreading depression (e.g., stroke or trauma) and terms are not interchangeable, the full terms are used.

To initiate SD in the rodent cortex, a minimum volume of approximately 1 mm<sup>3</sup> brain tissue needs to be depolarized [25]. Only strong stimuli such as hyperexcitability, seizures, ischemia, and trauma are sufficient to encumber clearance mechanisms for potassium and therefore trigger SD [26-29]. A potassium concentration of 10–12 mM must be exceeded in the extracellular space [26, 30] and can reach a peak of 80 mM [31]. The rise in extracellular potassium leads to the depolarization of adjacent brain tissue, thereby allowing the wave to spread. Neuronal depolarization results in the opening of voltage-gated Ca<sup>2+</sup>- and Na<sup>+</sup>-channels [30, 32] while sodium and calcium ions stream into the cells, releasing certain neurotransmitters such as glutamate [33, 34]. With N-Methyl-D-aspartic acid (NMDA) receptor activation contributing to the self-generating propagation of SD, the neurotransmitter glutamate serves as an essential mediator for sustaining depolarization [35, 36].

Interestingly, it was also reported that glial glutamate release might precede the increase of potassium concentration and neuronal depolarization, thereby causing synchronous oscillatory field activity and synchronization of neuronal firing [37]. Synaptic transmission is unnecessary for generating an SD wave, as experimental studies with the sodium channel blocker tetrodotoxin (TTX) have shown [38, 39]. Synaptic transmission and action potentials cause brief, highly regulated changes (lasting milliseconds) in voltage (amplitude in microvolts) along the cell membrane that travels at a rate of meters per second [20]. These electrophysiological mechanisms differ from SD, which lasts for minutes, creates a potential shift of up to -30 mV in amplitude, and propagates in a creeping fashion (millimeters per minute or 50–83 μm/sec) [6, 20].

On the contrary, the development of epileptic activity heavily depends on signaling that is established by α-amino-3-hydroxy-5-methyl-4-isoxazolepropionic acid (AMPA) receptors and synaptic transmission [3, 40]. Epileptic seizures represent clinical manifestations of excessive, hypersynchronous discharges in neurons [41]. However, their electrophysiological pattern and initial topographic focus are very heterogeneous, and several mechanisms that contribute to their manifestation are described. The communication between and within the brain's neuronal networks is potentially

mediated through oscillations (rhythmic and/or repetitive electrical activity). Seizures probably develop due to increased neuronal excitability, synaptic transmission, and higher network connectivity with hypersynchronous neuronal ensembles. Further mechanisms secondarily facilitate the recruitment of larger areas [42].

The propagation velocity of human seizures can range from very slow (<200  $\mu\text{m/s}$ ) to very fast >10 mm/s [43]. Importantly, in studies using the 0  $\text{Mg}^{2+}$ -model (increased NMDA receptor activity), the speed of seizure spread ranged from 160 to 250  $\mu\text{m/s}$  [44, 45]. Therefore, hyperexcitability can induce seizures with propagation velocities comparable to SD.

Although the initiating events of both phenomena have been extensively researched, it is still unclear what determines the transition from hyperexcitability to either SD or seizures [3].

Section 4 presents the state of current research and is followed by section 5 that presents the objectives and significance of this dissertation. Section 6 describes the methods, and section 7 the results of the publication that this dissertation is based on. Section 8 discusses the relationship between SD and seizures that is characterized by intriguing overlaps of migraine and epilepsy. This dissertation mainly focuses on the close bidirectional interactions between seizures and SD, which are the pathophysiological correlates of migraine and epilepsy. Although physicians often encounter puzzling cases that unify features of migraine and epilepsy, their clinical manifestations are typically interpreted as distinct conditions.

Therefore, this research addresses the current gap in knowledge concerning the missing links needed for a better understanding of both conditions. It offers a current review exploring facets and overlaps of both diseases by presenting their shared symptoms, triggers, and therapeutical strategies.

## 4. State of research\*

While epilepsy and migraine are both episodic diseases that have been extensively researched as distinct entities, their intriguing coexistence and the mechanisms underlying their relationship remain poorly understood. SD is a network phenomenon that connects both conditions as it is triggered by hyperexcitability. Furthermore, the hyperexcitable cortex is known to be particularly susceptible towards SD and seizures. This section begins with the historical characterization of SD as the pathophysiological correlate of migraine aura, followed by a detailed description of commonalities between epilepsy and migraine in the light of recent investigations in both fields.

### 4.1 Aura phenomenology: SD as the pathophysiological correlate of migraine aura.

Visual auras are flickering, colorful patterns with fortification figures and zigzag borders expanding from the center to the periphery of one visual field [3]. These hallucinations gradually float in a C-shape, leaving blindness in their wake (“scintillating scotoma”) [46]. Scientists first postulated the SD theory of migraine after comparing the progression rate of aural symptoms to SD. They hypothesized that scintillating hallucinations were caused by a leading wave of neuronal excitation (i.e., spreading depolarization), whereas the expanding scotoma was related to the extensive suppression of electrical activity (i.e., accompanying spreading depression). The visual patterns moved at a rate of 3 mm/min, which resembles the propagation speed of the SD wave [47, 48]. Among all migraine auras, visual auras are most frequent [49], perhaps because the occipital cortex is particularly susceptible to SD due to its low glial—neuronal cell ratio and, therefore, limited ability to control the extracellular  $K^+$  concentration [50].

Functional magnetic resonance imaging (MRI) studies later confirmed these observations. In the otherwise healthy brain, the massive depolarization during SD is followed by a rise in CBF (“spreading hyperemia”) to meet the heightened metabolic demand. A moderate decrease of CBF (“spreading oligemia”) can be detected after tissue recovers from the depolarization. Visual aura symptoms and headache could be matched topographically and timewise to neurovascular changes that resemble the

---

\* Parts of this section have been extensively researched in an unpublished academic essay by the author, and were revised and adapted from **Tamim, I.**, *Seizures versus Cortical Spreading Depolarization – Implications for Migraine with Aura and Epilepsy*. Charité Universitätsmedizin Berlin.

hemodynamic response to SD in functional magnetic resonance imaging (MRI) [3, 51, 52]. Ample evidence from experimental studies provides further insights. SD activates the trigeminovascular system that connects meninges and blood vessels with trigeminal ganglion cells [2]. More specifically, SD causes the release of pro-inflammatory players such as arachidonate, adenosine, and nitric oxide [5, 53-56]. However, it is important to note that this evidence is by no means definitive as magnetoencephalographic measurements remain the only direct evidence in support of the SD theory of migraine [57]. Electrophysiological data concerning the co-occurrence of SD and migraine aura remain rare as subdural recordings need to be obtained to detect SDs. In such cases, patients have usually suffered from an injury requiring surgery, which complicates the differentiation between pathology-induced and typical aura SD [58]. Furthermore, the causal relationship between headache and SD is controversial as 60–70 % of migraine patients do not experience auras [59, 60], and 9% of patients with auras do not suffer from headaches [61]. SD and headache may be independently initiated, which would significantly impact the role of SD as a therapeutic target [3]. When occurring in the ineloquent cortex, SD possibly leads to a silent aura that is mistakenly diagnosed as a migraine “without aura” [62]. The fact that prophylactic anti-migraine medications efficiently inhibit SD and migraine with or without aura [63] seems to support this assumption.

#### **4.2 Symptoms in the borderland: Post-ictal headache and visual disturbance.**

Headaches are not only prominent in migraine as they commonly occur as a post-ictal event in epilepsy, although the symptom is relatively innocuous and often neglected. Migraine-like post-ictal headaches are mainly related to specific seizure foci such as the occipital cortex. Especially younger patients with post-ictal headaches are more likely to report interictally occurring migraine attacks with headaches [64-66]. It appears that neuronal networks that promote vision are particularly prone to seizures and migraine during their development. Congenital ocular and visual dysfunctions in children are highly correlated to occipital electroencephalogram (EEG) abnormalities. Congruently, peri-ictal events such as blindness and hemianopia predominantly affect children [67, 68], and photosensitive epilepsy mainly occurs in young females [69]. The apparent similarity in the clinical manifestations can make a diagnosis difficult, as migraine with visual aura and simple partial occipital lobe seizures with post-ictal migraine-like headache and/or visual disturbance can imitate each other. Seizure-

triggered visual hallucinations require detailed descriptions and expertise to distinguish them from visual migraine aura [70], and without EEG recordings, judgment remains speculative. These patients may present a spectrum of intercalated symptoms on the borderland between migraine and epilepsy.

#### **4.3 Visual hypersensitivity, stress, and hyperexcitability: triggers in migraine and epilepsy.**

Visual disturbances during seizures and migraine attacks emphasize the importance of the visual cortex in the pathophysiology of both conditions. Furthermore, photic stimulation can trigger migraine attacks and seizures, indicating that subpopulations of patients suffering from migraine and photosensitive epilepsy show cortical hyperresponsivity to certain stimuli. Approximately 5% of patients with epilepsy are susceptible to visually induced seizures. Television, flickering lights, or striped patterns (especially when moving) readily induce EEG abnormalities and even seizures in susceptible individuals [71-73]. Several reports indicate that in these cases, ictal activity originates from the occipital cortex [74, 75] and can be mistaken for migraine aura [76]. Migraineurs often report visual discomfort and headache when viewing striped patterns [77, 78], and cortical arousal, sensitivity, and decreased habituation in different sensory modalities peak before a migraine attack [79-84]. Congruently, a decreased threshold for transcranial magnetic induction of phosphenes in migraineurs has been well described [85-87]. Phosphenes are transient conscious visual percepts that can be elicited with transcranial magnetic stimulation pulses applied to the occipital cortex without visual stimulation. Treatment with antiepileptic drugs (AED), particularly valproate, reduces phosphene occurrence [88-91] and migraine attack frequency. AEDs can inhibit SD [63], emphasizing cortical hyperexcitability as an important modulator in these patient groups.

Interestingly, in numerous studies, stress has been associated with heightened cortical excitability [92] and susceptible individuals report higher frequency rates of migraine attacks and seizures when exposed to stressors. Furthermore, stress can reduce the threshold for SD induction [93, 94] and promote seizures [92, 95], probably through actions mediated by glucocorticoid and specific adrenergic receptors. Hyperexcitability as a trigger of SD has been the subject of much debate. At the onset of SD, neuronal fast field activity has been reported to precede the elevation of the potassium concentration [26, 37, 96-99]. The synchronization of neurons and the subsequent

oscillations of this neuronal group can occur shortly before SD is triggered. Additionally, this state of altered excitability originates at a millimeter distance from the depolarization avalanche. It is possible that neuronal field oscillations are independent of synaptic transmission and could be mediated by glutamate [37] or via gap junctions [98].

Glutamate, an excitatory neurotransmitter, is a crucial mediator for generating an environment of hyperexcitability that facilitates focal seizures [100] and SD [97]. As mentioned previously, NMDA receptors are responsible for sustaining the depolarization wave of SD [101]. However, other low-affinity NMDA receptor antagonists (e.g., memantine) show robust efficiency in reducing headache frequency (i.e., SD occurrence) [102] and increase seizure threshold when co-administered with an AMPA receptor antagonist [103]. NMDA receptor antagonist MK-801 (see sections 6.3 and 7.3) and ketamine [104] can inhibit SD frequency. Interestingly, under specific circumstances such as refractory status epilepticus [105] or kindling models, these substances can act as potent anticonvulsants [106].

#### **4.4 Excessive neural activity as a treatment target in migraine and epilepsy**

Along with AMPA and NMDA receptors, calcium signaling mediated by astrocytic glutamate release plays a substantial role in SD and seizures, thereby revealing additional shared mechanisms that connect both network phenomena. In migraine prophylaxis, the clinical efficiency of specific antiepileptic drugs such as topiramate, levetiracetam, and ezogabine [63, 107, 108] is of particular interest. Valproate blocks astrocytic calcium-mediated hypersynchronous epileptiform activity in neighboring neuron groups. When administered for a more extended period, topiramate and valproate inhibit SD [63, 100] and reduce cortical hyperexcitability and headache frequency in migraine patients [89, 90, 109]. Similarly, long-term treatment with valproate decreases whole-brain glutamate levels [110] and reduces NMDA or kainate receptor-mediated synaptic transmission [111, 112]. While hyperexcitability and synaptic transmission may not be required to induce SD, they can still contribute to its triggering. Given the various lines of evidence, it is very likely that they are highly relevant to SD induction in the hyperexcitable and hyperresponsive migraine cortex, although, naturally, there are probably multiple mechanisms contributing to the efficiency of AEDs in migraine prophylaxis. Considering that only chronic treatment was thus far sufficient to reduce SD and migraine frequency, the long-term modulation

of gene expression affecting brain excitability might be particularly relevant in this context [113].

#### **4.5 Genetic underpinnings of migraine and epilepsy**

A common genetic basis for migraine and epilepsy has long been suspected [6, 114] as both disorders aggregate in families [115, 116]. The pathophysiology of migraine and epileptic syndromes is typically bound to several external factors (e.g., stress, see section 4.3), which promote susceptibility to the manifestations of these disorders. However, the familial hemiplegic migraine (FHM) syndromes are rare exceptions showing a strong genetic component. FHM is inherited in an autosomal dominant way and causes a severe type of migraine with aura. Apart from the hemiparesis and longer duration of attacks, FHM patients typically report symptoms similar to those of common forms of migraine [117] and its pathogenesis can thus be compared to that of other types of migraine. Alterations of specific ion channels account for heightened cortical excitability, leading to migraine, epilepsy, or both. All three genes related to FHM are associated with higher susceptibility towards SD and seizures.

Missense mutations in the *CACNA1A* gene (FHM type 1) can be found in more than 50% of the families with FHM. More specifically, in this scenario, the  $\alpha 1A$ -subunit that shapes the pore of the P/Q-type calcium channels (CaV2.1) in neurons is structurally changed [3, 118], leading to increased density of P/Q-type calcium channels and higher open probability [119]. P/Q-type calcium channels can be found on somatodendritic membranes and presynaptic terminals [120]. The mutation leads to enhanced open probability, followed by a large-scale release of the excitatory neurotransmitter glutamate at pyramidal cell synapses. Because inhibitory neurons are excluded from changes in synaptic transmission [121], the imbalance between excitation and inhibition is likely responsible for the heightened susceptibility towards SD and seizures in FHM type 1. FHM type 1 can be further differentiated into the subtypes R192Q and S218. Both gain of function mutations lead to the expression of the pathological ion channels mentioned. The state of cellular hyperexcitability can lead to the co-occurrence of epileptic seizures and migraine attacks (i.e., SD) in susceptible individuals [122]. Patients with FHM type 1 show a higher prevalence of idiopathic generalized epilepsy [123] and sudden unexpected death in epilepsy which was recently associated with SD in the brainstem [3, 124].

The ATP1A2 (ATPase Na<sup>+</sup>/K<sup>+</sup> Transporting Subunit Alpha 2) gene is relevant to the FHM type 2 genotypes in which patients show a loss of function mutation in the gene that expresses an isoform of the Na<sup>+</sup>/K<sup>+</sup> ATPase in astrocytes that is crucial for the stability of transmembrane gradients. Congruently, FHM type 2 is linked to a higher occurrence of SD and epileptiform activity [125, 126]. FHM type 3 is caused by mutations in the SCNA1 gene that expresses a voltage-gated sodium channel. Patients with FHM type 3 show comorbidity with generalized [127, 128] and partial epilepsy [129] [130]. In addition, patients with familial hemiplegic migraine, generalized epileptic seizures, and benign familial infantile epilepsy show all mutations in the proline-rich transmembrane protein 2 (PRRT2) gene encoding a transmembrane protein [3, 131]. Interestingly, the S218L mutation, a subtype of FHM type 1, only causes epileptic seizures during childhood which transition to migraine during adulthood [132-134]. Similar findings were reported for FHM type 3 [130] and children suffering from typical migraine with aura [14].



## 5. Objectives and significance of the work

Epilepsy and migraine show strong correlations as they share clinical and genetic features as well as epidemiologically evident co-occurrence. However, patients are still mainly treated by separate subspecialties, and the management of epilepsy and migraine lacks clinical dialogue. This is a challenge to effective treatment as an integral pathophysiological understanding is crucial for diagnosis and improved therapeutical strategies, particularly when both disorders co-occur in the same individuals. The question concerning why brain hyperexcitability transitions to seizures in epilepsy and to SD in migraine is of great importance, although the findings in this regard remain obscure. It seems plausible that SD, a propagating wave that silences brain activity and that can be triggered by hyperexcitability, represents a linkage in the borderland between migraine and epilepsy [3]. The present study examines the direct interactions between seizures and SD and discusses the role of SD in the borderland between epilepsy and migraine, thus adding significant work for both subspecialties.

It delineates the electrophysiological interfaces of both conditions, thereby potentially contributing to quick diagnosis and improved treatment strategies. Furthermore, SD is discussed as a mechanistic link in their pathophysiology, which provides a more balanced perspective on SD's role in neurological diseases.

Three elementary questions are addressed in the scope of this discussion:

1. Do seizures trigger SD?
2. What factors influence the incidence of SD in the event of a seizure?
3. Do SDs suppress seizure intensity and spread?

## 6. Methods

This research was originally published in Nature Communications as

*Tamim, I., Chung, D.Y., de Moraes, A.L., Loonen, I.C.M., Qin, T., Misra, A., Schlunk, F., Endres, M., Schiff, S.J., Ayata, C. Spreading depression as an innate antiseizure mechanism. Nat. Commun. 12, 2206 (2021).*

<https://doi.org/10.1038/s41467-021-22464-x>

The following section is adapted from the publication mentioned above and describes the methods in detail. The author's own contributions are highlighted in the relevant sections.

All procedures and experimental setups were conducted in accordance with the Committees NIH Guide for Use and Care of Laboratory Animals (NIH Publication No. 85-23, 1996) of the Massachusetts General Hospital Institutional Animal Care and Use [135]. The experimental design was continuously modified based on a rolling review of data to optimize controllable input factors, thereby determining the cause- and effect relationship between SDs and seizures.

### 6.1 Animals, housing, and husbandry

Because the interplay between both phenomena may rely on the susceptibility of animals towards SD and seizures, experiments were conducted with mice of several strains: wild-type Swiss CD1-mice ( $n = 165$ , male,  $3.2 \pm 0.1$  months, Charles River Laboratories, Wilmington, MA, USA), familial hemiplegic migraine mutant mice ( $n = 7$  males, 1 female;  $8.9 \pm 2.7$  months, Jackson Laboratories, Bar Harbor, ME, USA), wild-type mice from the same litter ( $n = 4$  males, 2 females;  $8.3 \pm 1.6$  months), and transgenic mice ( $n = 10$  males and 8 females,  $7.5 \pm 0.6$  months, Jackson Laboratories, Bar Harbor, ME, USA) [135]. In FHM type 1 knockin mice, the S218L missense mutation was heterozygous. The mutation in the *Cacna1a* gene causes a defect in the  $\alpha_1A$  pore-forming subunit of voltage-gated calcium channels. As mentioned, the S218L mutation causes a more severe clinical phenotype and higher susceptibility towards SD and seizures compared to the R192Q variant [122]. In contrast, CD1 mice do not show higher susceptibility towards seizures or SDs.

Transgenic mice (ChR2+, n=10 males and 8 females, 7.5±0.6 months, B6.Cg-Tg (Thy1-COP4/EYFP)18Gfng/J) were used [135-137] to study optogenetically induced SDs in comparison to chemically induced SDs in CD1-mice. Thy1-ChR2-YFP mice express channelrhodopsin-2, a fusion protein in layer 5 neurons of the cortex [136]. Their light-sensitive ChR2 cation channels allow SD induction by applying a brief blue light stimulus onto the intact skull with an optic fiber [138]. All mice were housed in the same facility room exposed to a 12-hour light/dark cycle (lights on from 7 a.m. to 7 p.m.) with unlimited access to water and food. The room temperature was set to approximately 25°C, and the relative air humidity was set at 45–65 percent. Groups of two to four animals shared one cage. On the day before the experiments were conducted, food was withheld overnight ( $17.4 \pm 0.3$  hours; n = 173) to increase susceptibility towards seizures.

### **6.2 Surgical procedures**

All surgical procedures were conducted by the author. The tail vein was incised to draw blood to perform blood glucose testing before anesthetic induction. The time of day at which the measurements were conducted was kept consistent, and all experiments were carried out during the light period between 7 a.m. and 6 p.m. The mice were initially anesthetized with 3% isoflurane that was quickly reduced to 1.25% to maintain anesthesia, and they were allowed to breathe spontaneously on 70% NO<sub>2</sub> and 30% O<sub>2</sub> throughout. The left femoral artery was catheterized to continuously measure blood pressure (PowerLab; ADInstruments) and to allow arterial blood gases measurements. Invasive blood pressure monitoring was established by an intra-arterial monitoring system consisting of an arterial cannula that was connected to a tube placed inside the femoral artery. The tube was filled with a saline column that conducted the blood pressure wave to a transducer. The blood pressure was used to control anesthesia depth and to manage intraarterial fluid administration. In all cases, arterial blood gases (pCO<sub>2</sub>, pO<sub>2</sub>) and pH were measured before applying the respective chemoconvulsant to ensure comparable physiological conditions after surgical preparation. After the initial recordings, the measurements were re-done to warrant reproducibility of the results. The rectal temperature was continuously

measured and automatically adjusted to 36.5–37.0°C by a heating pad that the mice were placed on to guarantee normothermia. Mineral oil was applied to the uncovered skull to prevent bone drying. Under saline cooling, burr holes were drilled based on electrode configurations in various cohorts. For the topical application of chemoconvulsants, the skull was thinned to create a two-millimeter wide occipital window with a small crack to place the epidural electrode and enhance drug diffusion (3 mm lateral and 2 mm anterior from the lambda). Throughout the experiment, care was taken to keep the dura wet and imperforated to prevent inadvertently triggered SD.

### 6.3 Pharmacological interventions

For this study, it was important to investigate the effect of SD in different experimental seizure models. Since epilepsy is a disease term that encompasses various clinical manifestations, research has generated an equally diverse variety of experimental animal models over the last decades, whereby each model represents an attempt to replicate a distinct kind of clinical epilepsy with its unique features and dynamics. The hypothesis was tested in four different seizure models to prove that SD plays a significant and reliable role in seizure expression. For this experimental series, 4-aminopyridine (4-AP; 5, 30 or 100 mM; Sigma-Aldrich, USA), penicillin G (PG; 188434 IU/ml, sodium salt; Sigma-Aldrich, St. Louis, MO, USA), 1(S),9(R)-(-)-bicuculline methiodide (BIC; 5 mM; 1mM, 0.5 mM, 0.05 mM, and 5  $\mu$ M; Sigma-Aldrich, USA) [135] or vehicle (0.9% saline) were applied topically onto thinned skull to induce microseizures. The application was repeated once (10 minutes after the first application), and the cortex was not washed afterward. All chemoconvulsants are reported to induce epileptiform activity *in vivo* and *in vitro*.

Concerning the mode of action, 4-AP generates seizure activity by inhibiting transient (A-type) or sustained voltage-dependent potassium channels in nerve terminals. At the presynaptic terminals, the drug's epileptiform action is also driven by the release of excitatory amino acid (mainly glutamate) molecules (Fig. 1B). In the somatodendritic region, the drug lowers the threshold for induction of action potentials and shortens the refractory phase. Importantly, 4-AP preserves neuronal inhibition [139, 140]. The antibiotic PG has epileptogenic properties that reversibly antagonize the  $\gamma$ -aminobutyric acid type A receptor (GABA<sub>A</sub>R) [141] and, thereby, inhibits chloride ion

## Methods

influx and synaptic inhibition [142] (Fig. 1A) while BIC functions as a competitive antagonist at GABA<sub>A</sub>R too (Fig.1A). It decreases both channel open durations and frequency of opening. Because its molecular weight is three times higher than that of GABA, BIC might attach to binding sites that cannot be reached by GABA [143]. In a subset of experiments, mice received intraperitoneal injections of kainic acid (KA; 60 mg/kg; Sigma-Aldrich, USA), an agonist at the kainate and AMPA receptors (Fig. 1C) [144-147]. After injection into the peritoneal cavity, KA is subsequently absorbed by blood vessels and transported to the brain through passive diffusion, where it crosses the blood-brain barrier [148]. The cortex was pretreated with a topical focal application of tetrodotoxin (TTX; 30  $\mu$ m in sodium citrate buffer, pH 4.8; Enzo Life Sciences, Farmingdale, NY, USA) [135] 30 minutes before 4-AP administration as TTX blocks sodium channels and action potentials by inhibiting sodium permeability without impairing the potassium conductance [149]. Interestingly, TTX does not abolish SD, which is a unique feature of the network phenomenon. Moreover, Na<sup>+</sup>-equilibrium potential and propagation velocity during SD remain unaffected by TTX. Classical voltage-gated Na<sup>+</sup>-channels are necessary for seizure formation but not for SD initiation [20, 38]. In contrast, MK-801, a noncompetitive NMDA receptor antagonist, reveals a different mechanism concerning SD as MK-801 blocks SD by hampering the glutamate-mediated Ca<sup>2+</sup> influx into the cell [150]. To block SD in a separate cohort, MK-801 was injected intraperitoneally 30 minutes before 4-AP application (1 mg/kg, n=7; 3 mg/kg, n=5; Sigma-Aldrich, USA) [135].



**Figure 1 | Mechanisms underlying pharmacological acute seizure models.**

**A** | BIC and PG antagonize ionotropic GABA<sub>A</sub>-receptors resulting in a blockage of the inhibitory actions of GABA on the postsynaptic site. Because the chloride influx into the postsynaptic excitatory neuron is not sufficient to hyperpolarize the membrane, the inhibitory postsynaptic potential (IPSP) is reduced. The resulting IPSP, in turn, fails to decrease the probability of the generation of a postsynaptic action potential. Note that BIC is a competitive GABA<sub>A</sub> receptor antagonist whereas PG reversibly binds to GABA<sub>A</sub> receptors. **B** | 4-AP binds to several voltage-activated potassium channels located on pre- and postsynaptic sites. A reduction of transient potassium outward current hampers the rectification of the depolarizing potential and leads to a reduced threshold for further action potential generation. In addition, 4-AP-sensitive calcium channels enhance glutamate release which activates NMDA and AMPA receptors on the postsynaptic site (increased excitatory postsynaptic potential, EPSP).

**C** | Kainic acid (KA) binds to pre- and postsynaptic kainate and AMPA receptors. The activation of kainate receptors on glutamatergic nerve terminals leads to an increased influx of sodium and calcium ions which promotes glutamate release. Together with the increased glutamate concentration, KA further increases action potential firing at the postsynaptic site by directly binding AMPA and kainate receptors. Additionally, at concentrations used in this study, KA inhibits GABA-release from inhibitory nerve terminals. The exact mechanisms underlying the suppression of GABA release are not fully understood but are probably related to actions involved in a G-protein coupled cascade.

**6.4 Cortical electrophysiological recordings**

All recordings were conducted by the author. Different experimental settings were used to elaborate the interplay between seizures and SD in terms of several aspects. The direct current (DC) potential and electrocorticogram (ECoG) were constantly monitored and processed as continuous data output. For this purpose, glass micropipettes were filled with 0.9 % sodium chloride (NaCl) and positioned epidurally. Three locations (E1–E3) were selected to capture SD occurrence, seizure activity, and generalization. Two electrodes were used for experiments in which the characteristics of SD-triggering seizures were determined. The local electrode, E1, was placed in the seizure focus (i.e., drug application window) while E2 was positioned on the ipsilateral frontal cortex (1.5 mm lateral, 1.5 mm anterior from bregma), and E3 was placed homotopically to the seizure focus (i.e., E1) on the contralateral hemisphere [135]. SDs were artificially induced with topical application of potassium chloride onto thinned skull from a remote site. In experiments with an anteriorly placed electrode (E2), KCl was applied between E1 and E2 to prevent the chemical from influencing measure-

ments at the recording site. In experiments without an electrode on the ipsilateral hemisphere, KCl was applied anteriorly. In experiments where SD was induced non-invasively, an optic fiber was positioned anteriorly and in parallel to the skull surface. Mineral oil was used to optimize the optical coupling between the probe tip and the skull surface. A 400- $\mu\text{m}$ -diameter fiber with a 470-nm LED (LED: MF470F3; LED driver: DC2100; Thorlabs, Newton, NJ, USA) was used for optogenetic light stimulation [135, 151]. The light intensity was adjusted to between 1 and 3 mW by using an analog-to-digital converter.

### **6.5 Hippocampal electrophysiological recordings**

The DC potential and local field potential (LFP) were recorded from the hippocampal CA1 region (2 mm posterior and 1.5 mm lateral from bregma at a depth of 1.4 mm) [135]. KA was injected at an isoflurane level of 1.5%. Anesthesia is a known suppressor of SD [152], and isoflurane, in particular, potentiates the neuromuscular blockade [153], masking motoric manifestations of generalized seizures. For this reason, isoflurane was gradually lowered after KA injection to  $\sim 0.58 \pm 0.08$  % over 45 minutes. The reduction of isoflurane was stopped when small-amplitude clonic leg movements appeared, representing generalized seizure. The movement pattern differed from purposeful movements that appear in response to pain.

A subcutaneous Ag/AgCl electrode was implanted in the neck to act as a reference for DC potential, ECoG, and LFP measurements.

### **6.6 Data processing**

Data processing and analysis were conducted by the author. For further computation, the signal was amplified (bandpass 0.3–300 Hz) and processed at a sampling rate of 1 kHz (PowerLab; ADInstruments). Unwanted frequency components over 20 Hz were removed using a digital low pass filter (LabChart 5 Pro, ADInstruments). In the first analytical step, the power spectrum density of the ECoG was calculated using the fast Fourier transform method (FFT, cosine-bell window, size 1024, window overlap 93.75 %) on uninterrupted 5-minute bins (LabChart 8 Pro, ADInstruments) [135]. Because seizure-triggered spontaneous SDs occurred at various time points, time bins of 1 minute were chosen to give higher accuracy of computed power spectrum densities in this cohort. For E1, the baseline was selected



close to the topical application of the respective chemoconvulsant to avoid field potential changes due to fluid application. The power spectrum densities were averaged for  $\delta$  (0–4 Hz),  $\theta$  (4–8 Hz), and  $\alpha$  (8–12 Hz) frequency bands within one selected time bin. The output for each bin was then plotted over time in every experiment. To aid with visualization, time-varying spectrograms were created with the Thomson's multitaper technique (window length 10 seconds, window step 1 second, bandwidth 20 Hz, number of tapers 9) [135]. The code used to compute and plot the graphs can be found in the Chronux toolbox, <http://chronux.org>; version 2.12 v03, 2018).

### **6.7 Intrinsic optical signal (IOS) imaging**

Intrinsic optical signals (IOS) are used to characterize changes in the exposed cortex's diffuse optical reflectance. They may result from changes in the cerebral blood volume (CBV) and oxygenation on a local level. Therefore, IOS, in combination with ECoG, is a valuable tool to study neurovascular coupling—i.e., the relationship between neuronal activity and local hemodynamic changes. Transcranial IOS imaging was used to examine CBV as a correlate of seizure activity and visually detect the origin and propagation [154-156]. The skull was exposed after a midline scalp incision, followed by removal of overlying connective tissue. Skull translucence was achieved by initially applying mineral oil and repeating this step for 15 minutes to prevent the skull from drying. The USB camera and light sources were positioned to minimize light reflections from the surface of the skull. IOS imaging was started before skull drilling in order to exclude animals in which SDs were inadvertently induced during the surgical procedure. Images were output in real-time to stop the experiment when SD was detected during surgical preparation, which was enabled by white light illumination. Time-lapse jpeg images were continuously taken (0.5 Hz, 640 x 480 pixels) with a pen USB camera during skull drilling and electrode positioning (YawCam 0.6.2, 2018). A MATLAB (R2018b) script was used to periodically generate different jpeg images [135, 154].

### 6.8 CBV measurement

For CBV measurements, a white or a green LED (M530L3, FB530-10, Thorlabs) with a wavelength of 530 nm and an aspheric condenser lens (ACL2520U-DG15-A, Thorlabs) were selected [135]. All experiments were conducted in a Faraday's cage whose doors were closed during recording in order to selectively illuminate the skull with the mentioned light sources. Full-field images (1 Hz, 640 x 480 pixels) were collected, downsampled to 320 x 240 pixels, and the pixel intensity in each frame over time was computed [135]. The pixel intensity corresponds to the diffusely reflected light that enters the brain, is dispersed throughout the cortex, and eventually exits from the surface to approach the USB camera. At a wavelength of 530 nm, oxygenated and deoxygenated hemoglobin shows the same absorption values (isosbestic point). Therefore, measurements taken at this wavelength are independent of oxygenation and sensitive to total hemoglobin alterations. For further examination, a new MATLAB algorithm was used to analyze the green channel in all images using a modified Beer-Lambert equation [157]. One line of interest (LOI) was put between the drug administration location (seizure focus) and the anterior electrode, and another LOI was placed homotopically on the contralateral cortex (Fig. 4). At a distance of 1 mm, regions of interest (ROIs) along the LOI were defined. The pixel intensity for each ROI and LOI was plotted throughout the recording. Full-field band power maps and pixel intensity were color-coded and plotted to visualize seizure appearance. Red corresponds to hyperemia representing local seizure spread, while blue corresponds to oligemia (e.g., during interictal phases or after SD). The measurements were acquired in parallel with the electrophysiological recordings by the author. The MATLAB script for image analysis was written in cooperation with a laboratory member.

### 6.9 Rigor and statistical analysis

A total of 197 mice were included in the present study. Cohorts that received intervention and control groups with vehicle application were randomized after surgical preparation by a laboratory member not involved in the study. Experiments in both groups were conducted in parallel. Due to real-time electrophysiological recordings and IOS images, it was not possible to conduct the experiments in a blinded fashion, although the confirmation of data processing and statistical analysis were conducted in a blinded fashion. Sample sizes were chosen to identify an effect size of at least

## Methods

30% with a coefficient of variation of 20% ( $\alpha = 0.05$ ). The reproducibility of the findings was ensured by replicating experiments of cohorts at multiple time points with an interval of three to six months during the study. Fresh drug batches were purchased every 3 to 4 months to prevent alterations in drug activity. The data were statistically analyzed using GraphPad/Prism 8. The exact p-values, statistical tests, and sample sizes are provided in the text and selected figure legends. Data from 16 experiments were excluded. Four experiments were excluded due to technical problems (discontinuous measurements of DC amplitudes), seven experiments were excluded after inadvertent SD induction recorded with optical imaging during surgical preparation (2 FHM1 mice, 5 CD1 mice in spontaneous SD cohort, 4-AP, PG). One FHM1 mutant mouse suddenly died during severe seizures and was excluded. Four experiments were excluded because the potency of 4-AP changed after altered temperature storage (SD pre-treatment cohort, CD1 mice-cohort). Statistical analysis was conducted by the author and supervised by the principal investigator.

## 7. Results

This research was originally published in Nature Communications as

*Tamim, I., Chung, D.Y., de Moraes, A.L., Loonen, I.C.M., Qin, T., Misra, A., Schlunk, F., Endres, M., Schiff, S.J., Ayata, C. Spreading depression as an innate antiseizure mechanism. Nat. Commun. 12, 2206 (2021).*

<https://doi.org/10.1038/s41467-021-22464-x>

The following sections describe the results in detail and are adapted from the above publication.

### 7.1 Seizures trigger SD.

#### Dynamics and characteristics of microseizures

Seizures induced with 4-AP started with synchronized monomorphic spiking that evolved into polyspikes for approximately 15–25 minutes. Discharges transformed into a burst pattern that recurred with increasing intervals and lasted about 2 hours. The initial pattern showed rhythmic discharges at a frequency of 1 Hz with large amplitudes (400% over baseline) that evolved into polyspikes with a frequency of about 4 Hz. The subsequent bursting pattern typically started with a single large-amplitude slow discharge (1 Hz) followed by fast oscillations starting at 18 Hz and rapidly decreasing to 6 Hz over 20–80 seconds. The highest power density (PD) increase was detected in the  $\delta$  frequency band (0–4 Hz; 7.3 fold), followed by the  $\theta$  (4–8 Hz, 3.2 fold) and  $\alpha$  (8–12 Hz, 3.4 fold) frequency bands. Penicillin G and bicuculline methiodide, both GABA<sub>A</sub> receptor antagonists, induced seizures with uninterrupted high-amplitude monomorphic spikes, while PG caused spike-wave activity. Initially, PG induced discharges that showed a 2.5 fold increase in amplitude, which subsequently transitioned to a 6 fold increase with a stable 0.5 Hz frequency [135]. The PD increase within the  $\alpha$ -frequency band (13.7 fold) lasted for about 90 minutes while the  $\theta$ -power increase (12.4 fold) remained stable for the entire recording of 4 hours in the PG-cohort. A 3.6 fold increase in PD was also detected in the  $\delta$  frequency range. BIC-induced seizures were typically shorter than those induced with 4-AP and PG and only lasted for < 60 minutes. Spikes began at a frequency of 0.2 Hz and increased to a 2 Hz activity over 40 minutes (Fig. 2A). Similarly, the amplitude increased from 120% to

## Results

250% over baseline. The PD increase was largest in the  $\alpha$  frequency band (19.9 fold), followed by the  $\theta$  (13.3 fold) band. In contrast to the 7.3 fold power increase in the  $\delta$  frequency band during 4-AP-induced seizures, only a 3.6 and 3.4 fold increase could be detected for the PG and BIC groups, respectively. It is interesting to note that the control vehicle application (0.9% NaCl) resulted in a stable ECoG morphology and power level for the entire recording time of 4 hours.

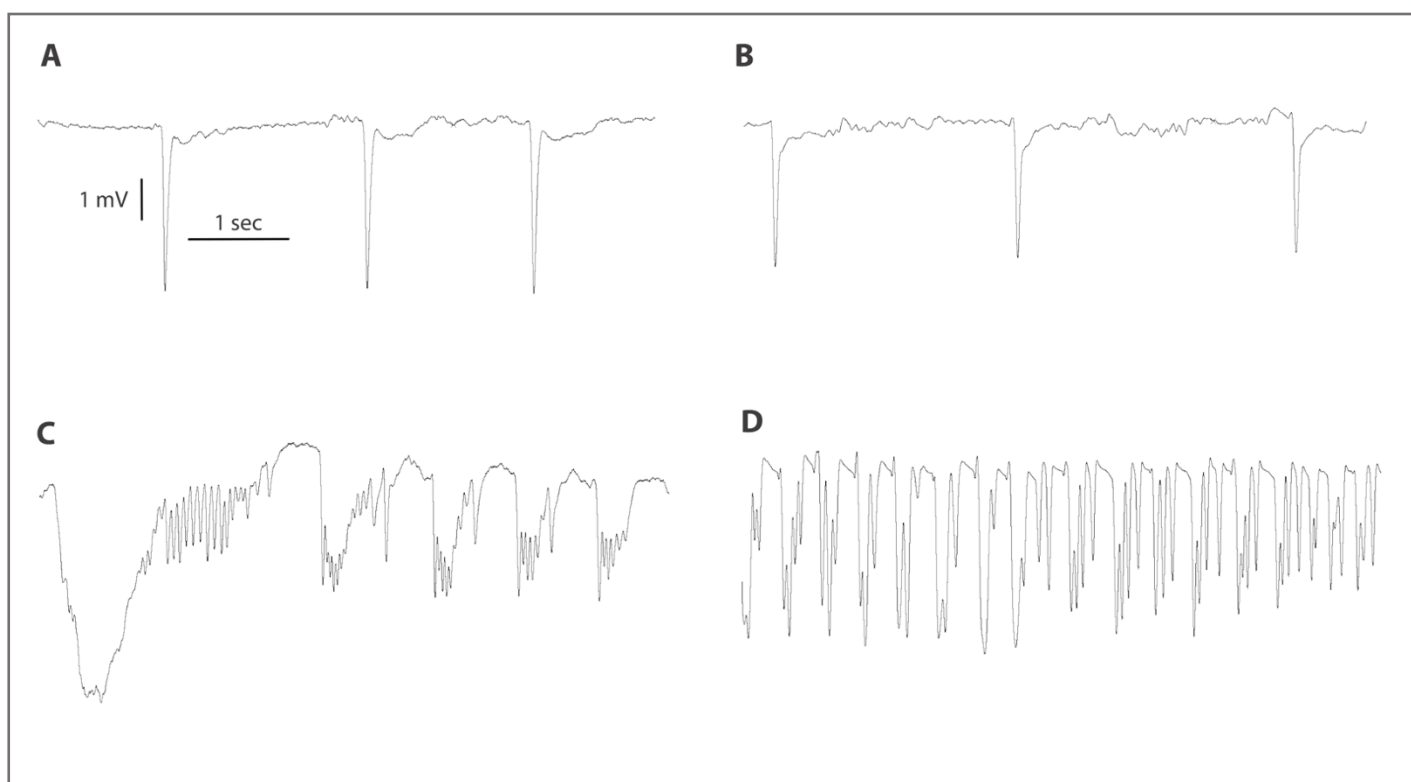


**Figure 2 | ECoG characteristics in the different seizure models.**

**A** | BIC- induced continuous monomorphic spiking that resembled the epileptiform pattern induced by PG **(B)**. Both chemoconvulsants share a similar mechanism of action. **C** | Seizures induced by 4AP eventually transformed to polymorphic spikes that appeared as bursting periods lasting for 20–80s.

**D** | Generalized seizures induced by KA were characterized by rhythmic discharges occurring as bursting periods every 1–3 minutes.

Cortical microseizures trigger SD.

4-AP-induced seizures triggered SDs in 69% (n = 32), PG in 33% (n = 9), and BIC in 9% (n = 11) of the mice (p = 0.002,  $\chi^2$ ) (Fig. 3). No SDs appeared in control experiments with vehicle application (n = 10). SDs were detected via direct current (DC) large slow potential shifts at the seizure focus recording site and IOS imaging. The initial SDs typically erupted singly, whereas subsequent SDs tended to appear in clusters. In the 4-AP group, SDs occurred at a frequency of  $0.89 \pm 0.22/h$ , followed by the BIC cohort with a frequency of  $0.74 \pm 0.74/h$ . The PG-induced seizures showed the lowest frequency of SD occurrence ( $0.26 \pm 0.17/h$ ) [135]. Subsequent SDs often caused uncharacteristic positive DC shifts, suggesting growing resistance towards SD over the course of the experiment as previously described elsewhere [158]. In the 4-AP group, 48% of the first SDs and 50% of subsequent SDs did not move to the original seizure core, whereas only 33% of the first SDs and 67% of the subsequent SDs were not capable of penetrating the seizure core in the PG group. In the BIC group that showed the shortest seizure duration, all SDs penetrated the seizure core. Additionally, SDs caused typical CBV alterations that were visible on IOS imaging. SDs mainly arose in the area of the seizure focus, although some emerged from the frontal lobe. The different origins of SDs across the cortex indicate seizure spread. All SDs propagated to the ipsilateral frontal cortex rather than occurring as non-spreading SDs that are typically caused by severe ischemia [135].

Blocked seizures prevent SD-occurrence

Because SDs were more prevalent in the 4-AP group, it was essential to study a potential SD-inducing effect of the chemoconvulsant independent of seizure activity. TTX was applied topically onto the cortex in the occipital window 30 minutes before the 4-AP-application. As a result, TTX blocked action potentials, silenced cortical activity, and prevented seizure emergence after 4-AP application. With neurons failing to generate action potentials, seizures were prevented and although 4-AP was applied according to the protocol, no SD was triggered (p = 0.005 4-AP + TTX vs. 4-AP alone, n = 5;  $\chi^2$ ). It was confirmed that TTX did not inhibit SD by remotely eliciting SD with KCl after each recording [135].

## Results

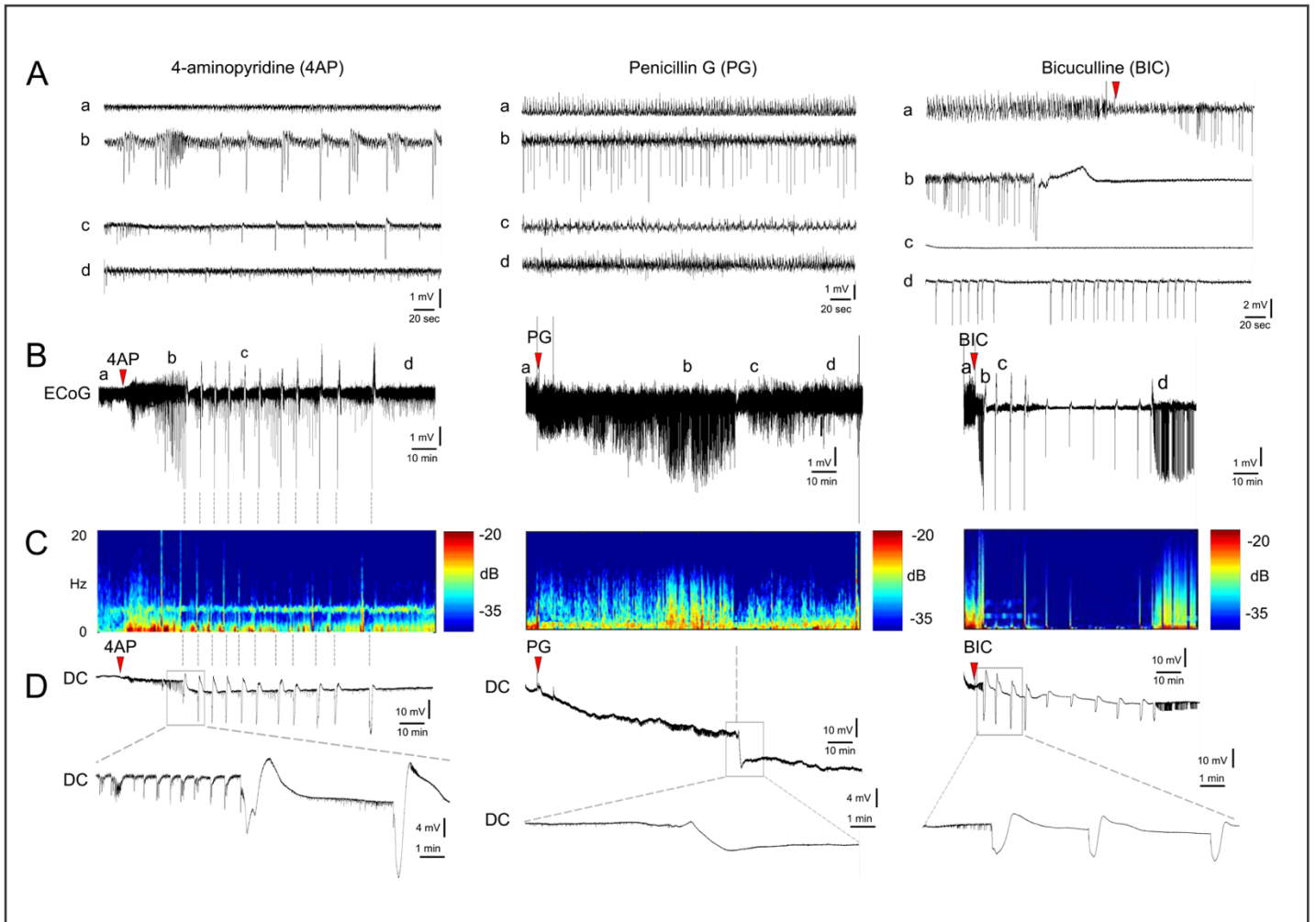


**Figure 3 | Focal cortical seizures trigger spreading depression.**

**A** | “Representative tracings show typical ECoG phases (a–d) of 4-AP, PG, or BIC microseizures, as indicated on the full ECoG timeline (**B**). Red arrowheads show the time of drug application. Vertical dashed lines indicate SDs. **C** | Time–frequency–power spectra of the full timeline shown in **B** calculated using Thomson’s multitaper method. **D** | Corresponding DC tracings show one or more SDs triggered during the seizures as large negative slow potential shifts. Boxes indicate expanded views. These were simultaneously confirmed on IOS as SD waves. A total of 11 spontaneous SDs originated from the 4-AP window starting 23 min after drug application in this animal. PG seizure triggered 1 SD at 134 min and BIC seizure triggered 10 SDs between 3 and 60 min.”

This figure and its legend were published open access under a [CC BY license](https://creativecommons.org/licenses/by/4.0/) (Creative Commons Attribution 4.0 International License) as Tamim, I., Chung, D.Y., de Moraes, A.L., Loonen, I.C.M., Qin, T., Misra, A., Schlunk, F., Endres, M., Schiff, S.J., Ayata, C. Spreading depression as an innate antiseizure mechanism. *Nat. Commun.* 12, 2206 (2021)

## 7.2 Power intensity and spatial extent influence the incidence of SD in the event of a seizure

Because the SD rate was significantly different in the three chemoconvulsants groups, it was essential to identify the determinants responsible for SD triggering.

A comparison of the peak PD in the three frequency bands  $\delta$  (0–4 Hz),  $\theta$  (4–8 Hz), and  $\alpha$  (8–12 Hz) identified the highest increase in the  $\delta$  band within the 4-AP group. Congruently, the greatest SD frequency was observed in the 4-AP cohort. The PD 5 minutes before the first spontaneously triggered SD was subsequently analyzed. For this purpose, the onsets of SDs and the respective power increases in the group without SDs were time-matched. An association between PD increase in the  $\delta$ -frequency band and SD frequency could be established. The PD increases at the remote recording sites were also quantified to further investigate the spatial dynamics of the seizures. Overall, 36% and 26% of the 4-AP treated animals showed epileptiform activity at the anterior ipsilateral and the homotopic contralateral recording site, respectively. Epileptiform activity on the remote recording sites was only observed in animals with triggered SDs ( $n = 9$ ). Mice that developed seizures, which were not interrupted by SDs ( $n = 8$ ) never showed any epileptiform activity on the remote recording sites ( $p = 0.032$ ,  $\chi^2$ ). The relationship between seizure spread (i.e., generalization) and SD occurrence was thus further analyzed.

Because neurovascular coupling leads to changes of CBV during seizure activity, the spatial extent of ictal events across the cortex over time was indirectly measurable via IOS imaging. Hyperemic transients detected with IOS were time-matched to bursting periods on ECoG (Fig. 4A), which allowed the use of CBV measurement as a surrogate for seizure generalization [135]. Five ROIs were set along an LOI that expanded anteriorly (1 mm distance between each ROI) (Fig. 4B), whereby the first ROI was placed in the seizure core. In addition, one ROI was placed homotopically to the focus and one LOI contralaterally to differentiate global CBV alterations from seizure-coupled CBV changes. The CBV was measured within each ROI and along the LOI over time (Fig. 4C), and CBV changes in the focus (ROI 1) were detected in 69% of the animals ( $n = 32$ ) treated with 4-AP. Although seizures were detectable via ECoG, hyperemic transients could not be identified in 31% of these animals, and only 28% showed hyperemic transients on the frontal cortex (ROI 5) (Fig. 4D). Notably, the spatial extent of seizures was most remarkable in animals with one or more triggered



## Results

SDs compared to animals in the non-SD group ( $p = 0.013$ ; Mann-Whitney test, Figs. 4E and F). No animal showed seizure spread to ROI 4 and 5 in the non-SD group. In contrast, 50% and 40% in the SD-group showed spread to ROI 4 and 5, respectively. Altogether, these data indicate that generalization of seizures predicts spontaneous SD occurrence [135].

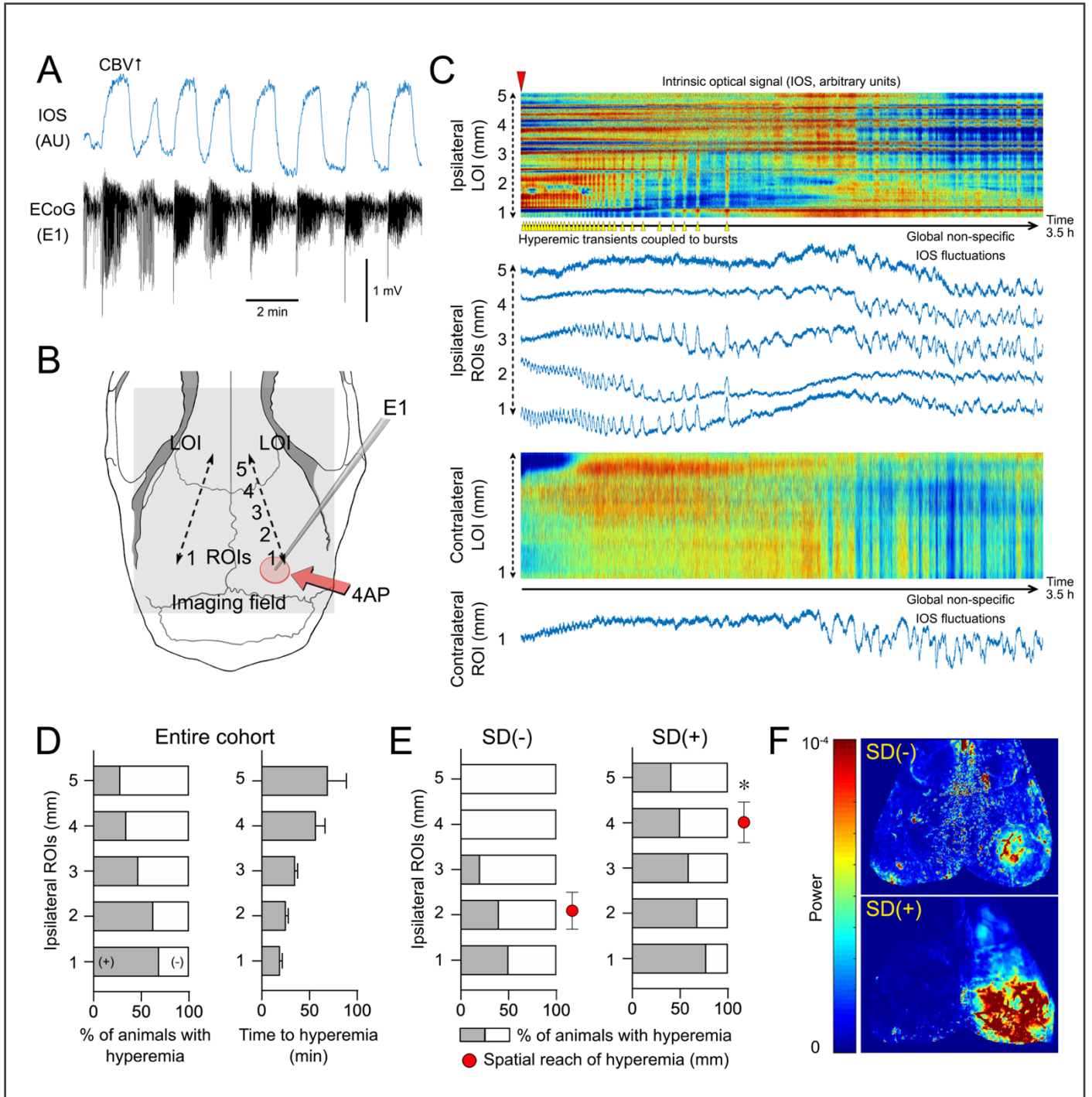


### Figure 4 | Spatial reach of seizures across the cortex predicts SD occurrence.

**A** | “Representative 4-AP experiment shows hyperemia coupled to seizure bursts (AU, arbitrary unit) used as a surrogate to examine the spatial spread of the seizure. **B** | We placed a line of interest (LOI) extending from the drug application site anteriorly on the ipsilateral hemisphere, and one symmetrically on the contralateral hemisphere (dashed lines). Five ROIs (1–5) were placed along with the ipsilateral LOI at 1 mm intervals and a contralateral ROI was placed symmetrically to ipsilateral ROI 1. **C** | IOS intensity along with the two LOIs and in each ROI are plotted over time. Red indicates an increase and blue decreases in CBV. Hyperemic transients (yellow arrowheads) reached ROI 3 within 25 min after 4-AP (red arrowhead) but did not extend to ROI 4 (experiment without SD). Contralateral LOI and ROI did not show hyperemic bursts, indicating a lack of generalization. Non-specific CBV fluctuations (e.g., due to blood pressure), were distinguishable by their global nature and time course. **D** | The proportion of animals that developed hyperemic transients within each ROI and the time of their onset after 4-AP application ( $\pm$ SEM). **E** | Hyperemic transients showed a farther spread in animals that eventually developed an SD. Red circles indicate the average distance hyperemic transients reached from the drug application site in each subgroup ( $*p = 0.012$ , unpaired t-test;  $\pm$ SEM). **F** | Representative CBV power maps show a larger area of cortex with the hyperemic transients in the animal that eventually developed an SD (red high and blue low power).”

This figure and its legend were published open access under a [CC BY license](#) (Creative Commons Attribution 4.0 International License) as Tamim, I., Chung, D.Y., de Moraes, A.L., Loonen, I.C.M., Qin, T., Misra, A., Schlunk, F., Endres, M., Schiff, S.J., Ayata, C. Spreading depression as an innate antiseizure mechanism. *Nat. Commun.* 12, 2206 (2021)

### 7.3 SDs suppress seizure intensity and spread.

Spectrograms of individual experiments suggested a potent antiseizure effect of spontaneously triggered SDs. Therefore, the effect on focal seizures was quantified, and the power time course between the SD- and non-SD groups were compared. Because of their highly variable timing, only the first SDs were examined. Spontaneously triggered SDs substantially decreased seizure severity in the  $\delta$  (0–4 Hz) and  $\theta$  (4–8 Hz) frequency ranges compared to animals that did not show SD ( $p = 0.012$  and  $p = 0.046$ , respectively; two-way ANOVA for repeated measurements). The antiseizure effect was subsequently investigated in a controlled setting. For this purpose, an SD was elicited on the frontal cortex by topical potassium chloride administration at  $37 \pm 3$  minutes after 4-AP,  $19 \pm 0$  minutes after PG, and  $13 \pm 2$  minutes after BIC application (Fig. 5). An abrupt seizure termination was observed

when SDs propagated across the cortex and entered the focus in the 4-AP, PG, and BIC groups. Seizures did not reoccur in the majority of the experiments. Moreover, suppression of seizure power lasted for a minimum of 30 min after SD induction (pre-SD seizure vs. post-SD  $p < 0.05$ – $0.001$ ; two-way ANOVA for repeated measures) (Fig. 5E). Although some animals showed occasional spike activity, the power never reached pre-SD levels. The fact that the epileptogenic agent was not washed off the cortex suggests that SD exerted a long-lasting, strong antiseizure effect [135].

### *Pre-treatment of the cortex with SD suppresses seizure emergence.*

The data thus far strongly demonstrated an acute, strongly suppressing effect on ongoing seizures. Because migraine and epilepsy are chronic disorders, it was examined how long the antiseizure effect of SD lasted. For this purpose, the cortex was pretreated with one remotely induced SD 5 and 30 minutes prior to the application of the chemoconvulsant. Animals were randomized to the SD group after surgical preparation. A single SD at 5 minutes before drug application prevented seizure emergence. An SD induced 30 minutes before the 4-AP application still strongly inhibited the development of epileptic activity, thereby implying that SD exerts a potent effect on seizures that lasts longer than 90 minutes. Moreover, SD exerted a suppressing effect on the whole cortex as no remote recording site showed abnormal ECoG activity [135].

### *SD limits seizure generalization across the cortex*

In the course of these experiments, SD thus showed a strong suppressing effect on regional seizure activity that persisted for a longer period than its typical ECoG silence. Subsequently, the effect of SDs on the generalization of seizures was analyzed. An SD induced 5 or 30 minutes prior and approximately 30 minutes after seizure induction reduced the involvement of distant ROIs. Additionally, the average distance to which hyperemic transients moved was shorter than the control group ( $p = 0.006$  for 4-AP,  $p = 0.010$  for PG, and  $p = 0.016$  for BIC, ordinary one-way ANOVA). Although no SD was induced in the control animals, seizures triggered spontaneous SDs in 22 animals in the 4-AP group, three animals in the PG group, and one in the BIC group. Pretreatment with KCl-induced SD showed the highest effect in preventing generalization, presumably because the onset of SDs influences the capability of the brain tissue to generate further epileptic activity.

## Results

Generalization was further investigated by placing a second electrode in close vicinity to the 4-AP application window. SD was induced from an anterior remote site when the spread of epileptiform activity was detected in this location. The suppressing effect on PD lasted for at least 30 minutes after SD ( $p < 0.001$ , one-way ANOVA). In summary, these data show that seizure generalization triggers SD, which, in turn, prevents the spatial extent of seizures [135].

### *Optogenetically induced SDs exert a similar strong antiseizure effect.*

Exposure of the cortex for application of KCl is an invasive method that can potentially influence SD characteristics. Therefore, it was tested whether non-invasively triggered SDs through intact skull were also capable of suppressing seizures. A single SD induced  $29 \pm 3$  minutes after 4-AP application in ChR2<sup>+</sup> mice significantly reduced seizure intensity in the  $\delta$ - and  $\theta$ - frequency bands compared to animals not treated with an SD ( $n = 10$  and  $n = 8$ , respectively,  $p = 0.01$ , two-way ANOVA). Optogenetic SDs tended to reduce generalization measured by IOS as well. These data confirm that non-invasively triggered SDs are also capable of suppressing seizures [135].

### *Pharmacological blockage of SDs intensifies seizures and facilitates generalization.*

To investigate the dynamics of seizures without the suppressing effect of SDs, SD occurrence was inhibited by intraperitoneal injection of the NMDA receptor blocker MK-801. SD occurred in only 33% of the mice treated with MK-801 ( $n = 12$ ), and MK-801 reduced the SD frequency to  $0.14 \pm 0.06/h$ .

In the group that did not receive MK-801 ( $n = 32$ ), 69% of the animals developed an SD, and the SD frequency was 6.3 fold higher ( $0.89 \pm 0.22/h$ ) compared to that of MK-801-treated mice.

In the MK-801 group, 92% of the animals showed spread to the ipsilateral remote recording site. In addition, 89% of the animals showed generalization to the contralateral recording site. Animals, in which development of spontaneous SDs was not inhibited (i.e., no administration of MK-801), spatial extent of ictal events to the ipsilateral frontal recording site occurred in only 36% and to the contralateral recording site in 26% of the animals. Furthermore, blockage of SD resulted in the increase of PD at the remote recording sites. However, the seizure intensity in the focus itself did not

## Results

differ compared to the controls, thereby suggesting that SD in particular influences seizure generalization. CBV variations coupled to epileptiform activity were used to further investigate generalization. Hyperemic fluctuations (i.e., seizure activity) showed significantly greater expansion in the MK-801 group compared to the control group ( $p = 0.04$ ,  $t$ -test with Welch's correction). In the MK-801 group, ECoG-coupled hyperemic fluctuations in the contralateral ROI occurred more frequently compared to the control group ( $p = 0.001$ ,  $\chi^2$ ). In summary, these data show that the suppression of SD and hence the elimination of the endogenous antiseizure effect facilitates generalization and enhances seizure intensity [135].

### *SDs and seizures in a migraine-relevant mutant mouse model*

The conclusions were supported by a migraine-relevant mutant mouse model (S218L; familial hemiplegic migraine type 1 mutation). As described previously, focal microseizures were chemically generated using 4-AP (100 mM). FHM type1 and their wild-type littermates showed characteristic seizures akin to 4-AP seizures induced in CD1 mice (see above). SD occurred in 88% of the FHM1 mice, whereas only 17% of their wild-type littermates developed SD ( $p = 0.008$ ,  $\chi^2$ ). Congruently, wild-type mice tended to show higher peak power increases in all frequency bands compared to FHM1 mice ( $p = 0.143$ , two-way ANOVA). SDs in FHM1 mice mainly appeared as clusters at a frequency of  $3.0 \pm 0.7$ /h compared to their wild-type littermates with an SD frequency of 1.3 SDs/h and CD1 mice with  $0.9 \pm 0.2$  SDs/h. In contrast to CD1 mice, all SDs except for one entered the seizure focus in the FHM1 group. However, the DC shifts gradually declined, indicating a growing resistance towards SD. Most importantly, spontaneously occurring SDs in FHM1 mice showed a similar suppressing effect on seizures ( $p = 0.002$ , two-way ANOVA for repeated measures) [135].

## Results

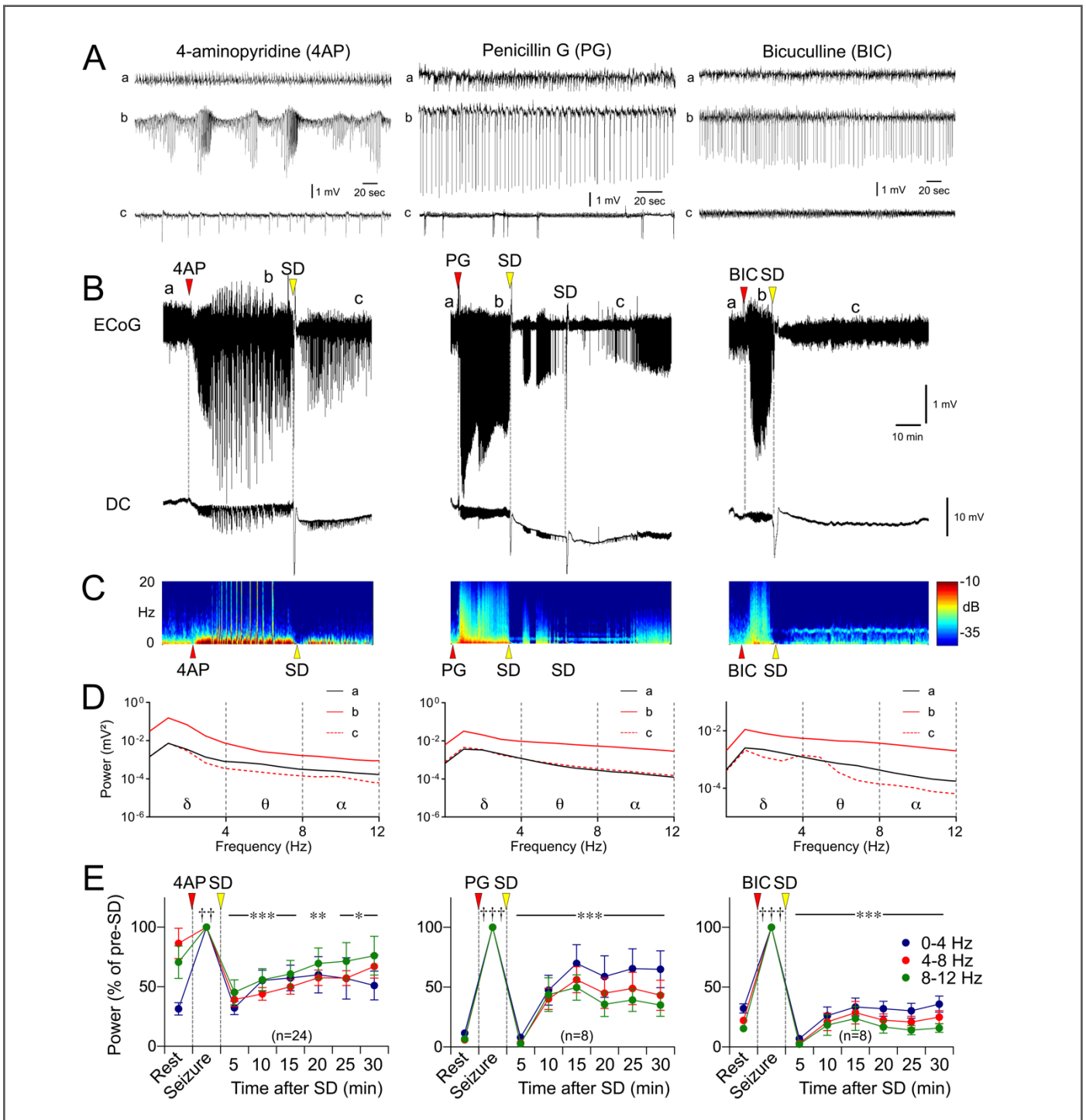


**Figure 5 | Exogenously induced SD terminates focal cortical seizures and limits their reemergence.**

**A** | Representative tracings show ECoG at baseline (a), during 4-AP, PG, or BIC microseizures (b), and after an exogenously induced SD (c), as indicated on the full ECoG timeline (**B**). Recordings are from the drug application site, (E1, Supplementary Fig. 1B, b). Red arrowheads show the time of drug application. Induced SDs (yellow arrowheads) and the abrupt seizure termination are seen on the DC and ECoG tracings, respectively.

## Results

Note that a second SD spontaneously originated from the seizure focus in this PG experiment.

**C** | Time–frequency–power spectra of the full timeline shown in **B** calculated using Thomson’s multitaper method also show an abrupt reduction in seizure power associated with SDs.

**D** | Power density at the three phases (a–c) computed using FFT further demonstrates the lasting seizure power reduction after SD. **E** | Average ECoG power time course in  $\delta$  (0–4 Hz),  $\theta$  (4–8 Hz), and  $\alpha$  (8–12 Hz) frequency bands show ECoG power at rest, during the seizure (5 min prior to SD, and every 5 min thereafter (5–30 min), expressed as % of pre-SD seizure power. All frequency bands show a significant reduction in seizure power for at least 30 min after SD. SD was induced at  $37 \pm 3$  min (13–69) after 4-AP application,  $19 \pm 0$  min (17–20) after PG application, and  $13 \pm 2$  min (10–18) after BIC application (mean  $\pm$  standard error and full range). Sample sizes are shown on the graphs. †††††  $p < 0.05$ – $0.001$  vs. R; \*–\*\*\* $p < 0.05$ – $0.001$  vs. S (two-way ANOVA for repeated measures;  $\pm$ SEM).”

This figure and its legend were published open access under a [CC BY license](#) (Creative Commons Attribution 4.0 International License) as Tamim, I., Chung, D.Y., de Moraes, A.L., Loonen, I.C.M., Qin, T., Misra, A., Schlunk, F., Endres, M., Schiff, S.J., Ayata, C. Spreading depression as an innate antiseizure mechanism. *Nat. Commun.* 12, 2206 (2021).

### Primarily generalized seizures and spontaneously triggered SDs.

To further support our findings, the theory was directly tested in a generalized seizure model. Electrophysiological recordings from the hippocampus CA1 area were obtained after systemic injection of KA (60mg/kg, intraperitoneal in CD1 mice,  $n = 7$ ) (Fig. 2D). All mice developed generalized seizures that gradually evolved within 30–60 minutes upon systemic KA injection. Bursting periods occurred every 1–3 minutes and lasted for 15–60s, respectively. The intervals between bursting periods increased over time, indicating the waning of the drug. Ictal phases were characterized by rhythmic discharges at a 15–30 Hz frequency with a peak amplitude of 300% over baseline. Every animal treated with KA developed hippocampal SD. Most importantly, SD suppressed hippocampal seizures for approximately 30 minutes despite the presence of the highly epileptogenic substance [135].

## 8. Discussion

The study findings show that cortical focal microseizures and generalized seizures in four different pharmacological models readily result in SD. Higher seizure severity is associated with SD as PD increases, and generalization of seizures determines the occurrence of SD. The mutation in a migraine-relevant gene locus can facilitate SD occurrence during seizures. SDs, in turn, interrupt seizures and directly suppress their intensity in the focus for more than 30 minutes when occurring during seizures. Notably, FHM1 mice carrying the S218L mutation typically show more severe forms of seizures (spontaneous generalized seizures, sudden unexpected death during seizures, coma) than the R192Q subtype [122]. Hence, the suppressing effect of SDs and their penetrating character during induced seizures despite the persistence of a pharmacological stimulus is particularly compelling.

Preconditioning with SD inhibits the development of seizures for a minimum of 90 minutes. SD moves across the cortex, whereby the phenomenon employs a wider antiseizure effect and limits the reemergence of seizures. Blocking SDs thus promotes seizure generalization.

Primarily generalized seizures also trigger SDs, which inhibit the seizures detected in the hippocampus for more than 30 minutes. In summary, SD functions as an inherent antiseizure mechanism in both focal and generalized seizure models. Because SD is an important event occurring during brain injury, the phenomenon was conceptualized as a surrogate and contributor of tissue deterioration and metabolic burden. In the present study, SD was triggered by seizures in a model without an injury component or a metabolic compromise, thereby mimicking the hyperexcitable migraine brain.

### 8.1 Clinical applications: Human microseizures as the trigger of SD in migraine brains.

As previously outlined, hyperexcitability and hyperresponsivity in the migraine brain represent a similitude to epileptic seizures. It is reasonable to use these shared trigger mechanisms to propose a theory for SD as an inherent defense mechanism of the central nervous system (Fig. 6). The cortical focal seizure model used simulates human “microseizures” and provides further knowledge on the borderland between migraine and epilepsy.



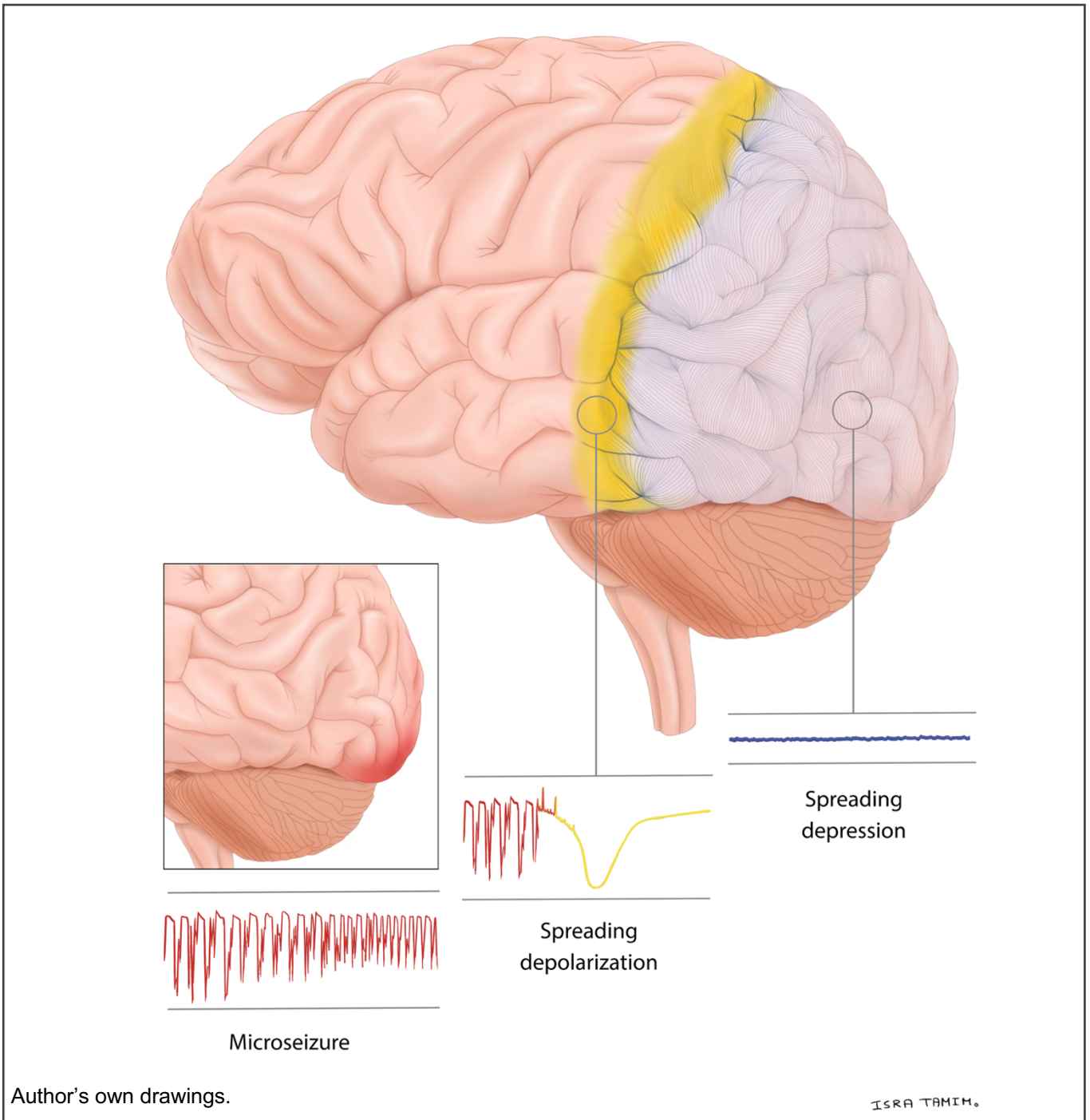


**Figure 6 | Theory: SD suppresses microseizures in migraineurs.**

From left to right: Microseizures in migraineurs develop at a sub-millimeter scale resulting from enhanced cortical excitability. Hyperexcitability (red) triggers spreading depolarization when potassium concentration is raised above the threshold of 12 mM in a sufficient volume of tissue. The depolarization-excitation front (yellow) moves along the hemisphere to exert a wide antiseizure effect. Spreading depolarization is followed by silence of cortical activity (spreading depression, blue). During this process, the formation of a large-scale seizure is prevented and spreading depression manifests as migraine aura.

Clinically overt seizures can begin at sub-millimeter scale hours in advance as microseizures [159] that cannot be probed with the macroelectrodes used in clinical EEG systems. Pathological neuronal clusters can develop at a scale of  $< 1.0 \text{ mm}^3$  after focal KA injection in the hippocampus [160] weeks to months before the occurrence of overt seizures. Interestingly, SD is evoked when a critical volume of  $1.0 \text{ mm}^3$  brain tissue is synchronized [161]. Microseizures can act as multifocal seed events for large-scale seizures by triggering powerful hypersynchronous bursts (Fig. 2) [160, 162-164]. Moreover, they might initiate chronic epilepsy by kindling the brain to develop microdomains of pathologically interconnected neurons. Microseizures have also been observed in normal brains, suggesting that epileptiform activity regularly occurs in healthy tissue. In this hypothesis of ictogenesis, the development of epileptic brain tissue depends on increased connectivity and the number of microdomains generating microseizures that become synchronized as more tissue is recruited. However, it is still unclear what determinants of homeostatic mechanisms are sufficient to restore the equilibrium before a large-scale seizure develops.

SD in migraine might function as a “control reset” or a “rescue mechanism” when a critical size of neuronal clusters in a microdomain is reached, and a large-scale seizure is looming [135]. In this unifying theory of the migraine aura (SD)-seizure continuum, SD quickly terminates the local seizures and exerts a broad antiepileptic effect by propagating along the hemisphere. This study provides further evidence to the theory of hyperexcitability as one of the triggers of aura in migraine.

The results and implications for the migraine aura (SD)-seizure continuum also offer clinical applications for the field. Patients suffering from occipital seizures with complex visual hallucinations and post-ictal headaches make differentiation from migraine with aura difficult. Furthermore, as outlined in the introduction, comorbidity of epileptic syndromes and migraine may further impede proper therapy. Treatment options that target the one upstream event which connects SD and seizures, namely hyperexcitability, might improve the outcome of such intermediate cases. Topiramate and valproate are excellent examples of prophylactic treatment strategies that are regularly used in both fields. The results of this study and scientific background allow the perception of migraine and epilepsy as a family of neurological disorders. Therefore, it is of great value to consider a shared understanding of pathophysiological knowledge in clinical practice. However, further research is needed to determine the exact factors that decide the transition of hyperexcitability to seizures in epilepsy and

to SD in migraine. The present study was limited by the fact that interventions that block SD often also influence seizure dynamics, making the identification of the underlying mechanisms difficult.

## **8.2 The antiseizure effect of SD in other models.**

The interplay between SD and seizures has intrigued neuroscientists since the days of pioneers like Van Harreveld and Stamm in 1954 [165]. They reported a protective effect akin to SD that followed convulsive activity in the rabbit cortex. The antiseizure effect of SDs has now also been reported in many experimental investigations utilizing a variety of seizure models [165-176].

Although seizures and their underlying pathological mechanisms are highly variable, SD showed a strong antiseizure effect in all of these models, indicating that SD is ubiquitous in seizure expression. Similar observations were made in the four different seizure models of the present study. The antiseizure effect in the different models lasted within a range of only a few minutes [177] to 90 minutes [178].

Among the studies describing an antiseizure effect of SD, one modeled genetic absence epilepsy in rats, which aims to generate generalized seizures. Here, a single mechanically-induced SD terminated epileptiform activity (spike-wave discharges) and limited its reemergence for at least 90 minutes [178]. In contrast to the microseizure-SD theory of migraine, seizures in this model were primarily generalized. A migraine aura lasts only 15–20 minutes and is caused by a single SD. This study used a pharmacological seizure model that included a sustained epileptogenic trigger that lasted hours and induced multiple SDs. In the genetic absence model of epilepsy, a single SD was sufficient to limit seizures, thereby adding evidence to the microseizure-SD theory of migraine. Additionally, SD likely exerts an even more potent effect on small-scale seizures than on generalized seizures.

Nevertheless, most previous studies have failed to systematically examine and quantify the suppressing effect of SD on seizures. The research to date has mainly focused on the local effect on seizures, excluding predictors of SD, spatial extent (generalization), preconditioning, and non-invasively triggered SD and the relevance for migraine-mutant mice. Therefore, the data presented in this dissertation add new and compelling evidence on the interplay between SD and seizures. Intriguingly, several studies have reported that SD is easier to initiate in the hyperexcitable brain than a seizure. Cortical penicillin foci have been reported to function as a generator

for spike-triggered SD in rats [179]. The phenomenon of spike-triggered SDs was encountered in several experiments in the present study as well.

In rats, isolated epileptiform spikes that develop 1 minute after systemic pentylenetetrazol injection reliably induced bilateral SD in the cortex and thalamus [180]. SD can be induced by a low-intensity electroshock stimulus and prevent behavioral convulsions [181]. Moreover, minimal disinhibition with a low concentration of the GABA<sub>A</sub>-receptor blocker bicuculline can induce SD [182]. However, it remains challenging to explain the neurobiological mechanisms underlying the suppressing effect of SDs on seizures. It was proposed that the transition of epileptic seizures to SD is associated with cell swelling and contraction related to osmotic pressure caused by alterations in potassium concentration. It is thus proposed that seizures and SD are involved in the continuum of the neuronal membrane and its microenvironment. Epileptiform activity is promoted if brain cells are exposed to an environment of hypoosmolarity with the resulting reduction of extracellular space [183].

In contrast, hyperosmolarity and increasing extracellular space suppress excitability and can lead to SD. Therefore, potassium concentrations between 8–12 mM promote seizure activity, whereas concentrations above 12 mM are more likely to result in SD [183]. A study showed that potassium accumulation reduces the amplitude and the number of action potentials after hyperpolarization, which could explain SD's suppressing effect on seizures. When potassium is driven into the extracellular space, the net loss of transmembrane potassium-current increases the duration needed for repolarization. Lower levels of repolarization result in a reduced membrane potential difference, which causes the inactivation of voltage-gated sodium channels whose inactivation curve is localized near the membrane resting potential. As a result, action potentials are suppressed, and the development of a full-grown seizure becomes unlikely [184]. Therefore, a transition to states of SD or seizures is potentially dependent on potassium levels that modify brain excitability.

### **8.3 Potential beneficial effects of SD.**

A recent study suggests that seizure-triggered SD is initiated in the superficial layers of the cortex and that seizure suppression is restricted to layers penetrated by SD [171]. Although the exact cortical layer to which SD and seizures reached was not identified in the present study, it was observed that the number of non-penetrating SDs increased over time, suggesting growing tissue resistance towards SD. Kindling is a

process by which healthy tissue gradually evolves into epileptic tissue. Repeated seizures result in a longer duration of subsequent seizures and more intensive behavioral involvement during this process. Both developments suggest a weakening of the homeostatic mechanisms or the growing resistance of the tissue towards these mechanisms and the increasing recruitment of neuronal clusters [185].

The continuous presence of the epileptogenic agents (KA systemically and 4-AP, PG, and BIC directly on the cortex) created an epileptogenic model that lasted for hours. It might have gradually created pathways of kindling mechanisms (e.g., modulated gene expression), resulting in enhanced susceptibility of the cortex towards seizures. Moreover, repetitive SDs might result in the suppression of GABAergic function [186] and enhanced excitability. Furthermore, *in vitro* studies have demonstrated that chronic epileptic tissue of humans and animals can become resistant towards SD [158, 180, 182]. In contrast, a separate model of chronic epilepsy demonstrated that diazepam therapy might overcome SD resistance [3, 187].

For this reason, the quantification of PD was restricted to the first SD. Nevertheless, epileptiform activity in the healthy brain without injury (e.g., in migraine) likely culminates in a single SD, resulting in inhibition. The latter manifests as a single migraine aura. However, in chronic migraine (> 15 migraine attacks per month), cortical inhibition can be impaired in comparison to episodic migraine [89].

Some may argue that SD occurrence may be related to the beginning of tissue deterioration in the present study. However, timelines showing the onset of SD suggest that this is unlikely. Many first SDs occurred only a few minutes after the beginning of seizures when the tissue was still healthy. Additionally, because of the continuous epileptic stimulus that topically applied chemoconvulsants represent, tissue was still capable of generating seizures several hours after SD onset. However, we did not perform an analysis of histology or immunohistochemistry on rodent brains to quantify cell death, and our conclusion concerning SD as a fundamental defense mechanism is thus not based on the degree of tissue injury. This is certainly a limitation of the study design. Nevertheless, it is assumed that suppression of seizures and their generalization must be beneficial in terms of acute survival advantage. Seizures, particularly when they spatially extend to generalized seizures, can be terminal when the patient loses consciousness.

Moreover, convulsions can cause physical injuries to the body, and prolonged status epilepticus can lead to irreversible neuronal loss and post-ictal encephalopathy. SD,

on the other hand, is viewed as a benign and self-limiting event [3] when it occurs in adequately supplied tissue, as was the case in the present study (i.e., in migraine) [188]. On the contrary, measurements of perfusion and oximetry dynamics during ictal discharges raise the question of whether the development of chronic epilepsy may pose a significant metabolic burden on brain tissue in the long run as progressive cognitive decline in some types of epilepsy could be caused by repetitive focal hypoxia. For instance, epileptic events induced by 4-AP have been shown to cause hypermetabolic increases of CBF in the seizure focus. Due to neurovascular coupling, vasodilatation in the focus accompanied by vasoconstriction in the surrounding tissue contributes to blood shunting from the adjacent surrounding tissue leading to brief focal ischemia [155, 156]. We observed similar increases of CBV in the seizure focus using IOS and used them as an indicator for seizure generalization. The CBV increases in the ROIs mainly diminished after SD occurrence.

Moreover, when SD was induced 30 to 5 minutes before the seizure, CBV alterations decreased to an absolute minimum. Although still highly theoretical at this stage, it is possible that SD plays a significant role in preventing repetitive focal ischemia due to multifocal microseizures in migraine brains. Notably, geometrical models of the thermodynamics of spreading depolarization and epileptiform activity characterize spreading depolarization as a more severe pathology in terms of energy burden [189]. However, although one would consequently conclude that migraine is a disorder associated with brain damage, patients nevertheless do not suffer from persistent neurological deficits after migraine attacks, except for rare migrainous infarcts. Therefore, it is justified to assume that SD can be fully reversible under normoxic conditions except when occurring in the brainstem [23, 124, 147]. Of course, in scenarios of metabolic compromise, SD signifies an energy-demand mismatch and can delay recovery.

#### **8.4 SD and seizures after brain injury: post-traumatic epilepsy and migraine**

There is a considerable amount of evidence that head trauma is causally associated with migraine and epileptic seizures. Heightened neuronal excitation after mild head trauma may be mechanically induced due to tissue shearing [190]. Increased concentrations of excitatory neurotransmitters such as glutamate and blood-brain barrier disruption might contribute to higher seizure susceptibility and development of post-traumatic epilepsy even at low levels of traumatic brain injury [191-193].

Congruently, about 10% of patients suffering from traumatic brain injury develop early seizures within a week following the incident, while post-traumatic epilepsy occurs in 2% of the patients [194, 195].

The interplay of spreading depolarization and seizures in trauma is highly complex, and the severity of injury must be taken into account to evaluate consequences. As shown by subdural recordings, SD and seizures co-occur in individuals with severe acute brain damage. In about 10% of the patients, seizures culminated in SD, which, in turn, interrupted the seizure [196]. SDs are linked with delayed cerebral ischemia and gradual tissue damage due to the increased metabolic load after such severe trauma [197-199]. Clusters of extended SDs with persistent depression were linked with substantially longer spreading ischemia than those associated with single spreading depolarizations [200]. Interestingly, patients who developed SDs early after trauma were more likely to develop late epilepsy [201]. Clusters of SDs may result in selective inhibition of GABAergic activity after severe brain damage [3, 186], leading to a disrupted balance of cortical excitability. SDs, in turn, can present with subsequent spreading convulsions rather than spreading depression [201, 202]. Moreover, the occurrence of several ictal-interictal continuum abnormalities (IICA) was linked to SDs and seizures as continuous EEG has become a standard tool in neurologic intensive care units.

After brain injury, the synaptic transmission may be the first process to fail [203], leading to the initiation of an avalanche reinforcing the metabolic burden on brain tissue. The resulting disinhibition might facilitate the generation of IICA or seizures, which eventually trigger SD. It is difficult to discern the causes of SD and seizure occurrence in severe brain injury. While SD and seizures can be triggered independently by the underlying injury, seizures can also culminate in SDs. Although SD might extinguish or shorten the duration of IICA and seizures [173], it does not resolve the underlying disease and intensifies the critical metabolic situation.

Intriguingly, trivial head trauma (e.g., heading a soccer ball without a subsequent loss of consciousness) has repeatedly been associated with new-onset migraine, which is sometimes referred to as “footballer’s migraine” [191, 204] and trauma on the occipital cortex, a location known to be particularly susceptible to SD, is most likely to be followed by migraine symptoms in children and young adults [205, 206]. Furthermore, post-traumatic headache frequency can efficiently be treated by amitriptyline and

propranolol, which also suppress SD [63, 207]. Notably, seizures and migraine attacks are common after head trauma in FHM patients [208].

In these cases, migraine symptoms start within a time window ranging from 1 min to 4 hours. Only a few patients report unprovoked attacks in the sense of a new-onset chronic migraine indicating permanent alterations to brain excitability after trauma. Typically, migraine attacks only occur after trauma, suggesting that concussion mechanically triggers heightened brain excitation leading to induction of SD [191]. Therefore, in trivial head trauma, SD could prevent a full-grown seizure due to mechanically induced hyperexcitability. Of course, SD accelerates metabolic demand after trauma, although the young age of the reported patient group and low-level injury might be capable of meeting the increased demand and does not delay recovery. A migraine aura accompanied by headache is clearly beneficial in terms of survival advantage compared to losing consciousness during generalized seizures.



## 9. Conclusions

This study unequivocally showed that SD acts as an endogenous antiseizure mechanism in the rodent brain. Neocortical microseizures and generalized seizures trigger SDs, which in turn terminate the seizure, prevent seizure generalization, and limit seizure recurrence. Starting from the seizure focus, SD then extends over the cortex to provide a wider antiseizure effect. Employment of optogenetics and migraine mutant mice further supports these conclusions. SD appears to be a reliable response to heightened excitability in the brain. Epilepsy and migraine are episodic, chronic disorders sharing a genetic basis, similar triggers, pharmacological interventions, and clinical features. Subspecialists must learn how to differentiate both conditions, in particular concerning occipital symptoms.

SD undoubtedly represents a linking phenomenon in the borderland of both diseases, and SD that is induced by hyperexcitability of the cortex might underly a subgroup of migraine auras. Prevention of a large-scale seizure or status epilepticus at the cost of a headache is preferable in terms of survival advantage. It is possible that potassium concentrations in the extracellular space and resulting altered cell volume are responsible for determining the transition from hyperexcitability to seizures or SD. The energy state of the tissue is crucial for the consequences that follow network phenomena such as SD and seizures and must be taken into account when characterizing their role in neurological diseases.

The work presented in this study can become the cornerstone of a novel unified theory of SD with a more balanced view of its beneficial and hazardous effects. Furthermore, the data open a new direction of research into the molecular mechanisms of this antiepileptic effect in search of more nuanced pathophysiological concepts and novel therapies.

## 10. References

1. Gowers, W.R., *Clinical Lectures ON THE BORDERLAND OF EPILEPSY. III.—MIGRAINE*. BMJ, 1906. **2**(2397): p. 1617–1622.
2. Pietrobon, D. and M.A. Moskowitz, *Chaos and commotion in the wake of cortical spreading depression and spreading depolarizations*. Nat. Rev. Neurosci., 2014. **15**(6): p. 379–393.
3. Tamim, I., *Seizures versus Cortical Spreading Depolarization – Implications for Migraine with Aura and Epilepsy*. 2020, Charité Universitätsmedizin Berlin.
4. Spong, K.E., R.D. Andrew, and R.M. Robertson, *Mechanisms of spreading depolarization in vertebrate and insect central nervous systems*. J. Neurophysiol., 2016. **116**(3): p. 1117–1127.
5. Karatas, H., S.E. Erdener, Y. Gursoy-Ozdemir, S. Lule, E. Eren-Koçak, Z.D. Sen, and T. Dalkara, *Spreading depression triggers headache by activating neuronal Panx1 channels*. Science, 2013. **339**(6123): p. 1092–1095.
6. Rogawski, M.A., *Migraine and Epilepsy—Shared Mechanisms within the Family of Episodic Disorders*, in *Jasper's Basic Mechanisms of the Epilepsies*, J.L. Noebels, et al., Editors. 2012: Bethesda (MD). 2012.
7. Collaborators, G.H., *Global, regional, and national burden of migraine and tension-type headache, 1990-2016: a systematic analysis for the Global Burden of Disease Study 2016*. Lancet Neurol., 2018. **17**(11): p. 954–976.
8. Lipton, R.B. and M.E. Bigal, *Migraine: epidemiology, impact, and risk factors for progression*. Headache, 2005. **45 Suppl 1**: p. S3–S13.
9. Schwedt, T.J., *Chronic migraine*. BMJ, 2014. **348**: p. 1416.
10. Hauser, W.A., J.F. Annegers, and L.T. Kurland, *Prevalence of epilepsy in Rochester, Minnesota: 1940–1980*. Epilepsia, 1991. **32**(4): p. 429–445.
11. Ottman, R. and R.B. Lipton, *Comorbidity of migraine and epilepsy*. Neurology, 1994. **44**(11): p. 2105–2110.
12. Haut, S.H., M.E. Bigal, and R.B. Lipton, *Chronic disorders with episodic manifestations— focus on epilepsy and migraine*. Lancet Neurol., 2006. **5**(2): p. 148–157.
13. Andermann, F., *Migraine–epilepsy relationships*. Epilepsy Res., 1987. **1**(4): p. 213–226.

## References

14. Toldo, I., E. Perissinotto, F. Menegazzo, C. Boniver, S. Sartori, L. Salviati, M. Clementi, P. Montagna, and P.A. Battistella, *Comorbidity between headache and epilepsy in a pediatric headache center*. *J. Headache Pain*, 2010. **11**(3): p. 235–240.
15. Leveing, E., *On Megrin, Sick-Headache, and Some Allied Disorders, a Contribution to the Pathology*. *Ind. Med. Gaz.*, 1873. **8**(11): p. 305–306.
16. Rajna, P., B. Clemens, E. Csibri, E. Dobos, A. Geregely, M. Gottschal, I. György, A. Horváth, F. Horváth, L. Mezöfi, I. Velkey, J. Veres, and E. Wagner, *Hungarian multicentre epidemiologic study of the warning and initial symptoms (prodrome, aura) of epileptic seizures*. *Seizure*, 1997. **6**(5): p. 361–368.
17. Wolff, H.G., *Headache and other head pain*. Vol. 2nd ed. New York. 1963: Oxford University Press.
18. Olesen, J., L. Friberg, T.S. Olsen, H.K. Iversen, N.A. Lassen, A.R. Andersen, and A. Karle, *Timing and topography of cerebral blood flow, aura, and headache during migraine attacks*. *Ann. Neurol.*, 1990. **28**(6): p. 791–798.
19. Schoonman, G.G., J. van der Grond, C. Kortmann, R.J. van der Geest, G.M. Terwindt, and M.D. Ferrari, *Migraine headache is not associated with cerebral or meningeal vasodilatation—a 3T magnetic resonance angiography study*. *Brain*, 2008. **131**(Pt 8): p. 2192–2200.
20. Ayata, C. and M. Lauritzen, *Spreading Depression, Spreading Depolarizations, and the Cerebral Vasculature*. *Physiol. Rev.*, 2015. **95**(3): p. 953–993.
21. Leao, A., *Spreading depression of activity in the cerebral cortex*. *J Neurophysiol*, 1944. **7**: p. 359–390.
22. Rogawski, M.A., *Common Pathophysiologic Mechanisms in Migraine and Epilepsy*. *Arch Neurol.*, 2008. **65**(6): p. 709–714.
23. Dreier, J.P., *The role of spreading depression, spreading depolarization and spreading ischemia in neurological disease*. *Nat. Med.*, 2011. **17**(4): p. 439–447.
24. Nedergaard, M., A.J. Cooper, and S.A. Goldman, *Gap junctions are required for the propagation of spreading depression*. *J. Neurobiol.*, 1995. **28**(4): p. 433–444.

## References

25. Matsuura, T. and J. Bures, *The minimum volume of depolarized neural tissue required for triggering cortical spreading depression in rat.* . Exp. Brain Res., 1971. **12**(3): p. 238–249.
26. Grafstein, B., *Mechanism of spreading cortical depression.* J. Neurophysiol., 1956. **19**(2): p. 154–171.
27. Vinogradova, L.V., *Comparative potency of sensory-induced brainstem activation to trigger spreading depression and seizures in the cortex of awake rats: Implications for the pathophysiology of migraine aura.* Cephalalgia, 2015. **35**(11): p. 979–986.
28. Strong, A.J., M. Fabricius, M.G. Boutelle, S.J. Hibbins, S.E. Hopwood, R. Jones, M.C. Parkin, and M. Lauritzen, *Spreading and synchronous depressions of cortical activity in acutely injured human brain.* Stroke, 2002. **33**(12): p. 2738–2743.
29. Bere, Z., T.P. Obrenovitch, G. Kozák, F. Bari, and E. Farkas, *Imaging reveals the focal area of spreading depolarizations and a variety of hemodynamic responses in a rat microembolic stroke model.* J. Cereb. Blood Flow Metab., 2014. **34**(10): p. 1695–1705.
30. Hansen, A.J. and T. Zeuthen, *Extracellular ion concentrations during spreading depression and ischemia in the rat brain cortex.* Acta Physiol. Scand., 1981. **113**(4): p. 437–445.
31. Lothman, E., J. Lamanna, G. Cordingley, M. Rosenthal, and G. Somjen, *Responses of electrical potential, potassium levels, and oxidative metabolic activity of the cerebral neocortex of cats.* Brain Res., 1975. **88**(1): p. 15–36.
32. Kraig, R.P. and C. Nicholson, *Extracellular ionic variations during spreading depression.* Neuroscience, 1978. **3**(11): p. 1045–1059.
33. Molchanova, S., P. Kööbi, S.S. Oja, and P. Saransaari, *Interstitial concentrations of amino acids in the rat striatum during global forebrain ischemia and potassium-evoked spreading depression.* Neurochem. Res., 2004. **29**(8): p. 1519–1527.
34. Fabricius, M., L.H. Jensen, and M. Lauritzen, *Microdialysis of interstitial amino acids during spreading depression and anoxic depolarization in rat neocortex.* Brain Res., 1993. **612**(1-2): p. 61–69.

## References

35. Wendt, S., E. Wogram, L. Korvers, and H. Kettenmann, *Experimental Cortical Spreading Depression Induces NMDA Receptor Dependent Potassium Currents in Microglia*. J. Neurosci., 2016. **36**(23): p. 6165–6174.
36. Tuttle, A., J. Riera Diaz, and Y. Mori, *A computational study on the role of glutamate and NMDA receptors on cortical spreading depression using a multidomain electrodiffusion model*. PLoS Comput Biol, 2019. **15**(12): p. e1007455.
37. Larrosa, B., J. Pastor, L. Lopez-Aguado, and O. Herreras, *A role for glutamate and glia in the fast network oscillations preceding spreading depression*. Neuroscience, 2006. **141**(2): p. 1057–1068.
38. Tobiasz, C. and C. Nicholson, *Tetrodotoxin resistant propagation and extracellular sodium changes during spreading depression in rat cerebellum*. Brain Res., 1982. **241**(2): p. 329–333.
39. Sugaya, E., M. Takato, and Y. Noda, *Neuronal and glial activity during spreading depression in cerebral cortex of cat*. J. Neurophysiol., 1975. **38**(4): p. 822–841.
40. Rogawski, M.A., *Revisiting AMPA receptors as an antiepileptic drug target*. Epilepsy Curr., 2011. **11**(2): p. 56–63.
41. Fisher, R.S., W. van Emde Boas, W. Blume, C. Elger, P. Genton, P. Lee, and J. Engel, Jr., *Epileptic seizures and epilepsy: definitions proposed by the International League Against Epilepsy (ILAE) and the International Bureau for Epilepsy (IBE)*. Epilepsia, 2005. **46**(4): p. 470–472.
42. John, S.D., W.S. Josemir, M.S. Sanjay, and C.W. Matthew, *Adult epilepsy*. The Lancet, 2006. **367**(9516): p. 1087–1100.
43. Trevelyan, A.J., D. Sussillo, and R. Yuste, *Feedforward inhibition contributes to the control of epileptiform propagation speed*. J. Neurosci., 2007. **27**(13): p. 3383–3387.
44. Trevelyan, A.J., D. Sussillo, B.O. Watson, and R. Yuste, *Modular Propagation of Epileptiform Activity: Evidence for an Inhibitory Veto in Neocortex*. J. Neurosci., 2006. **26**(48): p. 12447-12455.
45. Wong, B.Y. and D.A. Prince, *The lateral spread of ictal discharges in neocortical brain slices*. Epilepsy Res., 1990. **7**(1): p. 29–39.
46. Van Dongen, R.M. and J. Haan. *Symptoms related to the visual system in migraine*. F1000Res 2019 30.07.2019 [cited 2021 01.09.2021].

## References

47. Lashley, K., *Patterns of cerebral integration indicated by the scotomas of migraine*. Arch. Neurol. Psychiatry, 1941. **46**: p. 331–339.
48. Milner, P.M., *Note on a possible correspondence between the scotomas of migraine and spreading depression of Leao*. Electroencephalogr. Clin. Neurophysiol., 1958. **10**: p. 705.
49. Russell, M.B. and J. Olesen, *A nosographic analysis of the migraine aura in a general population*. Brain, 1996. **119** p. 355–361.
50. Lauritzen, M., *Pathophysiology of the migraine aura. The spreading depression theory*. Brain, 1994. **117**: p. 199-210.
51. Cao, Y., K.M.A. Welch, S. Aurora, and E.M. Vikingstad, *Functional MRI-BOLD of visually triggered Headache in Patients with Migraine*. Arch. Neurology, 1999. **56**: p. 548–554.
52. Hadjikhani, N., M. Sanchez Del Rio, O. Wu, D. Schwartz, D. Bakker, B. Fischl, K.K. Kwong, F.M. Cutrer, B.R. Rosen, R.B. Tootell, A.G. Sorensen, and M.A. Moskowitz, *Mechanisms of migraine aura revealed by functional MRI in human visual cortex*. Proc. Natl. Acad. Sci. USA, 2001. **98**(8): p. 4687-4692.
53. Lauritzen, M., A.J. Hansen, D. Kronborg, and T. Wieloch, *Cortical spreading depression is associated with arachidonic acid accumulation and preservation of energy charge*. J Cereb Blood Flow Metab, 1990. **10**(1): p. 115-22.
54. Read, S.J., M.I. Smith, A.J. Hunter, and A.A. Parsons, *The dynamics of nitric oxide release measured directly and in real time following repeated waves of cortical spreading depression in the anaesthetised cat*. Neurosci. Lett., 1997. **232**(3): p. 127–130.
55. Zhang, X., D. Levy, R. Nosedá, V. Kainz, M. Jakubowski, and R. Burstein, *Activation of meningeal nociceptors by cortical spreading depression: implications for migraine with aura*. J. Neurosci., 2010. **30**(26): p. 8807–8814.
56. Bolay, H., U. Reuter, A.K. Dunn, Z. Huang, D.A. Boas, and M.A. Moskowitz, *Intrinsic brain activity triggers trigeminal meningeal afferents in a migraine model*. Nat. Med., 2002. **8**(2): p. 136–142.
57. Bowyer, S.M., K.S. Aurora, J.E. Moran, N. Tepley, and K.M. Welch, *Magnetoencephalographic fields from patients with spontaneous and induced migraine aura*. Ann. Neurol., 2001. **50**(5): p. 582–587.
58. Major, S., S. Huo, C.L. Lemale, E. Siebert, D. Milakara, J. Woitzik, K. Gertz, and J.P. Dreier, *Direct electrophysiological evidence that spreading*

## References

- depolarization-induced spreading depression is the pathophysiological correlate of the migraine aura and a review of the spreading depolarization continuum of acute neuronal mass injury.* GeroScience, 2020. **42**(1): p. 57–80.
59. Harriott, A.M., T. Takizawa, D.Y. Chung, and S.P. Chen, *Spreading depression as a preclinical model of migraine.* J. Headache Pain, 2019. **20**(1): p. 45.
60. Kelman, L., *The aura: a tertiary care study of 952 migraine patients.* Cephalalgia, 2004. **24**(9): p. 728–734.
61. Viana, M., G. Sances, M. Linde, N. Ghiotto, E. Guaschino, M. Allena, S. Terrazzino, G. Nappi, P.J. Goadsby, and C. Tassorelli, *Clinical features of migraine aura: Results from a prospective diary-aided study.* Cephalalgia, 2017. **37**(10): p. 979–989.
62. Hansen, J.M., S.M. Baca, P. Vanvalkenburgh, and A. Charles, *Distinctive anatomical and physiological features of migraine aura revealed by 18 years of recording.* Brain, 2013. **136**(Pt 12): p. 3589–3595.
63. Ayata, C., H. Jin, C. Kudo, T. Dalkara, and M.A. Moskowitz, *Suppression of cortical spreading depression in migraine prophylaxis.* Ann. Neurol., 2006. **59**(4): p. 652–661.
64. Wang, X.Q., S.Y. Lang, X. Zhang, F. Zhu, M. Wan, X.B. Shi, Y.F. Ma, and S.Y. Yu, *Clinical factors associated with postictal headache in Chinese patients with partial epilepsy.* Seizure, 2014. **23**(3): p. 191–195.
65. Ito, M., Adachi, N., Nakamura, F., Koyama, T., Okamura, T., Kato, M., Kanemoto, K., Nakano, T., Matsuura, M., & Hara, S., *Characteristics of postictal headache in patients with partial epilepsy.* Cephalalgia, 2004. **24**(1): p. 23-28.
66. Panayiotopoulos, C.P., *Benign childhood epilepsy with occipital paroxysms: a 15-year prospective study.* Ann. Neurol., 1989. **26**(1): p. 51–56.
67. Panayiotopoulos, C.P., *Difficulties in Differentiating Migraine and Epilepsy, in Migraine and Epilepsy, F. Andermann and E. Lugaresi, Editors.* 1987, Butterworth Publishers. p. 31–45.
68. Shahar, E. and S. Barak, *Favorable outcome of epileptic blindness in children.* J. Child Neurol., 2003. **18**(1): p. 12–16.

## References

69. Martins da Silva, A. and B. Leal, *Photosensitivity and epilepsy: Current concepts and perspectives—A narrative review*. *Seizure*, 2017. **50**: p. 209–218.
70. Panayiotopoulos, C.P., *Elementary visual hallucinations, blindness, and headache in idiopathic occipital epilepsy: differentiation from migraine*. *J. Neurol. Neurosurg. Psychiatry*, 1999. **66**(4): p. 536–540.
71. Pantelakis, S.N., B.D. Bower, and H.D. Jones, *Convulsions and television viewing*. *Br. Med. J.*, 1962. **2**(5305): p. 633–638.
72. Enoki, H., T. Akiyama, J. Hattori, and E. Oka, *Photosensitive fits elicited by TV animation: an electroencephalographic study*. *Acta Paediatr. Jpn.*, 1998. **40**(6): p. 626–630.
73. Kasteleijn-Nolst Trenité, D.G., R. Guerrini, C.D. Binnie, and P. Genton, *Visual sensitivity and epilepsy: a proposed terminology and classification for clinical and EEG phenomenology*. *Epilepsia*, 2001. **42**(5): p. 692–701.
74. Naquet, R., L. Fegersten, and J. Bert, *Seizure discharges localized to the posterior cerebral regions in man, provoked by intermittent photic stimulation*. *Electroencephalogr. Clin. Neurophysiol.*, 1960. **12**: p. 305–316.
75. Guerrini, R. and P. Genton, *Epileptic syndromes and visually induced seizures*. *Epilepsia*, 2004. **45 Suppl 1**: p. 14–18.
76. Walker, M.C., S.J. Smith, S.M. Sisodiya, and S.D. Shorvon, *Case of simple partial status epilepticus in occipital lobe epilepsy misdiagnosed as migraine: clinical, electrophysiological, and magnetic resonance imaging characteristics*. *Epilepsia*, 1995. **36**(12): p. 1233–1236.
77. Schoenen, J., W. Wang, A. Albert, and P.J. Delwaide, *Potentiation instead of habituation characterizes visual evoked potentials in migraine patients between attacks*. *Eur. J. Neurol.*, 1995. **2**(2): p. 115–122.
78. Marcus, D.A. and M.J. Soso, *Migraine and stripe-induced visual discomfort*. *Arch. Neurol.*, 1989. **46**(10): p. 1129–1132.
79. Kropp, P. and W.D. Gerber, *Prediction of migraine attacks using a slow cortical potential, the contingent negative variation*. *Neurosci. Lett.*, 1998. **257**(2): p. 73–76.
80. Coppola, G., F. Pierelli, and J. Schoenen, *Is The Cerebral Cortex Hyperexcitable or Hyperresponsive in Migraine?* *Cephalalgia*, 2007. **27**(12): p. 1427–1439.



## References

81. Siniatchkin, M., N. Averkina, F. Andrasik, U. Stephani, and W.D. Gerber, *Neurophysiological reactivity before a migraine attack*. *Neurosci. Lett.*, 2006. **400**(1-2): p. 121–124.
82. Wang, W., M. Timsit-Berthier, and J. Schoenen, *Intensity dependence of auditory evoked potentials is pronounced in migraine: an indication of cortical potentiation and low serotonergic neurotransmission?* *Neurology*, 1996. **46**(5): p. 1404–1409.
83. Ambrosini, A., P. Rossi, V. De Pasqua, F. Pierelli, and J. Schoenen, *Lack of habituation causes high intensity dependence of auditory evoked cortical potentials in migraine*. *Brain*, 2003. **126**(Pt 9): p. 2009–2015.
84. Ozkul, Y. and A. Uckardes, *Median nerve somatosensory evoked potentials in migraine*. *Eur. J. Neurol.*, 2002. **9**(3): p. 227–232.
85. Aurora, S.K., B.K. Ahmad, K.M.A. Welch, P. Bhardhwaj, and N.M. Ramadan, *Transcranial magnetic stimulation confirms hyperexcitability of occipital cortex in migraine*. *Neurology*, 1998. **50**: p. 1111–1114.
86. Mulleners, W.M., E.P. Chronicle, J.E. Palmer, P.J. Koehler, and J.W. Vredeveld, *Visual cortex excitability in migraineurs*. *Headache*, 2001. **41**(6): p. 565-572.
87. Van der Kamp, W., A. Maassen Van Den Brink, M.D. Ferrari, and J. Gert van Dijk, *Interictal hyperexcitability in migraine patients demonstrated with transcranial magnetic stimulation*. *J. Neurol. Sci.*, 1996. **139**: p. 106–110.
88. Young, W., J. Shaw, M. Bloom, and C. Gebeline-Myers, *Correlation of increase in phosphene threshold with reduction of migraine frequency: observation of levetiracetam-treated subjects*. *Headache*, 2008. **48**(10): p. 1490–1498.
89. Aurora, S.K., P. Barrodale, E.P. Chronicle, and W.M. Mulleners, *Cortical inhibition is reduced in chronic and episodic migraine and demonstrates a spectrum of illness*. *Headache*, 2005. **45**(5): p. 546–452.
90. Mulleners, W.M., E.P. Chronicle, J.W. Vredeveld, and P.J. Koehler, *Visual cortex excitability in migraine before and after valproate prophylaxis: a pilot study using TMS*. *Eur. J. Neurol.*, 2002. **9**(1): p. 35–40.
91. Palermo, A., B. Fierro, G. Giglia, G. Cosentino, A.R. Puma, and F. Brighina, *Modulation of visual cortex excitability in migraine with aura: effects of valproate therapy*. *Neurosci. Lett.*, 2009. **467**(1): p. 26–29.

## References

92. Joëls, M., *Stress, the hippocampus, and epilepsy*. *Epilepsia*, 2009. **50**(4): p. 586–597.
93. Yapici-Eser, H., B. Donmez-Demir, K. Kilic, E. Eren-Kocak, and T. Dalkara, *Stress modulates cortical excitability via alpha-2 adrenergic and glucocorticoid receptors: As assessed by spreading depression*. *Exp. Neurol.*, 2018. **307**: p. 45–51.
94. Shyti, R., K. Eikermann-Haerter, S.H. van Heiningen, O.C. Meijer, C. Ayata, M. Joëls, M.D. Ferrari, A.M. van den Maagdenberg, and E.A. Tolner, *Stress hormone corticosterone enhances susceptibility to cortical spreading depression in familial hemiplegic migraine type 1 mutant mice*. *Exp. Neurol.*, 2015. **263**: p. 214–220.
95. Dubé, C.M., J. Molet, A. Singh-Taaylor, A. Ivy, P.M. Maras, and T.Z. Baram, *Hyper-excitability and epilepsy generated by chronic early-life stress*. *Neurobiol. Stress*, 2015. **2**: p. 10–19.
96. Ichijo, M. and S. Ochs, *Spreading depression of negative wave of direct cortical response and pyramidal tract responses*. *Brain Res.*, 1970. **23**(1): p. 41–56.
97. Herreras, O., *Electrical prodromals of spreading depression void Grafstein's potassium hypothesis*. *J. Neurophysiol.*, 2005. **94**(5): p. 3656; author reply 3656-3657.
98. Herreras, O., C. Largo, J.M. Ibarz, G.G. Somjen, and R. Martín del Río, *Role of neuronal synchronizing mechanisms in the propagation of spreading depression in the in vivo hippocampus*. *J. Neurosci.*, 1994. **14**(11 Pt 2): p. 7087–7098.
99. Higashida, H., G. Mitarai, and S. Watanabe, *A comparative study of membrane potential changes in neurons and neuroglial cells during spreading depression in the rabbit*. *Brain Res.*, 1974. **65**(3): p. 411–425.
100. Tian, G.F., H. Azmi, T. Takano, Q. Xu, W. Peng, J. Lin, N. Oberheim, N. Lou, X. Wang, H.R. Zielke, J. Kang, and M. Nedergaard, *An astrocytic basis of epilepsy*. *Nat. Med.*, 2005. **11**(9): p. 973–981.
101. Mei, Y.Y., M.H. Lee, T.C. Cheng, I.H. Hsiao, D.C. Wu, and N. Zhou, *NMDA receptors sustain but do not initiate neuronal depolarization in spreading depolarization*. *Neurobiol. Dis.*, 2020. **145**: p. 1050-1071.

## References

102. Shanmugam, S., K. Karunaikadal, S. Varadarajan, and M. Krishnan, *Memantine Ameliorates Migraine Headache*. Ann. Indian Acad. Neurol., 2019. **22**(3): p. 286–290.
103. Löscher, W. and D. Hönack, *Over-additive anticonvulsant effect of memantine and NBQX in kindled rats*. Eur J Pharmacol, 1994. **259**(2): p. R3-5.
104. Santos, E., A. Olivares-Rivera, S. Major, R. Sánchez-Porras, L. Uhlmann, K. Kunzmann, R. Zerelles, M. Kentar, V. Kola, A.H. Aguilera, M.G. Herrera, C.L. Lemale, J. Woitzik, J.A. Hartings, O.W. Sakowitz, A.W. Unterberg, and J.P. Dreier, *Lasting s-ketamine block of spreading depolarizations in subarachnoid hemorrhage: a retrospective cohort study*. Crit. Care, 2019. **23**(1): p. 427.
105. Fang, Y. and X. Wang, *Ketamine for the treatment of refractory status epilepticus*. Seizure, 2015. **30**: p. 14–20.
106. Sato, K., K. Morimoto, and M. Okamoto, *Anticonvulsant action of a non-competitive antagonist of NMDA receptors (MK-801) in the kindling model of epilepsy*. Brain Res., 1988. **463**(1): p. 12–20.
107. Po-Hua, Y., K. Yi-Chun, T. Ka-Wai, C. Chen-Chih, H. Chien-Tai, and H. Yao-Hsien, *Efficacy of levetiracetam for migraine prophylaxis: A systematic review and meta-analysis*. J. Formos. Med. Assoc., 2021. **120**(1): p. 755–764.
108. XiChun, Z., J. Moshe, B. Catherine, K. Vanessa, G. Michael, and B. Rami, *Ezogabine (KCNQ2/3 channel opener) prevents delayed activation of meningeal nociceptors if given before but not after the occurrence of cortical spreading depression*. Epilepsy & Behav., 2013. **28**(2): p. 243–248.
109. Bowyer, S.M., K.M. Mason, J.E. Moran, N. Tepley, and P.D. Mitsias, *Cortical hyperexcitability in migraine patients before and after sodium valproate treatment*. J. Clin. Neurophysiol., 2005. **22**(1): p. 65–67.
110. O'Donnell, T., S. Rotzinger, M. Ulrich, C.C. Hanstock, T.T. Nakashima, and P.H. Silverstone, *Effects of chronic lithium and sodium valproate on concentrations of brain amino acids*. Eur. Neuropsychopharmacol., 2003. **13**(4): p. 220–227.
111. Gean, P.W., C.C. Huang, C.R. Hung, and J.J. Tsai, *Valproic acid suppresses the synaptic response mediated by the NMDA receptors in rat amygdalar slices*. Brain Res. Bull., 1994. **33**(3): p. 333-336.

## References

112. Gobbi, G. and L. Janiri, *Sodium- and magnesium-valproate in vivo modulate glutamatergic and GABAergic synapses in the medial prefrontal cortex*. *Psychopharmacology (Berl.)*, 2006. **185**(2): p. 255–262.
113. Rogawski, M.A., *Antiepileptic Drugs and Migraine*, in *16th International Headache Research Seminar, "Innovative Drug Development For Headache Disorders"*. 2008: Copenhagen, Denmark.
114. Nye, B.L. and V.M. Thadani, *Migraine and epilepsy: review of the literature*. *Headache*, 2015. **55**(3): p. 359–380.
115. Russell, M.B., L. Iselius, and J. Olesen, *Migraine without aura and migraine with aura are inherited disorders*. *Cephalalgia*, 1996. **16**(5): p. 305–309.
116. Ferraro, T.N., D.J. Dlugos, and R.J. Buono, *Role of genetics in the diagnosis and treatment of epilepsy*. *Expert Rev. Neurother*, 2006. **6**(12): p. 1789–1800.
117. Thomsen, L.L., M.K. Eriksen, S.F. Roemer, I. Andersen, J. Olesen, and M.B. Russell, *A population-based study of familial hemiplegic migraine suggests revised diagnostic criteria*. *Brain*, 2002. **125**(Pt 6): p. 1379–1391.
118. Huang, Y., H. Xiao, X. Qin, Y. Nong, D. Zou, and Y. Wu, *The genetic relationship between epilepsy and hemiplegic migraine*. *Neuropsychiatr. Dis. Treat.*, 2017. **13**: p. 1175–1179.
119. Hans, M., S. Luvisetto, M.E. Williams, M. Spagnolo, A. Urrutia, A. Tottene, P.F. Brust, E.C. Johnson, M.M. Harpold, K.A. Stauderman, and D. Pietrobon, *Functional consequences of mutations in the human alpha1A calcium channel subunit linked to familial hemiplegic migraine*. *J. Neurosci.*, 1999. **19**(5): p. 1610–1619.
120. Westenbroek, R.E., T. Sakurai, E.M. Elliott, J.W. Hell, T.V. Starr, T.P. Snutch, and W.A. Catterall, *Immunochemical identification and subcellular distribution of the alpha 1A subunits of brain calcium channels*. *J. Neurosci.*, 1995. **15**(10): p. 6403–6418.
121. Tottene, A., R. Conti, A. Fabbro, D. Vecchia, M. Shapovalova, M. Santello, A.M. van den Maagdenberg, M.D. Ferrari, and D. Pietrobon, *Enhanced excitatory transmission at cortical synapses as the basis for facilitated spreading depression in Ca(v)2.1 knockin migraine mice*. *Neuron*, 2009. **61**(5): p. 762–773.
122. Eikermann-Haerter, K., I. Yuzawa, T. Qin, Y. Wang, K. Baek, Y.R. Kim, U. Hoffmann, E. Dilekoz, C. Waeber, M.D. Ferrari, A.M. van den Maagdenberg,

## References

- M.A. Moskowitz, and C. Ayata, *Enhanced subcortical spreading depression in familial hemiplegic migraine type 1 mutant mice*. *J. Neurosci.*, 2011. **31**(15): p. 5755–5763.
123. Chioza, B., H. Wilkie, L. Nashef, J. Blower, D. McCormick, P. Sham, P. Asherson, and A.J. Makoff, *Association between the alpha(1a) calcium channel gene CACNA1A and idiopathic generalized epilepsy*. *Neurology*, 2001. **56**(9): p. 1245–1246.
124. Loonen, I.C.M., N.A. Jansen, S.M. Cain, M. Schenke, R.A. Voskuyl, A.C. Yung, B. Bohnet, P. Kozlowski, R.D. Thijs, M.D. Ferrari, T.P. Snutch, A. van den Maagdenberg, and E.A. Tolner, *Brainstem spreading depolarization and cortical dynamics during fatal seizures in Cacna1a S218L mice*. *Brain*, 2019. **142**(2): p. 412-425.
125. Kros, L., K. Lykke-Hartmann, and K. Khodakhah, *Increased susceptibility to cortical spreading depression and epileptiform activity in a mouse model for FHM2*. *Sci. Rep.*, 2018. **8**(1): p. 16959.
126. Riant, F., A. Ducros, C. Ploton, C. Barbance, C. Depienne, and E. Tournier-Lasserre, *De novo mutations in ATP1A2 and CACNA1A are frequent in early-onset sporadic hemiplegic migraine*. *Neurology*, 2010. **75**(11): p. 967–972.
127. Escayg, A., B.T. MacDonald, M.H. Meisler, S. Baulac, G. Huberfeld, I. An-Gourfinkel, A. Brice, E. LeGuern, B. Moulard, D. Chaigne, C. Buresi, and A. Malafosse, *Mutations of SCN1A, encoding a neuronal sodium channel, in two families with GEFS+2*. *Nat. Genet.*, 2000. **24**(4): p. 343–345.
128. Kasperaviciute, D., C.B. Catarino, M. Matarin, C. Leu, J. Novy, A. Tostevin, B. Leal, E.V. Hessel, K. Hallmann, M.S. Hildebrand, H.H. Dahl, M. Ryten, D. Trabzuni, A. Ramasamy, S. Alhusaini, C.P. Doherty, T. Dorn, J. Hansen, G. Krämer, B.J. Steinhoff, D. Zumsteg, S. Duncan, R.K. Kälviäinen, K.J. Eriksson, A.M. Kantanen, M. Pandolfo, U. Gruber-Sedlmayr, K. Schlachter, E.M. Reinthaler, E. Stogmann, F. Zimprich, E. Théâtre, C. Smith, T.J. O'Brien, K. Meng Tan, S. Petrovski, A. Robbiano, R. Paravidino, F. Zara, P. Striano, M.R. Sperling, R.J. Buono, H. Hakonarson, J. Chaves, P.P. Costa, B.M. Silva, A.M. da Silva, P.N. de Graan, B.P. Koeleman, A. Becker, S. Schoch, M. von Lehe, P.S. Reif, F. Rosenow, F. Becker, Y. Weber, H. Lerche, K. Rössler, M. Buchfelder, H.M. Hamer, K. Kobow, R. Coras, I. Blumcke, I.E. Scheffer, S.F. Berkovic, M.E. Weale, N. Delanty, C. Depondt, G.L. Cavalleri, W.S. Kunz, and

## References

- S.M. Sisodiya, *Epilepsy, hippocampal sclerosis and febrile seizures linked by common genetic variation around SCN1A*. *Brain*, 2013. **136**(Pt 10): p. 3140–3150.
129. Liao, W.P., Y.W. Shi, Y.S. Long, Y. Zeng, T. Li, M.J. Yu, T. Su, P. Deng, Z.G. Lei, S.J. Xu, W.Y. Deng, X.R. Liu, W.W. Sun, Y.H. Yi, Z.C. Xu, and S. Duan, *Partial epilepsy with antecedent febrile seizures and seizure aggravation by antiepileptic drugs: associated with loss of function of Na(v) 1.1*. *Epilepsia*, 2010. **51**(9): p. 1669–1678.
130. Castro, M.J., A.H. Stam, C. Lemos, B. de Vries, K.R. Vanmolkot, J. Barros, G.M. Terwindt, R.R. Frants, J. Sequeiros, M.D. Ferrari, J.M. Pereira-Monteiro, and A.M. van den Maagdenberg, *First mutation in the voltage-gated Nav1.1 subunit gene SCN1A with co-occurring familial hemiplegic migraine and epilepsy*. *Cephalalgia*, 2009. **29**(3): p. 308–313.
131. Riant, F., et al., *PRRT2 mutations cause hemiplegic migraine*. *Neurology*, 2012. **79**(21): p. 2122–2124.
132. Chan, Y.C., J.M. Burgunder, E. Wilder-Smith, S.E. Chew, K.M. Lam-Mok-Sing, V. Sharma, and B.K. Ong, *Electroencephalographic changes and seizures in familial hemiplegic migraine patients with the CACNA1A gene S218L mutation*. *J. Clin. Neurosci.*, 2008. **15**(8): p. 891–894.
133. Zangaladze, A., A.A. Asadi-Pooya, A. Ashkenazi, and M.R. Sperling, *Sporadic hemiplegic migraine and epilepsy associated with CACNA1A gene mutation*. *Epilepsy Behav.*, 2010. **17**(2): p. 293–295.
134. Kors, E.E., A. Melberg, K.R.J. Vanmolkot, E. Kumlien, J. Haan, R. Raininko, R. Flink, H.B. Ginjaar, R.R. Frants, M.D. Ferrari, and A.M.J.M. van den Maagdenberg, *Childhood epilepsy, familial hemiplegic migraine, cerebellar ataxia, and a new CACNA1A mutation*. *Neurology*, 2004. **63**(6): p. 1136–1137.
135. Tamim, I., D.Y. Chung, A.L. de Moraes, I.C.M. Loonen, T. Qin, A. Misra, F. Schlunk, M. Endres, S.J. Schiff, and C. Ayata, *Spreading depression as an innate antiseizure mechanism*. *Nature Communications*, 2021. **12**(1): p. 2206.
136. Wang, H., J. Peca, M. Matsuzaki, K. Matsuzaki, J. Noguchi, L. Qiu, D. Wang, F. Zhang, E. Boyden, K. Deisseroth, H. Kasai, W.C. Hall, G. Feng, and G.J. Augustine, *High-speed mapping of synaptic connectivity using*

## References

- photostimulation in Channelrhodopsin-2 transgenic mice*. Proc. Natl. Acad. Sci. USA, 2007. **104**(19): p. 8143–8148.
137. Arenkiel, B.R., J. Peca, I.G. Davison, C. Feliciano, K. Deisseroth, G.J. Augustine, M.D. Ehlers, and G. Feng, *In vivo light-induced activation of neural circuitry in transgenic mice expressing channelrhodopsin-2*. Neuron, 2007. **54**(2): p. 205–218.
138. Houben, T., I.C. Loonen, S.M. Baca, M. Schenke, J.H. Meijer, M.D. Ferrari, G.M. Terwindt, R.A. Voskuyl, A. Charles, A.M. van den Maagdenberg, and E.A. Tolner, *Optogenetic induction of cortical spreading depression in anesthetized and freely behaving mice*. J. Cereb. Blood Flow Metab., 2017. **37**(5): p. 1641–1655.
139. Yamaguchi, S. and M.A. Rogawski, *Effects of anticonvulsant drugs on 4-aminopyridine-induced seizures in mice*. Epilepsy Res., 1992. **11**(1): p. 9–16.
140. Perreault, P. and M. Avoli, *Physiology and pharmacology of epileptiform activity induced by 4-aminopyridine in rat hippocampal slices*. J. Neurophysiol., 1991. **65**(4): p. 771–785.
141. Rossokhin, A.V., I.N. Sharonova, J.V. Bukanova, S.N. Kolbaev, and V.G. Skrebitsky, *Block of GABA(A) receptor ion channel by penicillin: electrophysiological and modeling insights toward the mechanism*. Mol. Cell Neurosci., 2014. **63**: p. 72–82.
142. Tsuda, A., M. Ito, K. Kishi, H. Shiraishi, H. Tsuda, and C. Mori, *Effect of penicillin on GABA-gated chloride ion influx*. Neurochem. Res., 1994. **19**(1): p. 1–4.
143. Johnston, G.A., *Advantages of an antagonist: bicuculline and other GABA antagonists*. Br. J. Pharmacol., 2013. **169**(2): p. 328–336.
144. Liou, J.Y., H. Ma, M. Wenzel, M. Zhao, E. Baird-Daniel, E.H. Smith, A. Daniel, R. Emerson, R. Yuste, T.H. Schwartz, and C.A. Schevon, *Role of inhibitory control in modulating focal seizure spread*. Brain, 2018. **141**(7): p. 2083–2097.
145. Akdogan, I., E. Adiguzel, I. Yilmaz, M.B. Ozdemir, M. Sahiner, and A.C. Tufan, *Penicillin-induced epilepsy model in rats: dose-dependant effect on hippocampal volume and neuron number*. Brain Res. Bull., 2008. **77**(4): p. 172–177.
146. Pitkanen, A., P.A. Schwartzkroin, and S.L. Moshe, *Models of seizures and epilepsy*. 2006: Elsevier.

## References

147. Aiba, I.a.J.L.N., *Spreading depolarization in the brainstem mediates sudden cardiorespiratory arrest in mouse SUDEP models*. *Sci. Transl. Med.*, 2015. **7**: p. 282.
148. Rusina, E., C. Bernard, and A. Williamson, *The Kainic Acid Models of Temporal Lobe Epilepsy*. *eneuro*, 2021. **8**(2).
149. Narahashi, T., J.W. Moore, and W.R. Scott, *Tetrodotoxin Blockage of Sodium Conductance Increase in Lobster Giant Axons*. *J. Gen. Physiol.*, 1964. **47**(5): p. 965–974.
150. Gill, R., P. Andiné, L. Hillered, L. Persson, and H. Hagberg, *The effect of MK-801 on cortical spreading depression in the penumbral zone following focal ischaemia in the rat*. *J. Cereb. Blood Flow Metab.*, 1992. **12**(3): p. 371–379.
151. Chung, D.Y., H. Sadeghian, T. Qin, S. Lule, H. Lee, F. Karakaya, S. Goins, F. Oka, M.A. Yaseen, T. Houben, E.A. Tolner, A. van den Maagdenberg, M.J. Whalen, S. Sakadžic, and C. Ayata, *Determinants of Optogenetic Cortical Spreading Depolarizations*. *Cereb Cortex*, 2019. **29**(3): p. 1150-1161.
152. Kudo, C., A. Nozari, M.A. Moskowitz, and C. Ayata, *The impact of anesthetics and hyperoxia on cortical spreading depression*. *Exp. Neurol.*, 2008. **212**(1): p. 201–206.
153. Kobayashi, O., Y. Ohta, and F. Kosaka, *Interaction of sevoflurane, isoflurane, enflurane and halothane with non-depolarizing muscle relaxants and their prejunctional effects at the neuromuscular junction*. *Acta Med. Okayama*, 1990. **44**(4): p. 209–215.
154. Chung, D.Y., K. Sugimoto, P. Fischer, M. Bohm, T. Takizawa, H. Sadeghian, A. Morais, A. Harriott, F. Oka, T. Qin, N. Henninger, M.A. Yaseen, S. Sakadžic, and C. Ayata, *Real-time non-invasive in vivo visible light detection of cortical spreading depolarizations in mice*. *J Neurosci Methods*, 2018. **309**: p. 143-146.
155. Zhao, M., H. Ma, M. Suh, and T.H. and Schwartz, *Spatiotemporal Dynamics of Perfusion and Oximetry during Ictal Discharges in the Rat Neocortex*. *J. Neurosci.*, 2009. **29**: p. 2814-2823.
156. Zhao, M., J. Nguyen, H. Ma, N. Nishimura, C.B. Schaffer, and T.H. Schwartz, *Preictal and ictal neurovascular and metabolic coupling surrounding a seizure focus*. *J. Neurosci.*, 2011. **31**(37): p. 13292–13300.



## References

157. Ma, Y., M.A. Shaik, S.H. Kim, M.G. Kozberg, D.N. Thibodeaux, H.T. Zhao, H. Yu, and E.M. Hillman, *Wide-field optical mapping of neural activity and brain haemodynamics: considerations and novel approaches*. Philos. Trans. R. Soc. Lond. B. Biol. Sci., 2016. **371**(1705): p. 20150360.
158. Maslarova, A., M. Alam, C. Reiffurth, E. Lapilover, A. Gorji, and J.P. Dreier, *Chronically epileptic human and rat neocortex display a similar resistance against spreading depolarization in vitro*. Stroke, 2011. **42**(10): p. 2917–2922.
159. Litt, B., R. Esteller, J. Echauz, M. D'Alessandro, R. Shor, T. Henry, P. Pennell, C. Epstein, R. Bakay, M. Dichter, and G. Vachtsevanos, *Epileptic seizures may begin hours in advance of clinical onset: a report of five patients*. Neuron, 2001. **30**(1): p. 51–64.
160. Bragin, A., C.L. Wilson, and J.J. Engel, *Chronic Epileptogenesis Requires Development of a Network of Pathologically Interconnected Neuron Clusters A Hypothesis*. Epilepsia, 2000. **41**: p. 144–152.
161. Matsuura, T. and J. Bures, *The minimum volume of depolarized neural tissue required for triggering cortical spreading depression in rat*. Exp Brain Res, 1971. **12**(3): p. 238-49.
162. Schevon, C.A., S.K. Ng, J. Cappell, R.R. Goodman, G. McKhann, Jr., A. Waziri, A. Branner, A. Sosunov, C.E. Schroeder, and R.G. Emerson, *Microphysiology of epileptiform activity in human neocortex*. J. Clin. Neurophysiol., 2008. **25**(6): p. 321–330.
163. Bower, M.R., M. Stead, F.B. Meyer, W.R. Marsh, and G.A. Worrell, *Spatiotemporal neuronal correlates of seizure generation in focal epilepsy*. Epilepsia, 2012. **53**(5): p. 807–816.
164. Stead, M., M. Bower, B.H. Brinkmann, K. Lee, W.R. Marsh, F.B. Meyer, B. Litt, J. Van Gompel, and G.A. Worrell, *Microseizures and the spatiotemporal scales of human partial epilepsy*. Brain, 2010. **133**(9): p. 2789–2797.
165. Van Harreveld, A. and J.S. Stamm, *Consequences of cortical convulsive activity in rabbit*. J. Neurophysiol., 1954. **17**(6): p. 505-520.
166. Bures, J. and O. Buresova, *The influencing of reflex acoustic epilepsy and reflex inhibition (animal hypnosis) by spreading EEG depression*. Physiol Bohemoslov, 1956. **5**(4): p. 395-400.

## References

167. de Azeredo, F.A. and M.L. Perret, *Cortical slow potential changes during convulsions induced by maximal electroshock or penicillin focus*. *Metab. Brain Dis.*, 1992. **7**(2): p. 101-113.
168. Vinogradova, L.V., V.Y. Vinogradov, and G.D. Kuznetsova, *Unilateral cortical spreading depression is an early marker of audiogenic kindling in awake rats*. *Epilepsy Res.*, 2006. **71**(1): p. 64-75.
169. Bragin, A., M. Penttonen, and G. Buzsaki, *Termination of epileptic afterdischarge in the hippocampus*. *J Neurosci*, 1997. **17**(7): p. 2567-79.
170. Van Harreveld, A. and J.S. Stamm, *Cortical responses to metrazol and sensory stimulation in the rabbit*. *Electroencephalogr. Clin. Neurophysiol.*, 1955. **7**(3): p. 363-370.
171. Zakharov, A., K. Chernova, G. Burkhanova, G.L. Holmes, and R. Khazipov, *Segregation of seizures and spreading depolarization across cortical layers*. *Epilepsia*, 2019. **60**(12): p. 2386-2397.
172. Aquino-Cias, J. and J. Bures, *The effect of thalamic spreading depression on the epileptic discharge in rats*. *Comparative and cellular pathophysiology of epilepsy*. *Excerpta Medica Int. Congr. Ser.*, ed. Z. Servit. Vol. 124. 1966, Amsterdam: Excerpta Medica.
173. Schoknecht, K., M. Kikhia, C.L. Lemale, A. Liotta, S. Lublinsky, S. Mueller, P. Boehm-Sturm, A. Friedman, and J.P. Dreier, *The role of spreading depolarizations and electrographic seizures in early injury progression of the rat photothrombosis stroke model*. *J Cereb Blood Flow Metab*, 2020: p. 271678x20915801.
174. Vinogradova, L.V., *Audiogenic kindling in WAG/Rij rats: change in behavioral and electrophysiological responses to repetitive short acoustic stimulation*. *Zh Vyssh Nerv Deiat Im I P Pavlova*, 2004. **54**(5): p. 638–647.
175. Vinogradova, L.V., G.D. Kuznetsova, and A.M. Coenen, *Audiogenic seizures associated with a cortical spreading depression wave suppress spike-wave discharges in rats*. *Physiol. Behav.*, 2005. **86**(5): p. 554–558.
176. Kesner, R.P., L.I. O'Kelly, and G.J. Thomas, *EFFECTS OF CORTICAL SPREADING DEPRESSION AND DRUGS UPON AUDIOGENIC SEIZURES IN RATS*. *J Comp Physiol Psychol*, 1965. **59**: p. 280-2.

## References

177. Ueda, M. and J. Bures, *Differential effects of cortical spreading depression on epileptic foci induced by various convulsants*. *Electroencephalogr. Clin. Neurophysiol.*, 1977. **43**(5): p. 666–674.
178. Samotaeva, I.S., N. Tillmanns, G. van Luijtelaar, and L.V. Vinogradova, *Intracortical microinjections may cause spreading depression and suppress absence seizures*. *Neuroscience*, 2013. **230**: p. 50-55.
179. Koroleva, V.I. and J. Bures, *Cortical penicillin focus as a generator of repetitive spike-triggered waves of spreading depression in rats*. *Exp. Brain Res.*, 1983. **51**(2): p. 291-297.
180. Koroleva, V.I., L.V. Vinogradova, and J. Bures, *Reduced incidence of cortical spreading depression in the course of pentylenetetrazol kindling in rats*. *Brain Res.*, 1993. **608**(1): p. 107-114.
181. Rebert, C.S., G.T. Pryor, and J.A. Schaeffer, *Slow cortical potential consequences of electroconvulsive shock in rats*. *Physiol. Behav.*, 1974. **12**(1): p. 131-134.
182. Köhling, R., U.R. Koch, G. Hagemann, C. Redecker, H. Straub, and E.J. Speckmann, *Differential sensitivity to induction of spreading depression by partial disinhibition in chronically epileptic human and rat as compared to native rat neocortical tissue*. *Brain Res.*, 2003. **975**(1-2): p. 129-134.
183. Ullah, G., Y. Wei, M.A. Dahlem, M. Wechselberger, and S.J. Schiff, *The Role of Cell Volume in the Dynamics of Seizure, Spreading Depression, and Anoxic Depolarization*. *PLoS Comput Biol*, 2015. **11**(8): p. e1004414.
184. Foley, J., H. Nguyen, C.B. Bennett, and M. Muschol, *Potassium accumulation as dynamic modulator of neurohypophysial excitability*. *Neuroscience*, 2010. **169**(1): p. 65-73.
185. Bertram, E., *The relevance of kindling for human epilepsy*. *Epilepsia*, 2007. **48** **Suppl 2**: p. 65-74.
186. Kruger, H., H.J. Luhmann, and U. Heinemann, *Repetitive SD causes selective suppression of GABAergic function*. *NeuroReport*, 1996. **7**: p. 2733-2736.
187. Guedes, R.C. and E.A. Cavalheiro, *Blockade of spreading depression in chronic epileptic rats: reversion by diazepam*. *Epilepsy Res.*, 1997. **27**(1): p. 33-40.

## References

188. Nedergaard, M. and A.J. Hansen, *Spreading depression is not associated with neuronal injury in the normal brain*. Brain Res., 1988. **449**(1-2): p. 395-398.
189. Dreier, J.P., T. Isele, C. Reiffurth, N. Offenhauser, S.A. Kirov, M.A. Dahlem, and O. Herreras, *Is spreading depolarization characterized by an abrupt, massive release of gibbs free energy from the human brain cortex?* Neuroscientist, 2013. **19**(1): p. 25-42.
190. Shaw, N.A., *The neurophysiology of concussion*. Prog Neurobiol, 2002. **67**(4): p. 281-344.
191. Solomon, S., *Posttraumatic headache*. Med. Clin. North Am., 2001. **85**(4): p. 987-96, vii-viii.
192. Shlosberg, D., M. Benifla, D. Kaufer, and A. Friedman, *Blood-brain barrier breakdown as a therapeutic target in traumatic brain injury*. Nat. Rev. Neurol., 2010. **6**(7): p. 393-403.
193. Hayes, R.L. and C.E. Dixon, *Neurochemical changes in mild head injury*. Semin. Neurol., 1994. **14**(1): p. 25-31.
194. Kiriakopoulos, E. *Traumatic Brain Injury and Epilepsy*. 2020 [11.09.21]; Available from: <https://www.epilepsy.com/learn/epilepsy-due-specific-causes/structural-causes-epilepsy/specific-structural-epilepsies/traumatic-brain-injury-and-epilepsy>.
195. Takahashi, H., S. Manaka, and K. Sano, *Changes in extracellular potassium concentration in cortex and brain stem during the acute phase of experimental closed head injury*. J. Neurosurg., 1981. **55**(5): p. 708-717.
196. Fabricius, M., S. Fuhr, L. Willumsen, J.P. Dreier, R. Bhatia, M.G. Boutelle, J.A. Hartings, R. Bullock, A.J. Strong, and M. Lauritzen, *Association of seizures with cortical spreading depression and peri-infarct depolarisations in the acutely injured human brain*. Clin. Neurophysiol., 2008. **119**(9): p. 1973-1984.
197. Oliveira-Ferreira, A.I., D. Milakara, A. Mesbah, D. Jorks, S. Major, J.A. Hartings, J. Lueckl, P. Martus, R. Graf, C. Dohmen, G. Bohner, J. Woitzik, and J.P. Dreier, *Experimental and preliminary clinical evidence of an ischemic zone with prolonged negative DC shifts surrounded by a normally perfused tissue belt with persistent electrocorticographic depression*. J. Cereb. Blood Flow & Metab., 2010. **30**: p. 1504-1519.

## References

198. Dreier, J.P., J. Woitzik, M. Fabricius, R. Bhatia, S. Major, C. Drenckhahn, T.N. Lehmann, A. Sarrafzadeh, L. Willumsen, J.A. Hartings, O.W. Sakowitz, J.H. Seemann, A. Thieme, M. Lauritzen, and A.J. Strong, *Delayed ischaemic neurological deficits after subarachnoid haemorrhage are associated with clusters of spreading depolarizations*. Brain, 2006. **129**(Pt 12): p. 3224-3237.
199. Dreier, J.P., S. Major, A. Manning, J. Woitzik, C. Drenckhahn, J. Steinbrink, C. Tolia, A.I. Oliveira-Ferreira, M. Fabricius, J.A. Hartings, P. Vajkoczy, M. Lauritzen, U. Dirnagl, G. Bohner, A.J. Strong, and C.s. group, *Cortical spreading ischaemia is a novel process involved in ischaemic damage in patients with aneurysmal subarachnoid haemorrhage*. Brain, 2009. **132**(Pt 7): p. 1866-1881.
200. Bosche, B., R. Graf, R.I. Ernestus, C. Dohmen, T. Reithmeier, G. Brinker, A.J. Strong, J.P. Dreier, J. Woitzik, and D. Members of the Cooperative Study of Brain Injury, *Recurrent spreading depolarizations after subarachnoid hemorrhage decreases oxygen availability in human cerebral cortex*. Ann. Neurol., 2010. **67**(5): p. 607-617.
201. Dreier, J.P., S. Major, H.W. Pannek, J. Woitzik, M. Scheel, D. Wiesenthal, P. Martus, M.K. Winkler, J.A. Hartings, M. Fabricius, E.J. Speckmann, A. Gorji, and C.s. group, *Spreading convulsions, spreading depolarization and epileptogenesis in human cerebral cortex*. Brain, 2012. **135**(Pt 1): p. 259-275.
202. Van Harreld, A. and J.S. Stamm, *Spreading Cortical Convulsions and Depressions*. J. Neurophysiol., 1953. **16**(4): p. 352-366.
203. Hofmeijer, J. and M.J. van Putten, *Ischemic cerebral damage: an appraisal of synaptic failure*. Stroke, 2012. **43**(2): p. 607-615.
204. Matthews, W.B., *Footballer's migraine*. BMJ, 1972. **2**(5809): p. 326-327.
205. Greenblatt, S.H., *Posttraumatic transient cerebral blindness. Association with migraine and seizure diatheses*. JAMA, 1973. **225**(9): p. 1073-1076.
206. Haas, D.C. and R.D. Sovner, *Migraine attacks triggered by mild head trauma, and their relation to certain post-traumatic disorders of childhood*. J. Neurol. Neurosurg. Psychiatry, 1969. **32**(6): p. 548-554.
207. Weiss, H.D., B.J. Stern, and J. Goldberg, *Post-traumatic migraine: chronic migraine precipitated by minor head or neck trauma*. Headache, 1991. **31**(7): p. 451-456.

## References

208. Stam, A.H., G.J. Luijckx, B.T. Poll-Thé, I.B. Ginjaar, R.R. Frants, J. Haan, M.D. Ferrari, G.M. Terwindt, and A.M. van den Maagdenberg, *Early seizures and cerebral oedema after trivial head trauma associated with the CACNA1A S218L mutation*. J. Neurol. Neurosurg. Psychiatry, 2009. **80**(10): p. 1125-1129.



## 11. Eidesstattliche Versicherung

„Ich, Isra Tamim, versichere an Eides statt durch meine eigenhändige Unterschrift, dass ich die vorgelegte Dissertation mit dem Thema:

*Spreading depression as an endogenous antiseizure mechanism:*

*The interplay on the borderland between migraine and epilepsy*

-

*Spreading depression als endogener antiepileptischer Mechanismus:*

*Das Zusammenspiel in der Grenzzone zwischen Migräne und Epilepsie*

selbstständig und ohne nicht offengelegte Hilfe Dritter verfasst und keine anderen als die angegebenen Quellen und Hilfsmittel genutzt habe.

Alle Stellen, die wörtlich oder dem Sinne nach auf Publikationen oder Vorträgen anderer Autoren/innen beruhen, sind als solche in korrekter Zitierung kenntlich gemacht. Die Abschnitte zu Methodik (insbesondere praktische Arbeiten, Laborbestimmungen, statistische Aufarbeitung) und Resultaten (insbesondere Abbildungen, Graphiken und Tabellen) werden von mir verantwortet.

Ich versichere ferner, dass ich die in Zusammenarbeit mit anderen Personen generierten Daten, Datenauswertungen und Schlussfolgerungen korrekt gekennzeichnet und meinen eigenen Beitrag sowie die Beiträge anderer Personen korrekt kenntlich gemacht habe (siehe Anteilserklärung). Texte oder Textteile, die gemeinsam mit anderen erstellt oder verwendet wurden, habe ich korrekt kenntlich gemacht.

Meine Anteile an etwaigen Publikationen zu dieser Dissertation entsprechen denen, die in der untenstehenden gemeinsamen Erklärung mit dem/der Erstbetreuer/in, angegeben sind. Für sämtliche im Rahmen der Dissertation entstandenen Publikationen wurden die Richtlinien des ICMJE (International Committee of Medical Journal Editors; [www.icmje.org](http://www.icmje.org)) zur Autorenschaft eingehalten. Ich erkläre ferner, dass ich mich zur Einhaltung der Satzung der Charité – Universitätsmedizin Berlin zur Sicherung Guter Wissenschaftlicher Praxis verpflichte.



Weiterhin versichere ich, dass ich diese Dissertation weder in gleicher noch in ähnlicher Form bereits an einer anderen Fakultät eingereicht habe.

Die Bedeutung dieser eidesstattlichen Versicherung und die strafrechtlichen Folgen einer unwahren eidesstattlichen Versicherung (§§156, 161 des Strafgesetzbuches) sind mir bekannt und bewusst.“

Datum

Unterschrift



## 12. Anteilserklärung an der erfolgten Publikation im Top-Journal

Tamim, I., D.Y. Chung, A.L. de Moraes, I.C.M. Loonen, T. Qin, A. Misra, F. Schlunk, M. Endres, S.J. Schiff, and C. Ayata, *Spreading depression as an innate antiseizure mechanism*. Nat. Commun., 2021. **12**(1): p. 2206.

- Literaturrecherche zur Methodik mit nachfolgender Etablierung des Modells zur Induktion epileptischer Anfälle an der Maus (Durchführung einer Pilotstudie, aus der die publizierte Studie hervorging)
- Planung, Durchführung und Anpassung aller Experimente je nach Teilergebnissen im Sinne eines „rolling reviews“ (Datenakquirierung der Daten in *Figures 1-10, Supplementary Figures 1-9, Supplementary Tables 1, Supplementary Movies 1-2*)
- Konzipierung einer Datenprozessierung und Analyse der Elektrokortikogramm-Daten mittels LabChart (der Daten in *Figures 1-10, Supplementary Figures 1-9, Supplementary Tables 1, Supplementary Movies 1-2*)
- Bilddaten-Prozessierung mittels selbstkodiertem MATLAB-Script und anschließender Analyse und Auswertung
- Statistische Aufbereitung der Daten mittels Graphpad (Datenauswertung in *Figures 1-10, Supplementary Figures 3-9, Supplementary Table 1, Supplementary Movie 1*)
- Definition der Einschluss- und Ausschlusskriterien anhand der Interpretation von Vitalparametern, Blutgasen, Blutzucker und nach Durchsicht der Bilddaten (*Supplementary Table 1*)
- Erstellung der Illustrationen und Animation zur Visualisierung der Methodik mittels ProCreate und Adobe (*Figures 1-10, Supplementary Figures 1-9, Supplementary Movies 1-2*)
- Datenvisualisierung mittels Photoshop und Graphpad (*Figures 1-10, Supplementary Figures 1-9, Supplementary Tables 1, Supplementary Movies 1-2*)
- Entwurf des Manuskripts, Einreichung bei *Nature Communications* und Adressierung der Kommentare der Reviewer, sowie Planung, Konzipierung und Analyse der Revisionsexperimente
- Vorstellung der Studie auf wissenschaftlichen Kongressen

---

Unterschrift der Doktorandin

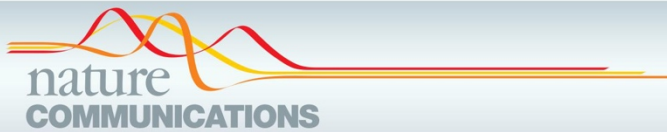
## 13. Journal Summary List

Journal Data Filtered By: **Selected JCR Year: 2018** Selected Editions: SCIE,SSCI  
 Selected Categories: **"MULTIDISCIPLINARY SCIENCES"** Selected Category  
 Scheme: WoS

**Gesamtanzahl: 69 Journale**

Rank	Full Journal Title	Total Cites	Journal Impact Factor	Eigenfactor Score
1	NATURE	745,692	43.070	1.285010
2	SCIENCE	680,994	41.037	1.070190
3	National Science Review	1,842	13.222	0.006500
4	Science Advances	21,901	12.804	0.110010
5	Nature Communications	243,793	11.878	1.103290
6	Nature Human Behaviour	1,230	10.575	0.006550
7	PROCEEDINGS OF THE NATIONAL ACADEMY OF SCIENCES OF THE UNITED STATES OF AMERICA	661,118	9.580	1.022190
8	Science Bulletin	3,569	6.277	0.009840
9	Scientific Data	3,240	5.929	0.015610
10	Frontiers in Bioengineering and Biotechnology	1,994	5.122	0.006540
11	Journal of Advanced Research	2,691	5.045	0.004780
12	Research Synthesis Methods	1,932	5.043	0.005420
13	GigaScience	2,674	4.688	0.012510
14	Annals of the New York Academy of Sciences	46,385	4.295	0.025840
15	Scientific Reports	302,086	4.011	1.061540
16	Journal of the Royal Society Interface	12,933	3.224	0.029190
17	NPJ Microgravity	203	3.111	0.000670
18	PHILOSOPHICAL TRANSACTIONS OF THE ROYAL SOCIETY A-MATHEMATICAL PHYSICAL AND ENGINEERING SCIENCES	19,227	3.093	0.028200

## 14. Print copy of publication










ARTICLE



<https://doi.org/10.1038/s41467-021-22464-x>

OPEN

# Spreading depression as an innate antiseizure mechanism

Isra Tamim <sup>1,2</sup>, David Y. Chung <sup>1,3</sup>, Andreia Lopes de Morais <sup>1</sup>, Inge C. M. Loonen <sup>1</sup>, Tao Qin<sup>1</sup>, Amrit Misra<sup>3</sup>, Frieder Schlunk<sup>2</sup>, Matthias Endres <sup>2</sup>, Steven J. Schiff <sup>4</sup> & Cenk Ayata <sup>1,3</sup>✉

Spreading depression (SD) is an intense and prolonged depolarization in the central nervous systems from insect to man. It is implicated in neurological disorders such as migraine and brain injury. Here, using an in vivo mouse model of focal neocortical seizures, we show that SD may be a fundamental defense against seizures. Seizures induced by topical 4-aminopyridine, penicillin or bicuculline, or systemic kainic acid, culminated in SDs at a variable rate. Greater seizure power and area of recruitment predicted SD. Once triggered, SD immediately suppressed the seizure. Optogenetic or KCl-induced SDs had similar antiseizure effect sustained for more than 30 min. Conversely, pharmacologically inhibiting SD occurrence during a focal seizure facilitated seizure generalization. Altogether, our data indicate that seizures trigger SD, which then terminates the seizure and prevents its generalization.

<sup>1</sup>Neurovascular Research Unit, Department of Radiology, Massachusetts General Hospital, Harvard Medical School, Boston, MA, USA.

<sup>2</sup>Charité-Universitätsmedizin Berlin, Klinik und Hochschulambulanz für Neurologie und Centrum für Schlaganfallforschung Berlin (CSB), Berlin, Germany.

<sup>3</sup>Department of Neurology, Massachusetts General Hospital, Harvard Medical School, Boston, MA, USA. <sup>4</sup>Center for Neural Engineering, Departments of Engineering Science and Mechanics and Physics, The Pennsylvania State University, State College, PA, USA. ✉email: [CAYATA@mgh.harvard.edu](mailto:CAYATA@mgh.harvard.edu)

**S**preading depression (also known as spreading depolarization, SD) is an intense but self-limited neuronal and glial depolarization wave that slowly propagates (millimeters/minute) in the gray matter by way of chemical contiguity<sup>1</sup>. Near-total loss of transmembrane ion gradients during SD precludes action potential generation and silences synaptic transmission for more than a minute. These properties prompted Leão to name the phenomenon “spreading depression” more than 75 years ago<sup>2</sup>.

All known triggers for SD are strong and sustained depolarizing events (e.g., ischemia, trauma) elevating extracellular  $[K^+]$  above a critical threshold of 12 mM. Yet SD is also the physiological basis of migraine aura<sup>3</sup>, and how and why such an intense depolarization event is initiated in ostensibly normal brains of migraine sufferers has perplexed scientists for decades. In fact, SD has been observed in the central nervous systems of all species studied to date from insect to man. It appears to be a fundamental intrinsic property of neurons and neuronal ensembles that somehow affords a survival advantage. The nature of the survival advantage (i.e., the selection pressure) and the significance of SD for normal brain function, however, have been a mystery.

Migraine aura and epilepsy are comorbid paroxysmal disorders, and hyperexcitability, also implicated in migraine, is one mechanism that can incite SD. For example, mutations in  $Ca_v2.1$  voltage-gated calcium channels in familial hemiplegic migraine<sup>4</sup> and pharmacological disinhibition by GABA<sub>A</sub> receptor blockers<sup>5</sup> facilitate and trigger SD. Both are also known to predispose to seizures. Moreover, seizures and SD share common triggers<sup>1</sup>, and seizures culminate in SD both in experimental animals<sup>6,7</sup> and in humans<sup>8</sup>. Indeed, a mixed dynamic of seizure and SD is predicted by an extended Hodgkin–Huxley model incorporating cell volume changes and oxygen availability, suggesting that seizures and SD represent a dynamic continuum of neuronal membranes<sup>9,10</sup>.

These observations raise the intriguing hypothesis that highly focal seizure activity triggers SD, and SD, by its electrical silencing effect, terminates the seizure. Here, we tested this hypothesis by undertaking a comprehensive examination of the reciprocal interactions between highly focal cortical seizures and SD. Our data provide the first direct proof-of-concept for an antiseizure role for SD and implicate highly focal seizures as potential triggers for migraine aura.

## Results

**Focal cortical seizures induced by topical application of epileptogenic agents.** In animals with topical vehicle application (0.9% NaCl), ECoG morphology and power density remained normal and stable for the entire duration of recordings (Fig. 1; setup as in Supplementary Fig. 1B, a). All three epileptogenic agents induced seizures within 10 min after topical application. Seizure morphology, duration, and the increase in ECoG power density within each frequency band differed among the three agents, recorded for a maximum of 4 h (Fig. 1, also see Supplementary Fig. 2 for ECoG at expanded time scale). Potassium channel blocker 4AP (100 mM) induced synchronized monomorphic spiking that gradually evolved into a periodic burst pattern. The electrographic pattern consisted of large amplitude (~400% of baseline) rhythmic discharges that started at ~1 Hz and evolved to ~4 Hz before attenuation. The cycle repeated itself over a ~30-min period. During bursting, the largest peak power density increase was within the  $\delta$  frequency range (0–4 Hz, 7.3-fold) followed by  $\theta$  (4–8 Hz, 3.2-fold) and  $\alpha$  (8–12 Hz, 3.4-fold) bands. Seizures typically lasted well over 2 h with gradually decreasing synchronization and burst duration. In contrast, GABA-A receptor antagonist PG (188434 IU/ml) induced near-continuous high-amplitude periodic spikes that changed polarity

in a subset of experiments after  $41 \pm 13$  min. The electrographic pattern started as ~0.5 Hz spike-wave activity with an amplitude ~250% over baseline and evolved in amplitude to ~600% over baseline with continuous ~0.5 Hz activity. This pattern developed over a ~70-min period. The largest peak power density increase with PG was within the  $\alpha$  (13.7-fold) and  $\theta$  (12.4-fold) bands followed by  $\delta$  (3.6-fold) band; power increase in the  $\theta$  band lasted for the duration of the recordings (4 h), while a band power increase resolved within 90 min. The second GABA-A receptor antagonist BIC (5 mM) induced seizures that were similar to PG in morphology and peak power density increase (19.9-fold in  $\alpha$ , 13.3-fold in  $\theta$ , 3.4-fold in  $\delta$ ), but spikes typically remained negative and lasted less than an hour (note time scale on Fig. 1). The electrographic pattern started as ~0.2 Hz spike-wave activity with an amplitude of ~120% of baseline and evolved into ~2 Hz spike-wave activity with an amplitude of ~250%. This pattern developed over a ~40-min period. The epileptogenic effect was concentration-dependent when tested for 4AP and BIC.

**Focal cortical seizures trigger spreading depression.** Neocortical seizures culminated in one or more SDs associated with large slow (DC) potential shifts in the seizure focus (Fig. 2; setup as in Supplementary Fig. 1B, a). These always propagated to the remote ipsilateral recording site, coupled to characteristic CBV transients on IOS imaging (Supplementary Movie 1). The highest proportion of animals that developed SD was during 4AP-induced seizures (69%,  $n = 32$  mice), followed by PG (33%,  $n = 9$  mice) and BIC (9%,  $n = 11$  mice;  $p = 0.002$ ,  $\chi^2$ ; Fig. 3A). Lower concentrations of 4AP (5 or 30 mM) or BIC (0.005, 0.5, and 1 mM) led to smaller and shorter-lasting concentration-dependent ECoG power density elevations but did not trigger SD ( $n = 9$  total). In most cases, SDs recurred singly or in clusters (Fig. 3B); all recurrent SDs appeared de novo rather than as reentrant or circling SDs on IOS imaging. The frequency of SDs was  $0.89 \pm 0.22/h$ ,  $0.26 \pm 0.17/h$ , and  $0.74 \pm 0.74/h$  after 4AP, PG, and BIC, respectively. The overall frequency of SDs decreased over time (only 4AP shown; Fig. 3C) associated with a gradual weakening of seizure power (Fig. 1). Full-field IOS imaging showed that although most SDs originated in the vicinity of the seizure focus, some emerged as far away as the frontal cortex, suggesting that they were triggered by generalized seizure activity (Fig. 3D). Vehicle application did not result in SD.

A proportion of SDs failed to fully penetrate the center of the seizure focus, as previously reported with repetitive ictal events<sup>11</sup>. These non-penetrant SDs were detected mainly as smaller positive DC shifts (Fig. 3E). The non-penetrant SD proportions for the first and the subsequent SDs were 48% and 50%, respectively, after 4AP, and 33% and 67%, respectively, after PG. In contrast, all SDs penetrated the seizure focus during BIC-induced seizures. The non-penetrant SD rate appeared to increase over time suggesting a growing resistance at the focus (Fig. 3F).

**Inhibition by tetrodotoxin confirms seizures as the immediate trigger for SD.** To test whether SDs that developed during a seizure is indeed triggered by seizure activity itself rather than by a direct SD-inducing effect of 4AP, we topically pretreated the cortex with the voltage-gated  $Na^+$  channel blocker tetrodotoxin (TTX, 30  $\mu$ M) 30 min before 4AP application (Supplementary Fig. 3; setup as in Supplementary Fig. 1B, b). TTX depressed ECoG power, blocked seizure induction after 4AP (compare with Fig. 1B), and completely prevented SD occurrence ( $n = 5$ ;  $p = 0.005$  4AP + TTX vs. 4AP alone,  $\chi^2$ ). Importantly, at the end of the experiments, we confirmed that TTX did not directly block SD by successfully inducing an SD via topical KCl application at the remote site and detecting the characteristic negative DC

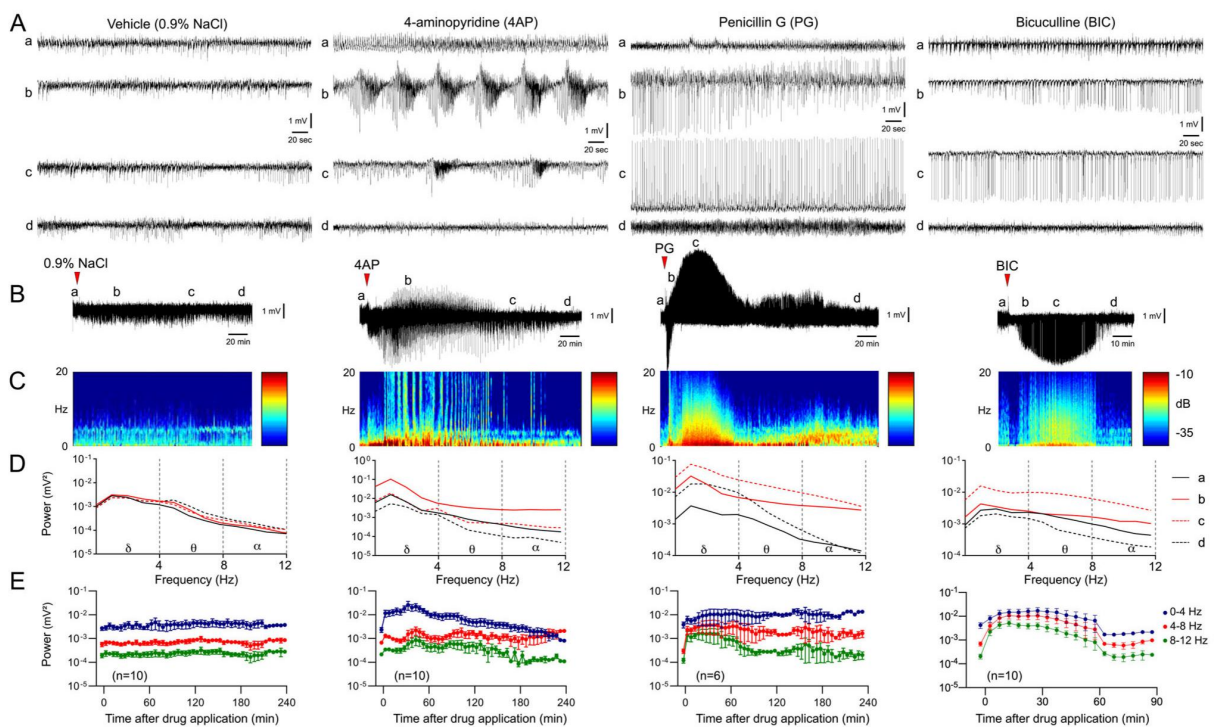


**Fig. 1** Characteristics of focal cortical seizures induced by 4AP, PG, and BIC. **A** Representative ECoG tracings show baseline (a), early and late seizure activity (b, c), and resolution (d) during 4AP, PG, or BIC microseizures, as indicated on the full ECoG timeline (**B**). **C** Time–frequency–power spectra of the full timeline shown in (**B**) calculated using Thomson’s multitaper method. **D** Power density at the four phases (a–d) computed using FFT. **E** Average ECoG power time course in  $\delta$  (0–4 Hz),  $\theta$  (4–8 Hz) and  $\alpha$  (8–12 Hz) frequency bands are shown on a logarithmic scale ( $\pm$ SEM). Sample sizes are indicated on the graphs.

potential shift at the TTX application site (Supplementary Fig. 3, upper right panel).

**Power density increase in the  $\delta$  frequency range predicts SD occurrence.** We next sought to elucidate the determinants of SD occurrence during focal seizures. Comparison of peak power increase in  $\delta$  (0–4 Hz),  $\theta$  (4–8 Hz) and  $\alpha$  (8–12 Hz) bands among the three epileptogenic agents showed that  $\delta$  band power increase was greatest after 4AP (Supplementary Fig. 4A), where SD occurrence rate was also the highest (Fig. 3A). Comparison of ECoG power immediately preceding an SD in the  $\delta$ ,  $\theta$  and  $\alpha$  bands between experiments with or without a spontaneous SD further supported an association between power increase in  $\delta$  range and SD occurrence (Supplementary Fig. 4B). Of note, arterial blood pressure, pH,  $p\text{CO}_2$ ,  $p\text{O}_2$ , and glucose remained within physiological ranges and did not predict SD occurrence in any of the experiments (Supplementary Table 1).

**Generalization of seizures across the cortex predicts SD occurrence.** In a subset of mice, 4AP-induced epileptiform activity appeared at the remote ipsilateral anterior recording site and the contralateral homotopic recording sites (36% and 26% of animals, respectively) suggesting seizure generalization (Supplementary Fig. 5, representative tracings a–c and representative spectrograms d–e). We, therefore, examined the relationship between generalization and spontaneous SD occurrence in the 4AP cohort. All nine mice that showed electrophysiological evidence of seizure generalization at the remote sites developed an SD, whereas none of the eight mice that never developed an

SD showed such generalization ( $p = 0.031$ ,  $\chi^2$ ), suggesting that seizure generalization predicts SD occurrence.

To better examine the relationship between seizure generalization and SDs, we determined the spatial reach of seizures across the cortex by making use of the cortical hyperemic response to seizure activity detected with IOS imaging. The periodic bursts induced by 4AP created conspicuous hyperemic transients on IOS images<sup>12</sup> that were locally tightly coupled to epileptic bursts (Supplementary Movie 1; Fig. 4A). Using this surrogate, we tested whether the spatial extent of cortical seizures predicted SD occurrence by placing five regions of interest (ROIs 1–5) 1 mm apart on a line of interest (LOI) extending anteriorly (Fig. 4B). This approach allowed us to visualize the spatial reach of hyperemic transients caused by the periodic burst pattern both along with the LOI and within each ROI over time (Fig. 4C). We found that 69% of all animals ( $n = 32$ ) showed hyperemic transients at the 4AP application site (Fig. 4D, ROI 1); the rest of the cohort (31%) did not show IOS transients despite the presence of electrographic seizures. The fraction of animals showing hyperemic transients in each ROI decreased as a function of distance such that only 28% of animals showed hyperemic transients farthest from the 4AP application site (i.e., ROI 5). Moreover, the latency to the onset of hyperemic transients in each ROI increased as a function of distance, suggesting that the spatial extent of cortical involvement with seizure activity gradually increased over time. When we segregated the experiments based on SD occurrence, we found that focal cortical seizures spread significantly farther from the 4AP application site in experiments where SDs occurred compared with those without an SD ( $p = 0.013$ ; Mann–Whitney test; Fig. 4E). The power map of CBV fluctuations linked to

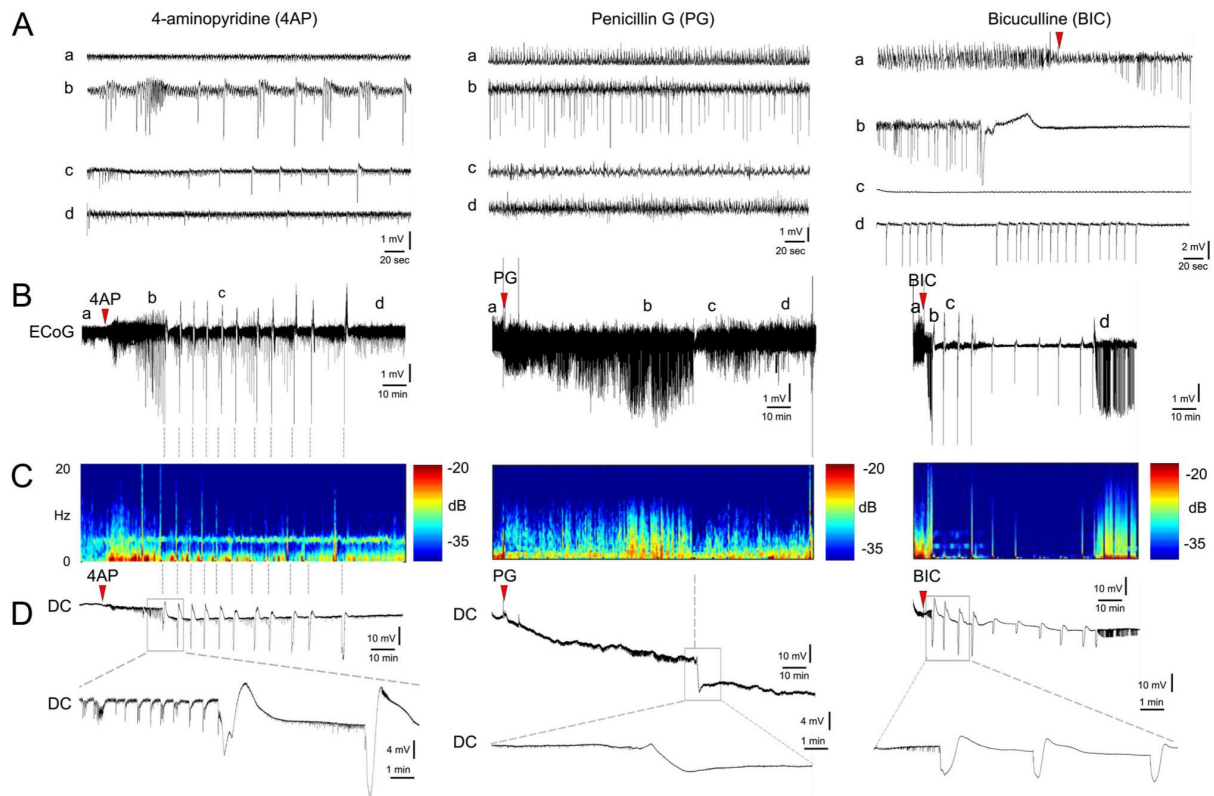


**Fig. 2 Focal cortical seizures trigger spreading depression.** **A** Representative tracings show typical ECoG phases (a–d) of 4AP, PG, or BIC microseizures, as indicated on the full ECoG timeline (**B**). Red arrowheads show the time of drug application. Vertical dashed lines indicate SDs. **C** Time–frequency–power spectra of the full timeline shown in **B** calculated using Thomson’s multitaper method. **D** Corresponding DC tracings show one or more SDs triggered during the seizures as large negative slow potential shifts. Boxes indicate expanded views. These were simultaneously confirmed on IOS as SD waves. A total of 11 spontaneous SDs originated from the 4AP window starting 23 min after drug application in this animal. PG seizure triggered 1 SD at 134 min and BIC seizure triggered 10 SDs between 3 and 60 min.

cortical bursts confirmed this finding (Fig. 4F for representative maps). These data showed that the wider the spatial reach of cortical seizure activity, the higher the likelihood of spontaneous SD occurrence. Importantly, IOS changes during seizure-induced SDs (see Supplementary Fig. 6 for a representative experiment) were similar to hemodynamic changes during SDs induced by other methods (e.g., topical KCl) in migraine models<sup>13,14</sup>. When an SD did not penetrate the seizure focus, it did not cause major IOS changes.

**SD terminates focal cortical seizures and limits their reemergence.** With all three epileptogenic agents, a highly conspicuous effect of SD was seizure suppression that lasted far beyond the characteristic ECoG depression after SD. To systematically test this, we induced SD by topical KCl application at a remote site after seizure onset and quantified its effect on local seizure activity (Fig. 5, setup as in Supplementary Fig. 1B, b). Induced SDs that propagated to and penetrated the seizure focus immediately extinguished all epileptiform activity triggered by 4AP, PG, or BIC. In the wake of SD, ECoG recovered within 10 min but never returned to power levels associated with the seizure activity prior to SD (Fig. 5E). In most cases, seizures did not reignite even when occasional spike activity returned, despite the continued presence of the seizure-inducing agent on the cortex.

Moreover, an SD induced shortly before the application of the seizure-inducing agent diminished the emergence of seizure activity with all three drugs (Fig. 6A). Even when induced 30 min

prior to the 4AP application, SD was still capable of depressing seizure intensity for at least 60 min, suggesting that the antiseizure effect of SD lasts more than 90 min (Fig. 6B). These data showed that SD is a powerful and lasting inhibitor of seizure activity.

**SD limits the generalization of seizures across the cortex.** To determine the effect of induced SD on the spatial reach of seizures across the cortex, we once again used the hyperemia coupled to seizure activity on IOS imaging (Fig. 7). As expected from diminished seizure activity at the focus, an SD induced 30 or 5 min before, or approximately 30 min after 4AP, all decreased seizure generalization assessed by the proportion of distant ROIs showing seizure-induced hyperemia, as well as the average distance from the drug application site (ROI 1) to which the hyperemia reached (Fig. 7B–D, red circles;  $p = 0.006$  for 4AP,  $p = 0.010$  for PG,  $p = 0.016$  for BIC data set; one-way ANOVA).

We also confirmed this by ECoG recordings outside the 4AP site (Supplementary Fig. 7). An SD induced after the generalization of seizure activity to this location strongly suppressed the seizure. The ECoG power returned to the pre-seizure baseline within 10 min but did not reach pre-SD seizure levels for at least 30 min ( $p < 0.001$ , one-way ANOVA; Supplementary Fig. 7C). These data suggested that SD also limits seizure generalization. Hence, not only larger areas of the neocortex recruited into the seizure increased the chance of SD occurrence (see Fig. 4E above), but SDs, in turn, diminished the area of neocortex recruited into



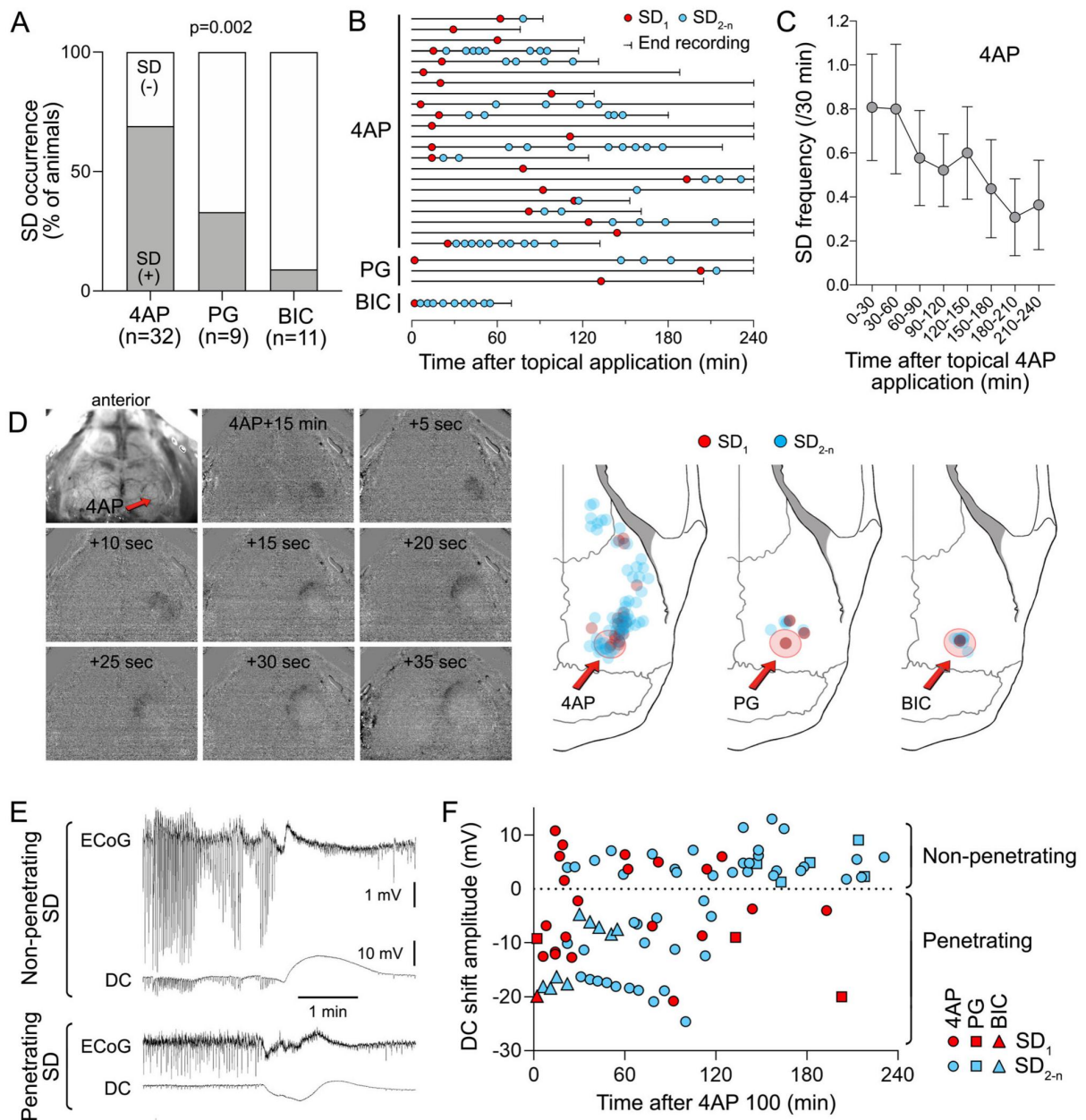


**Fig. 3** Characteristics of SDs triggered by focal cortical seizures. **A** The proportion of animals developing SD with each epileptogenic agent ( $p = 0.002$ ;  $\chi^2$ ). Sample sizes are indicated below each bar. **B** Experimental timelines showing first ( $SD_1$ , red symbols) and subsequent SDs ( $SD_{2-n}$ , blue symbols). Each line represents the duration of recording in one experiment and each symbol represents one SD. Only experiments with at least one SD are shown. **C** The decrease in SD occurrence overtime after 4AP application (30-min bins) likely reflects weakening seizures ( $\pm$ SEM). **D** Time-lapse IOS subtraction images of an SD originating and spreading anteriorly 15 min after 4AP application (red arrow). The right panel shows the origins of the first and subsequent SDs for each drug. Most SDs originated in the vicinity of the seizure focus. In 4AP seizures, subsequent SDs were more likely to erupt farther from the seizure focus, presumably due to generalization. **E** Representative ECoG and DC tracings of penetrating and non-penetrating SDs recorded by the epidural electrode over the seizure focus. Seizure-induced SDs were uncharacteristically variable in amplitude and duration. **F** The slow (DC) potential shift of the first and subsequent SDs transformed from predominantly negative to predominantly positive over time as the seizure focus became more resistant to SD penetration. Each drug is represented by a different symbol.

the seizure, displaying a feedback mechanism to limit seizure generalization.

**Optogenetically-induced SDs also show the strong antiseizure effect.** Because topical KCl application is an invasive method requiring a craniotomy to trigger SD, we next tested whether

optogenetic SDs induced non-invasively through the intact skull in  $Chr2^+$  mice<sup>15</sup> also suppress seizures. We found that a single optogenetic SD induced approximately 30 min after 4AP application indeed extinguished the focal seizure (Supplementary Fig. 8A) and tended to reduce its spatial reach (Supplementary Fig. 8B), non-invasively confirming the antiseizure effect of SD.

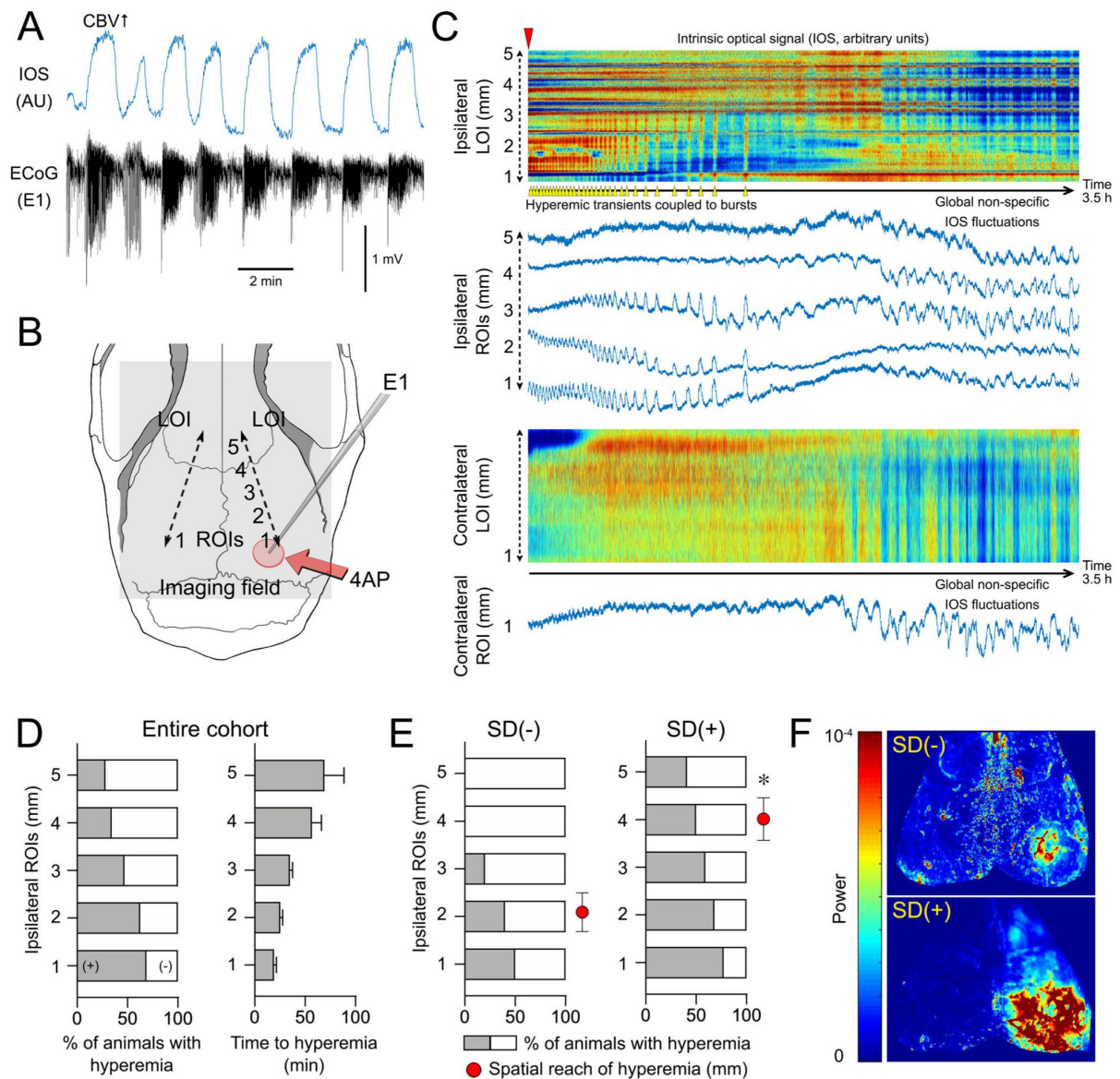


**Fig. 4 Spatial reach of seizures across the cortex predicts SD occurrence.** **A** Representative 4AP experiment shows hyperemia coupled to seizure bursts (AU, arbitrary unit) used as a surrogate to examine the spatial spread of the seizure. **B** We placed a line of interest (LOI) extending from the drug application site anteriorly on the ipsilateral hemisphere, and one symmetrically on the contralateral hemisphere (dashed lines). Five ROIs (1–5) were placed along with the ipsilateral LOI at 1 mm intervals and a contralateral ROI was placed symmetrically to ipsilateral ROI 1. **C** IOS intensity along with the two LOIs and in each ROI are plotted over time. Red indicates an increase and blue decreases in CBV. Hyperemic transients (yellow arrowheads) reached ROI 3 within 25 min after 4AP (red arrowhead) but did not extend to ROI 4 (experiment without SD). Contralateral LOI and ROI did not show hyperemic bursts, indicating a lack of generalization. Non-specific CBV fluctuations (e.g., due to blood pressure), were distinguishable by their global nature and time course. **D** The proportion of animals that developed hyperemic transients within each ROI and the time of their onset after 4AP application ( $\pm$ SEM). **E** Hyperemic transients showed a farther spread in animals that eventually developed an SD. Red circles indicate the average distance hyperemic transients reached from the drug application site in each subgroup ( $*p = 0.012$ , unpaired *t*-test;  $\pm$ SEM). **F** Representative CBV power maps show a larger area of cortex with the hyperemic transients in the animal that eventually developed an SD (red high and blue low power).

**Suppression of spontaneous SD occurrence enhances seizure intensity and generalization.** Data thus far strongly suggested that KCl-induced or optogenetic SDs exerted a potent antiseizure effect. We also examined the effect of spontaneous SDs on seizure power and found a significant suppression (Fig. 8). Because the timing of spontaneous SDs was variable among the experiments (unlike induced SDs as above), we only examined the first SD in each experiment. Next, we pharmacologically blocked

spontaneous SDs with NMDA receptor blocker MK-801 to test whether eliminating the SDs and thus their antiseizure effect, facilitates 4AP seizures and their generalization. MK-801 decreased the proportion of mice that developed an SD (33%), and reduced SD frequency by more than 80% ( $0.14 \pm 0.06/h$ ,  $n = 12$  mice) compared with control experiments ( $0.89 \pm 0.22/h$ ,  $n = 32$  mice), without suppressing the seizure intensity. On the contrary, SD-suppression by MK-801 facilitated seizure generalization to the

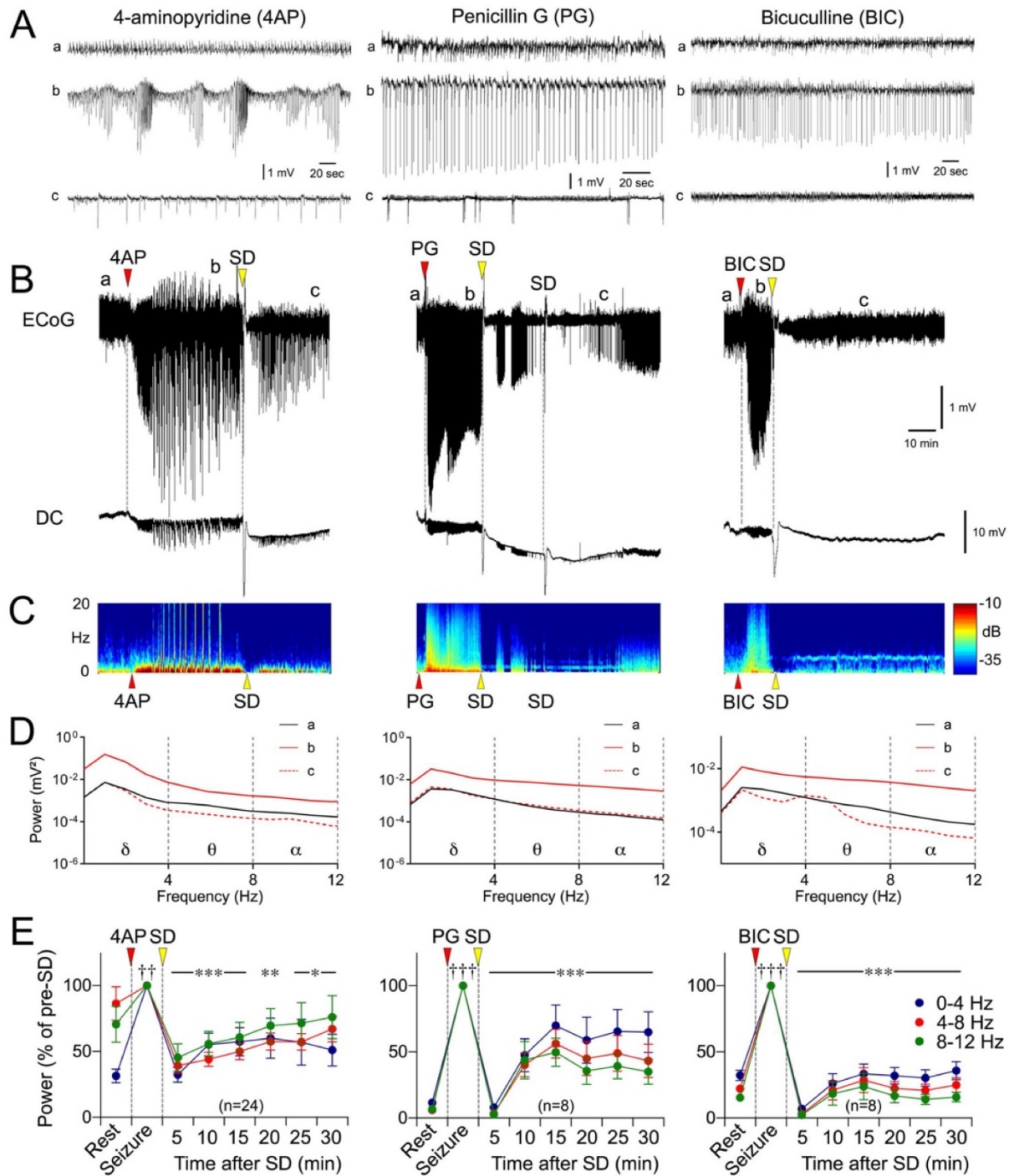


**Fig. 5 Exogenously induced SD terminates focal cortical seizures and limits their reemergence.** **A** Representative tracings show ECoG at baseline (a), during 4AP, PG, or BIC microseizures (b), and after an exogenously induced SD (c), as indicated on the full ECoG timeline (**B**). Recordings are from the drug application site, (E1, Supplementary Fig. 1B, b). Red arrowheads show the time of drug application. Induced SDs (yellow arrowheads) and the abrupt seizure termination are seen on the DC and ECoG tracings, respectively. Note that a second SD spontaneously originated from the seizure focus in this PG experiment. **C** Time–frequency–power spectra of the full timeline shown in **B** calculated using Thomson’s multitaper method also show an abrupt reduction in seizure power associated with SDs. **D** Power density at the three phases (a–c) computed using FFT further demonstrates the lasting seizure power reduction after SD. **E** Average ECoG power time course in  $\delta$  (0–4 Hz),  $\theta$  (4–8 Hz), and  $\alpha$  (8–12 Hz) frequency bands show ECoG power at rest, during the seizure (5 min prior to SD, and every 5 min thereafter (5–30 min), expressed as % of pre-SD seizure power. All frequency bands show a significant reduction in seizure power for at least 30 min after SD. SD was induced at  $37 \pm 3$  min (13–69) after 4AP application,  $19 \pm 0$  min (17–20) after PG application, and  $13 \pm 2$  min (10–18) after BIC application (mean  $\pm$  standard error and full range). Sample sizes are shown on the graphs. †–††† $p < 0.05$ –0.001 vs. R; \*–\*\*\* $p < 0.05$ –0.001 vs. S (two-way ANOVA for repeated measures;  $\pm$ SEM).

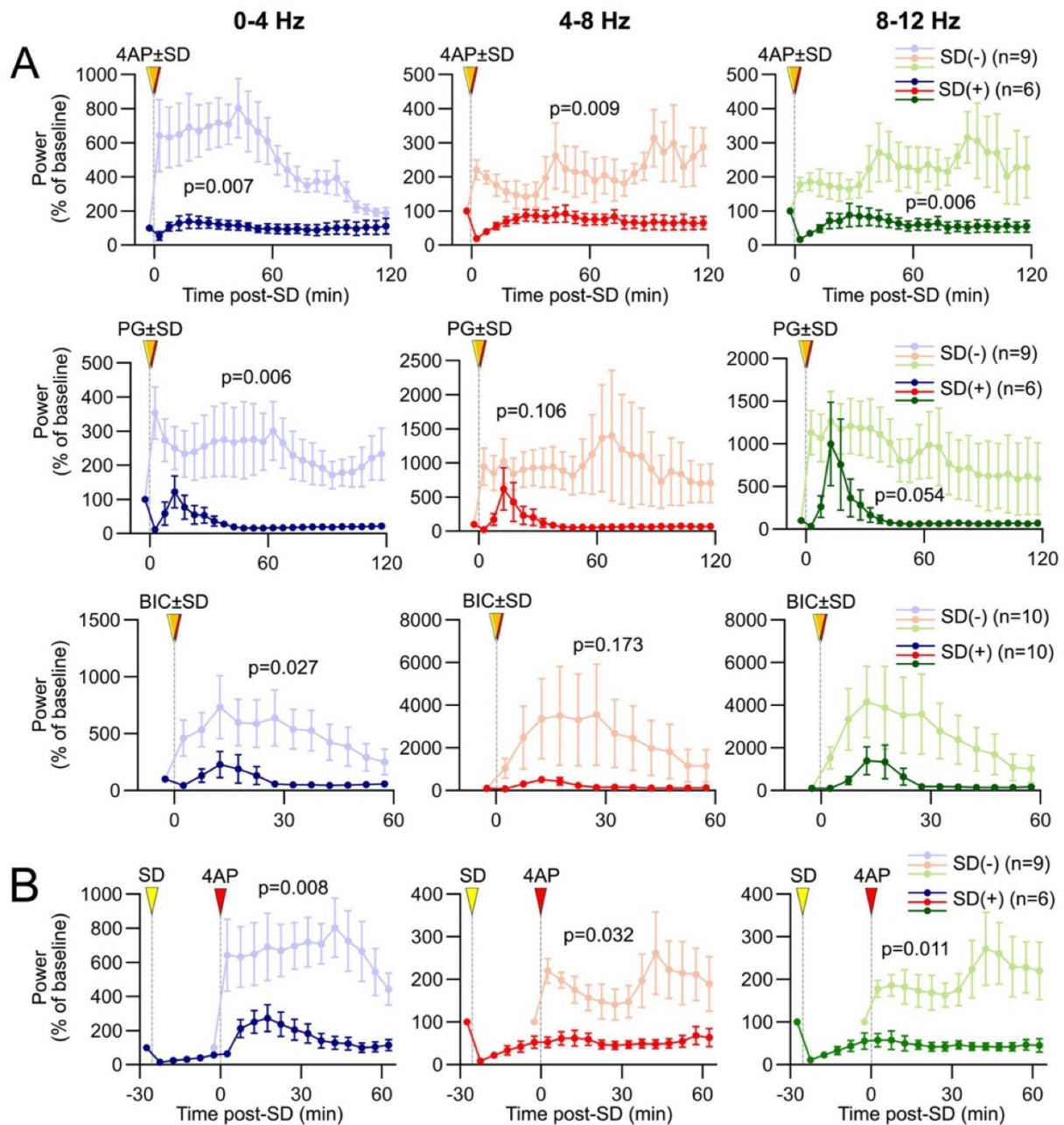


**Fig. 6 Pre-treatment with SD strongly inhibits the emergence of seizure activity. A** Average ECoG power time course graphs (5-min bins) expressed as % of baseline (-5 min) show that an SD induced (yellow arrowheads) 5 min before 4AP, PG or BIC application (red arrowheads) significantly diminished seizure intensity (bold curves) compared with controls without an SD (faint curves). **B** An SD induced 30 min before 4AP application still significantly suppressed subsequent seizure activity for at least 90 min. Data are from the drug application site (E1, Supplementary Fig. 1B). Each frequency band is shown separately. Exact p values are shown for SD (-) vs. SD (+), using two-way repeated-measures ANOVA.

ipsilateral and the contralateral remote recording sites (92% and 89%, respectively; Fig. 9A), compared with control animals (see above). Indeed, ECoG power increase after 4AP was significantly larger in both the ipsilateral and the contralateral remote recording sites in the MK-801 group (Fig. 9B). Once again using the hyperemic transients coupled to periodic bursts, we further confirmed robust seizure generalization in both the ipsilateral and the contralateral ROIs after MK-801 on IOS images (Fig. 9C). Altogether, these data indicated that spontaneously occurring SDs

during highly focal seizures are capable of exerting an antiseizure effect. Suppression of SD occurrence by MK-801 eliminated this endogenous antiseizure mechanism.

**Familial hemiplegic migraine knock-in mice.** We next sought to reproduce our findings in a migraine-relevant knock-in mouse model expressing the S218L familial hemiplegic migraine type 1 (FHM1) mutation in the Cav2.1 voltage-gated Ca<sup>2+</sup> channels.

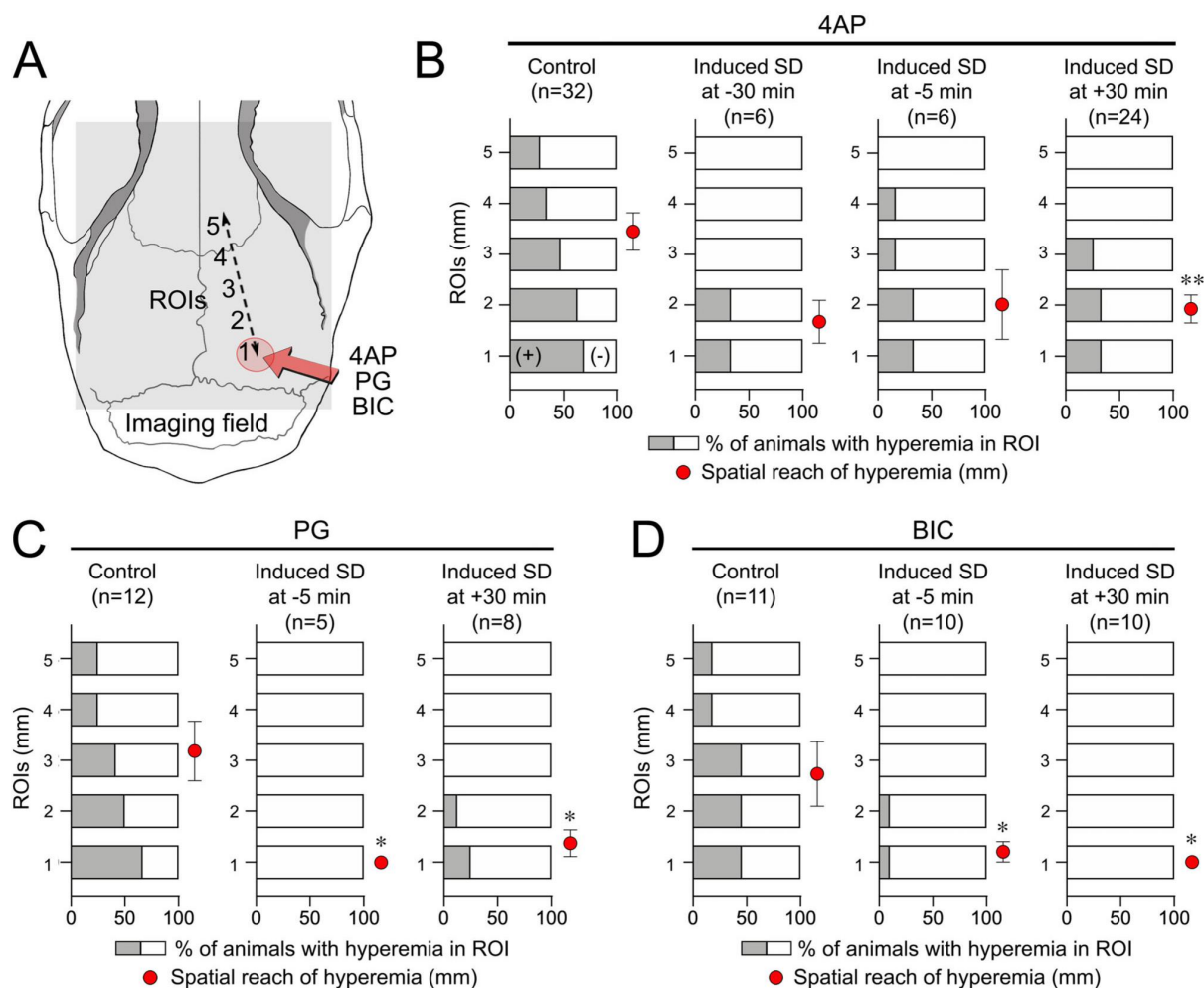


**Fig. 7 SD limits the spatial reach of seizures across the cortex. A** Diagram showing the ROI placement for IOS analysis. **B–D** The proportion of animals that developed hyperemia within each of the five ROIs coupled to 4AP, PG, or BIC seizures show that the spatial reach of seizures was diminished by an SD induced 30 min before (–30 min), 5 min before (–5 min) or 30 min after (+30 min) drug application. All SDs were remotely induced by topical KCl application using the setup shown in Supplementary Fig. 1B, b. The control group did not receive any SD intervention from outside, but 22 animals in 4AP, 3 animals in PG, and 1 animal in the BIC control group developed spontaneous SDs (as summarized in Fig. 3A, B). Red circles indicate the average distance hyperemic transients reached from the drug application site in each subgroup (no hyperemic transients in any ROI is 0 mm). \*–\*\*\* $p < 0.05$ –0.01 vs. control, one-way ANOVA followed by Dunnett’s multiple comparison’s tests ( $\pm$ SEM).

Topical application of 4AP (100 mM) induced typical seizures in both the FHM1 knock-in mice and their wild-type (WT) littermates (Supplementary Fig. 9). Despite lower peak power levels reached during the seizures, 7 out of 8 FHM1 mutants developed SDs, compared with only 1 out of 6 of their WT littermates ( $p = 0.008$ ,  $\chi^2$ ; Supplementary Fig. 9B). In FHM1 mutants, SDs often occurred in clusters (Supplementary Fig. 9C). The average SD frequency in FHM1 mutants ( $3.0 \pm 0.7$  SDs/h) was markedly higher than the WT littermate that developed an SD (1.3 SDs/h), as well as the CD1 mice ( $0.9 \pm 0.2$  SDs/h). The majority of SDs in FHM1 mutants penetrated the seizure focus and thus were associated with negative DC potentials shifts. However, the DC shift amplitude decreased over time suggesting a gradually developing resistance to SD at the seizure focus similar to CD1 mice (Supplementary Fig. 9D). More importantly, spontaneously developing SDs in FHM1 mutants also suppressed seizure intensity (Supplementary Fig. 9E).

**Generalized seizures upon systemic kainate administration.** Lastly, we extended our findings to a generalized seizure model using systemic kainate injection (60 mg/kg, intraperitoneal in CD1 mice,  $n = 7$ ). Electrophysiological recordings from the hippocampal CA1 region revealed a characteristic pattern of recurrent seizures consistent with electrographic status epilepticus in all mice that started gradually and gained strength within 30–60 min of kainate administration. Seizures were characterized by rhythmic 15–30 Hz activity with evolution in amplitude to 300% of baseline followed by the onset of 1–2 Hz rhythmic discharges measuring up to 8 mV. Discharges slowed and decreased in amplitude after 15–60 s giving way to post-ictal voltage attenuation. These recurred every 1–3 min with increasing intervals (Fig. 10A). All mice developed a hippocampal SD during kainate seizures. SDs occurred either during a seizure burst or shortly thereafter, the latter suggesting an SD origin farther from the recording site. In the wake of an SD, seizures were completely

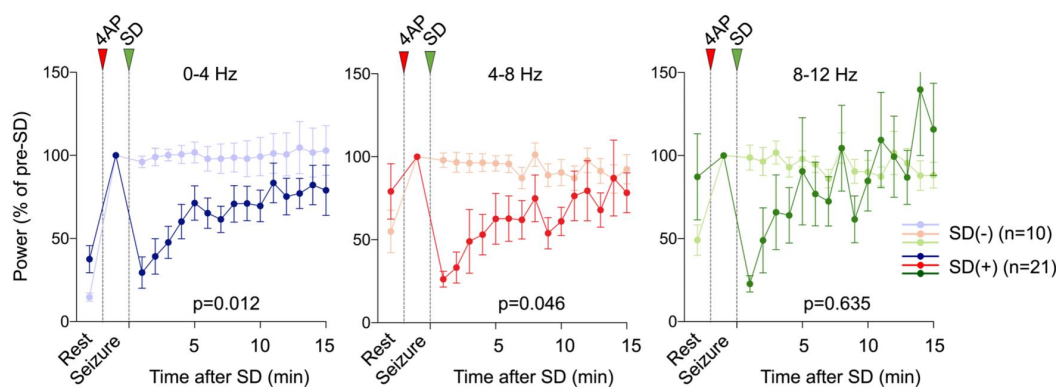


**Fig. 8 Spontaneously occurring SD terminates focal cortical seizures and limits their reemergence.** Average ECoG power time course in  $\delta$  (0–4 Hz),  $\theta$  (4–8 Hz), and  $\alpha$  (8–12 Hz) frequency bands show ECoG power at rest, during the seizure (5 min prior to SD, and every minute thereafter, expressed as % of pre-SD seizure power). Spontaneously arising SD significantly diminished seizure intensity (bold curves) compared with controls without an SD (faint curves) in  $\delta$  (0–4 Hz) and  $\theta$  (4–8 Hz) bands (two-way ANOVA for repeated measures;  $\pm$ SEM). Sample sizes are shown on the graph. Only the first SD in each experiment is analyzed.

suppressed for 10 min, and seizure power did not return to pre-SD levels for at least 30 min (Fig. 10B).

## Discussion

Our systematic examination using topical application of three different seizure-inducing agents shows that highly focal cortical seizures are capable of triggering SD. Both the ECoG's greater power increase in the  $\delta$  frequency band and greater spatial extent of generalization were positive predictors of SD occurrence, which was also enhanced by a human migraine mutation. In turn, SDs suppress seizures for more than 30 min, far beyond the brief electrophysiological silence associated with SD. Generalized seizures upon systemic kainate administration reproduced nearly identical findings.

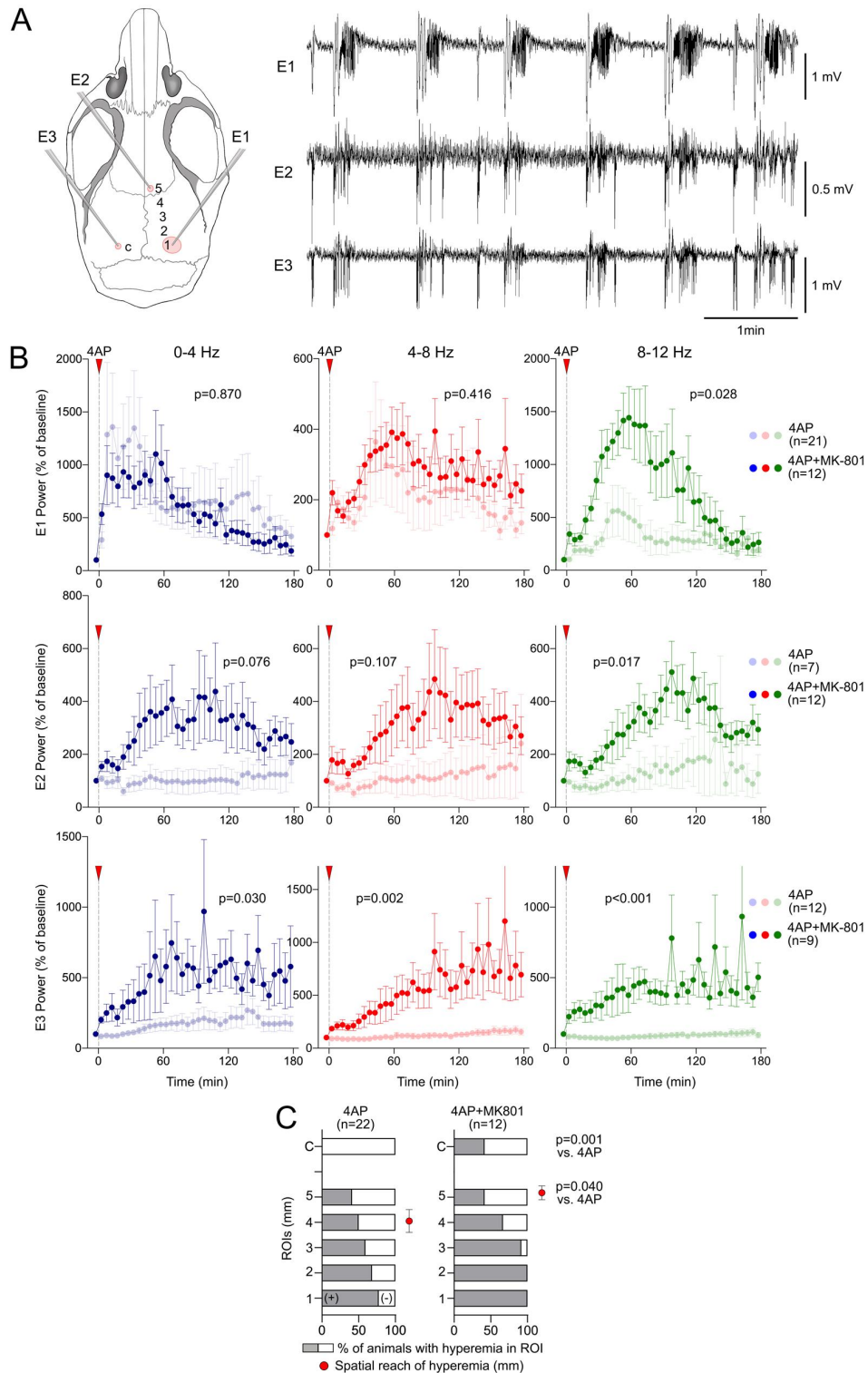
**A unifying theory.** Based on these findings, we propose a unifying theory wherein SD is a fundamental endogenous antiseizure mechanism in the central nervous system. As such, SD is triggered if and when synchronized focal neuronal network activity collectively raises extracellular  $K^+$  above the 12 mM threshold in a minimum critical volume of tissue, which is estimated to be  $\sim 1$  mm<sup>3</sup><sup>16</sup>. SD then acts as an ‘emergency brake’ or ‘reboot’ extinguishing the seizure and propagates centimeters away from the focus to exert a broader antiseizure effect. The latter is clinically perceived as a migraine aura (Supplementary Movie 2). Clearly, the organism is better off experiencing a migraine aura than seizures, status epilepticus, or generalized convulsions in terms of survival advantage, because they can lead to loss of consciousness, bodily harm, and prolonged post-ictal encephalopathy, and may even be terminal. Therefore, SD can be beneficial in the context of seizures. As such, our theory may explain the evolutionary purpose and persistence of SD.

Our theory can also explain the clinical overlap between epilepsy and migraine with aura, two comorbid, chronic-episodic, paroxysmal disorders. As eloquently outlined by Rogawski<sup>17</sup>, epilepsy, and migraine with aura share a number of common features: (a) higher prevalence of epilepsy in migraine with aura sufferers than the general population and vice versa<sup>18,19</sup>; (b) hyperexcitability in both migraine with aura and epilepsy<sup>20,21</sup>; (c) strong genetic underpinnings (e.g., *CACNA1A*, *ATP1A2*, *SCN1A*, *NOTCH3*, and *PRRT2*) associated with both migraine with aura and epilepsy<sup>17,22,23</sup>; (d) frequent occurrence of postictal migrainous headaches after seizures<sup>24,25</sup>; and (e) efficacy of antiepileptic drugs, such as valproate and topiramate, in migraine prophylaxis.

All these shared features support the notion that microseizures may serve as triggers for migraine aura, i.e., SD. Of course, it is unlikely that all auras are triggered by focal seizures and other trigger mechanisms exist.

**Relevance for microseizures.** Given their average spatial reach of only a few millimeters, the focal epileptiform activity generated in our model was akin to human microseizures that are typically below the spatial detection limit of conventional EEG and only detected using implanted microelectrodes in epilepsy patients, as well as in normal subjects<sup>26–28</sup>. Such localized, subclinical epileptiform activity can in fact precede clinical seizures by many hours<sup>29</sup>. Microseizures can spread by recruiting neighboring tissue, and as such, act as a precursor or seed for clinically overt seizure activity<sup>30</sup>. Moreover, microseizures can lead to potentiation of synapses and kindling over time and may be considered an intermediate stage in epileptogenesis<sup>31</sup>. Given the high rate of SD occurrence we detected under a general anesthetic regimen known to suppress SD susceptibility<sup>32</sup>, seizures may trigger SD even more frequently in the unanesthetized brain. Once triggered, SD propagates regionally to prevent seizure spread, and perhaps even kindling, thereby exerting a lasting antiepileptic effect. Most importantly, seizures can perpetuate and lead to excitotoxic cell death, whereas in the absence of metabolic compromise, SD is fundamentally self-limiting (typically < 1 min) and non-injurious even after numerous events<sup>33</sup>, except when prolonged, under hypoxic/ischemic conditions or involving the brainstem<sup>1,34,35</sup>.

**Evidence from other model systems.** Seizures culminating in SD have been observed under various experimental and clinical conditions. For example, focal cortical seizures after topical application of sodium penicillin salt triggered cortical SD waves in rats<sup>36</sup>, spontaneous focal seizures in both post-cerebral malaria and tetanus toxin mouse models of epilepsy triggered SDs<sup>37</sup>, focal cortical seizures after electrical stimulation or topical application of 4AP triggered cortical and/or brain stem SD and death in mutant mouse models<sup>6,35</sup>, and generalized seizures (e.g., maximal electroshock; systemic pentylentetrazol, tetanus toxin or flurothyl; audiogenic; absence) triggered cortical or subcortical SD in multiple species<sup>37–39</sup>. Moreover, in the acutely injured human brain, subdural recordings showed that more than half of the patients who developed seizures also developed SDs, and in most cases, seizures appeared to trigger SD<sup>8</sup>. These data suggest that SD triggered by seizure activity is a ubiquitous phenomenon.



Even recurrent SDs were predicted by the extended Hodgkin–Huxley model<sup>9,10</sup>. More importantly, SDs that developed during focal or generalized seizures were associated with seizure termination, after SD seizures did not return for more than 20 min, and when an SD did not develop seizures typically intensified<sup>38–41</sup>. Similarly, SDs that developed during seizures in

the acutely injured human brain was followed by suppression of seizure activity for more than 15 min even when ECoG activity has recovered<sup>8</sup>. Mechanically or KCl-induced SDs also potently extinguished and/or prevented focal and generalized seizures, sometimes for more than 90 min<sup>42–45</sup>. Altogether, the data strongly suggest that SD is a fundamental endogenous

**Fig. 9 Suppression of spontaneous SDs enhances seizure intensity and generalization.** **A** Left panel: Diagram showing electrode (E1-E3) and ROI (1-5, C) placement. Representative ECoG tracings showing seizure generalization to the remote ipsilateral (E2) and contralateral (E3) electrodes. Such synchronized electrophysiological generalization was common in the MK-801 group but rarely observed in control animals that were allowed to develop SDs. **B** Averaged ECoG power time courses normalized to pre-seizure baseline are shown separately for each electrode and frequency band. Seizure generalization to the remote ipsilateral (E2) and contralateral (E3) electrodes is significantly higher in the MK-801 group (bold symbols) that did not develop any SD compared with time controls that were allowed to develop spontaneous SDs (4AP alone, faint symbols). Seizure intensity at the local electrode (E1) is much less affected (only in 8-12 Hz band). Red arrowheads show the time of the 4AP application. Exact p values are shown on the graphs (two-way ANOVA for repeated measures;  $\pm$ SEM). **C** The proportion of animals that developed hyperemia within each of the six ROIs coupled to 4AP seizures are shown with and without MK-801 treatment. The proportion of animals that showed hyperemic transients in the contralateral ROI (c) was significantly higher in the MK-801 group compared with controls ( $p = 0.001$ ,  $\chi^2$ ). The average distance hyperemic transients reached from the drug application site was significantly higher in the MK-801 group ( $p = 0.040$ ,  $t$ -test with Welch's correction; red circles; no hyperemic transients in any ROI = 0;  $\pm$ SEM).

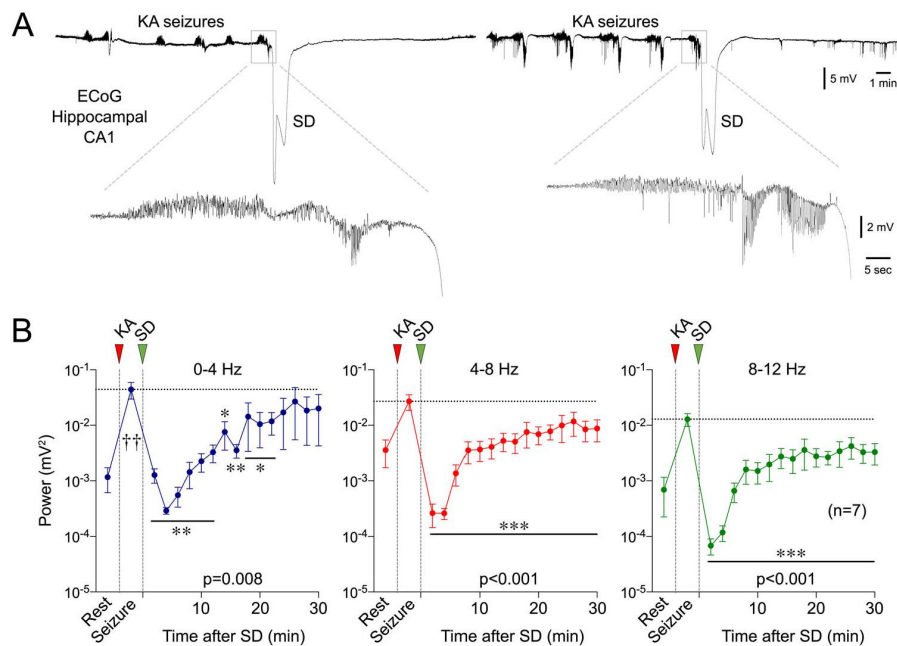


**Fig. 10 Spontaneous SDs during systemic kainic acid-induced global seizures terminate the seizures and limit their reemergence.** **A** Representative hippocampal recordings (DC) show seizure characteristics and SD emergence in two animals. **B** Average ECoG power time course in  $\delta$  (0-4 Hz),  $\theta$  (4-8 Hz), and  $\alpha$  (8-12 Hz) frequency bands show ECoG power at rest, during the seizure (5 min prior to SD, and every 2 min thereafter). All frequency bands showed a significant reduction in seizure power for at least 20 min after SD. The sample size is shown on the graph. \*-\*\*\* $p < 0.05$ -0.001 vs. pre-SD seizure power (one-way ANOVA for repeated measures;  $\pm$ SEM).

antiepileptic mechanism that is recruited when the intensity of network activity reaches a threshold. Indeed, SDs triggered by acute brain insults (e.g., concussion, intracranial hemorrhage) may also serve to suppress focal seizure activity that might be triggered by the insult, or its generalization, providing yet another potential survival advantage for the organism.

The duration of the antiseizure effect appeared to be highly variable among studies, ranging from just a few minutes to more than 90 min. This was likely due to the intensity of the seizure-inducing stimulus or the chronic epilepsy model used in each study. For example, when high concentrations of drugs were topically applied on a wide area of cortex, seizures returned shortly after SD<sup>43</sup>, whereas spike-wave discharges in a genetic model of absence epilepsy were suppressed for at least 4 h by a single SD<sup>44</sup>. The latter is clearly a translationally more relevant model than the topical application of potent seizure-inducing drugs. Therefore, we believe in the majority of cases where weak focal epileptiform activity evolves into a generalized seizure relatively infrequently, the antiseizure effect of SD is likely to be efficacious for longer periods of time. Nevertheless, recurrent

seizures also resulted in recurrent SDs in most studies, including ours, which was reminiscent of symptomatic occipital lobe epilepsy presenting with status migrainosus and diffusion-weighted MRI abnormalities consistent with SD<sup>46</sup>. Regardless of the context, however, on the whole, the occurrence of recurrent SDs significantly reduced the seizure burden in experimental models and is likely to do so in the clinical setting as well. It should be noted that chronic epileptic brains become resistant to SD<sup>11,47</sup> and acute but lasting seizures also render the tissue relatively resistant to SD<sup>43</sup>. This was evident in the failure of many SDs to propagate into the seizure core particularly during the later stages of our experiments as well. Indeed, persistent seizure activity in the process of kindling makes seizures less likely to culminate in SD<sup>48</sup>.

**Potential mechanisms.** The mechanisms triggering SD during intense neural activity are almost certainly related to elevated extracellular  $[K^+]$ . It is also possible that SD occurrence in our model simply reflects the deterioration of tissue health, but this is



unlikely as SDs occurred in some cases within mere minutes after seizure onset, at a time when the tissue was robust, healthy, and capable of sustaining more seizures thereafter. The mechanism(s) by which SD exerts its antiseizure effect is more difficult to discern. Profound shifts in extracellular concentrations of most if not all ions, elevated levels of numerous neurotransmitters and neuromodulators, metabolic and hemodynamic alterations, and morphological and gene expression changes, can all contribute to the antiseizure effect to some extent. It has been proposed that the concept of the ictus in epilepsy could be broadened to include a trajectory of seizures terminated by SD, seen in spontaneous epilepsy<sup>7</sup> and predicted by biophysics<sup>9,10</sup>. Given the overlapping cellular and electrophysiological mechanisms of seizures and SD, it is not easy to find an intervention that directly and selectively blocks SD occurrence without affecting the seizures to dissect the causality between these two phenomena and their mechanisms. Any intervention that inhibits one is also likely to directly affect the other. Regardless, data overwhelmingly show that the net effect of SD on seizure activity is a lasting suppression.

**Is SD physiological?** Research into SD over the past two decades, heavily in the context of acute brain injury, has portrayed SD as a pathological depolarization state associated with membrane failure. Both as a consequence of and contributor to brain injury, SD signified harm. However, older studies paint a different picture, where SD could be readily induced by single epileptiform spikes<sup>36,48</sup>, and even by sensory activation if the cortex was hyperexcitable<sup>38,49</sup>. The latter is intriguing given that migraine attacks can be triggered by sensory stimuli as well<sup>50</sup>. Intense synaptic activation via long-range inputs could also trigger SD<sup>51,52</sup>, and spontaneous SDs have been unequivocally demonstrated in genetically susceptible mice<sup>35</sup>. In fact, SD may be easier to develop than a seizure<sup>53</sup>, and recent models suggest seizures and SD are part of a dynamic continuum of neuronal membrane state<sup>9,10</sup>. There are many physiological (i.e., part of normal function, or beneficial) processes that can be pathological when they are overactive or occur at the wrong place and time, and SD might be one of those. When SD occurs in the wrong context (e.g., brain injury), it can have pathological consequences. But even in the injured brain, the interplay of seizures and SD is complex<sup>8,54–56</sup>, and seizures can be terminated by SDs<sup>56,57</sup>. In conclusion, SD may be an integral part of the brain function and serve fundamental roles (e.g., antiseizure effect). Further research into the potential beneficial effects of SD may reveal other mechanisms that facilitated evolutionary selection and conservation of SD.

## Methods

All experiments were approved by the Massachusetts General Hospital Institutional Animal Care and Use Committees and followed the NIH Guide for Use and Care of Laboratory Animals (NIH Publication No. 85-23, 1996).

**Animal preparation.** We used wild-type mice ( $n = 165$ , CD1, male,  $3.2 \pm 0.1$  months, Charles River Laboratories, Wilmington, MA, USA), familial hemiplegic migraine type 1 (FHM1) knockin mice heterozygous for the S218L mutation in the mouse *Cacna1a* gene encoding for the  $\alpha_1A$  pore-forming subunit of  $Ca_v2.1$  voltage-gated calcium channels ( $n = 7$  males, 1 female;  $8.9 \pm 2.7$  months) and their wild type littermates ( $n = 4$  males, 2 females;  $8.3 \pm 1.6$  months), and transgenic mice expressing channelrhodopsin-2 (ChR2<sup>+</sup>,  $n = 10$  males and 8 females,  $7.5 \pm 0.6$  months, B6.Cg-Tg (Thy1-COP4/EYFP)18Gfng/J, Jackson Laboratories, Bar Harbor, ME, USA)<sup>58,59</sup>. Mice were kept under diurnal lighting conditions, room temperature of approximately 25 °C and relative air humidity of 45–65%. Animals were kept in one cage in groups of two to four. The majority of mice were fasted overnight ( $17.4 \pm 0.3$  h;  $n = 173$ ), while a small cohort was studied without fasting ( $n = 17$ ); results did not differ and were pooled. Before anesthesia induction blood glucose was measured via the tail vein (Accu-Chek Guide, Hague Road, Indianapolis, USA). Mice were then anesthetized with isoflurane (3% induction, 1.25% maintenance) and allowed to breathe spontaneously on a mixture of 70% N<sub>2</sub>O/30% O<sub>2</sub>. The femoral artery was cannulated for continuous blood pressure (PowerLab; ADInstruments, Colorado Springs, MO, USA),

pCO<sub>2</sub>, pO<sub>2</sub>, and pH measurements. Rectal temperature was kept at 36.5–37.0 °C using a thermostatically controlled heating pad (CWE Inc., Ardmore, PA, USA). Mice were then placed on a stereotaxic frame. The skull was exposed, and mineral oil applied to prevent bone drying. Burr holes were drilled under saline cooling and the dura was kept intact.

**Cortical electrophysiological recordings and data processing.** Slow (DC) potential and electrocorticogram (ECoG) were continuously recorded using epidural glass micropipettes filled with 0.9% saline and a differential extracellular amplifier (bandpass 0.3–300 Hz; EX4-400, Dagan Corporation, Minneapolis, MN) and digitized at 1 kHz for offline analyses (PowerLab; ADInstruments, Colorado Springs, MO, USA). An Ag/AgCl reference electrode was placed subcutaneously in the neck. To eliminate non-physiological signals a 20 Hz digital low-pass filter was applied (Labchart 5 Pro, ADInstruments, Colorado Springs, MO, USA). The ECoG power spectrum density was computed using fast Fourier transform (FFT, cosine-bell window, size 1024, window overlap 93.75%) on 5-min bins of continuous noise-free segments (Labchart 8 Pro, ADInstruments, Colorado Springs, MO, USA). These were then averaged for  $\delta$  (0–4 Hz),  $\theta$  (4–8 Hz),  $\alpha$  (8–12 Hz) bands, and plotted over time. In addition, time-varying spectrograms were computed using Thomson's multitaper method (window length 10 s, window step 1 s, bandwidth 20 Hz, number of tapers 9; Chronux toolbox, <http://chronux.org>; version 2.12 v03, 2018).

**Hippocampal recordings.** DC potential and ECoG were continuously recorded using a glass micropipette in the hippocampal CA1 region (2 mm posterior and 1.5 mm lateral from bregma at a depth of 1.4 mm). After kainic acid administration isoflurane was gradually lowered from 1.5 to  $-0.58 \pm 0.08\%$  over 45 min until small-amplitude clonic leg movements appeared as a sign of generalized seizure in the absence of purposeful movements in response to pain.

**Intrinsic optical signal (IOS) imaging.** We simultaneously performed transcranial IOS imaging of cerebral blood volume (CBV) changes to complement electrophysiological recordings in all experiments to visualize the origins and propagation of SDs and the spatial extent of seizure activity as previously reported<sup>12,14,60</sup>. IOS imaging started prior to skull drilling to detect inadvertently triggered SDs during the preparation as an exclusion criterion. We achieved skull translucence using topical mineral oil application and diffusely illuminated the skull surface using a white or 530 nm green LED (M530L3, FB530-10, Thorlabs, Newton, NJ, USA) and an aspheric condenser lens (ACL2520U-DG15-A, Thorlabs, Newton, NJ, USA). We acquired full-field images using a USB camera (1 Hz, 640 × 480 pixels; Yaw-Cam 0.6.2, 2018). The camera and light source was positioned to minimize surface glare. The green channel of all images was processed with an in-house MATLAB (R2018b) code using the modified Beer-Lambert law as previously described<sup>61</sup> to enhance the signal changes reflecting total hemoglobin, and thus CBV. Images were downsampled to 320 × 240 pixels and the reflected light intensity of each pixel in each frame over the whole recording time was calculated. Two lines of interest (LOIs) were placed, one between the drug application site (hereafter referred to as the *focus*) and the anterior recording site, and one symmetrically on the contralateral hemisphere. In addition, regions of interest (ROIs) were placed along with the LOI at 1-mm intervals, and full-field band power maps were generated, to quantify regional seizure spread.

**Drugs.** We applied 4-aminopyridine (4AP; 5, 30, or 100 mM; Sigma-Aldrich), penicillin G (PG; 188434 IU/ml, sodium salt; Sigma-Aldrich, St. Louis, MO, USA), 1(S),9(R)-(–)-bicuculline methiodide (BIC; 5 mM; 1 mM, 0.5 mM, 0.05 mM, and 5  $\mu$ M; Sigma-Aldrich) or vehicle (0.9% saline) topically and repeated it once 10 min later. Cortex was not washed afterwards. In a subset of experiments, tetrodotoxin (TTX; 30  $\mu$ M in sodium citrate buffer, pH 4.8; Enzo Life Sciences, Farmingdale, NY, USA) was topically applied 30 min prior to 4AP. MK-801 (1 mg/kg,  $n = 7$ ; 3 mg/kg,  $n = 5$ ; Sigma-Aldrich) and KA (60 mg/kg; Sigma-Aldrich) were administered intraperitoneally. Topical concentrations and systemic doses were selected based on the literature<sup>6,62–64</sup>.

**Experimental design and setup.** Electrophysiology and optical imaging were carried out simultaneously in the same anesthetized animal throughout the experiment (Supplementary Fig. 1A). Various electrode, fiberoptic, and burr hole configurations were used depending on the experimental design. Basic configurations used in the majority of experiments are shown in Supplementary Fig. 1B. Variations to this configuration, when present, are indicated on subsequent figures where the relevant data are presented. The maximum duration of recordings was 240 min. We stopped the recordings if seizure activity diminished (<3 spikes/20 s) for at least 10 min suggesting waning of drug effect ( $n = 10$ ). Three experiments (76, 90, and 117 min) were additional controls done at later stages of the project to ensure the stability of the model system, and to record high-quality movies. Only one wild type and two FHM1 mice died during the recordings.

**Rigor and statistics.** Real-time electrophysiological recordings and IOS images precluded blinding. In the absence of a priori experience with the experimental

approach, sample sizes were chosen empirically. Data were analyzed using Prism 8 (GraphPad Software) and expressed as mean and standard error. Statistical tests used for each dataset and the sample sizes are indicated where they are presented in text, on the figures, or in figure legends.

**Reporting summary.** Further information on research design is available in the Nature Research Reporting Summary linked to this article.

### Data availability

The data that support the findings of this study are available from the corresponding author upon reasonable request. Source data are provided with this paper.

### Code availability

The MATLAB code for calculating CBV changes can be accessed through the following link: [https://github.com/t078/CBV\\_Pixel\\_Analysis\\_Seizure\\_Spread.git](https://github.com/t078/CBV_Pixel_Analysis_Seizure_Spread.git).

Received: 27 May 2020; Accepted: 15 March 2021;

Published online: 13 April 2021

### References

- Dreier, J. The role of spreading depression, spreading depolarization and spreading ischemia in neurological disease. *Nat. Rev.* **17**, 439–447 (2011).
- Leao, A. Spreading depression of activity in the cerebral cortex. *J. Neurophysiol.* **7**, 359–390 (1944).
- Lauritzen, M. et al. Clinical relevance of cortical spreading depression in neurological disorders: migraine, malignant stroke, subarachnoid and intracranial hemorrhage, and traumatic brain injury. *J. Cereb. Blood Flow. Metab.* **31**, 17–35 (2011).
- Eikermann-Haerter, K. et al. Genetic and hormonal factors modulate spreading depression and transient hemiparesis in mouse models of familial hemiplegic migraine type 1. *J. Clin. Invest.* **119**, 99–109 (2009).
- Köhling, R. et al. Differential sensitivity to induction of spreading depression by partial disinhibition in chronically epileptic human and rat as compared to native rat neocortical tissue. *Brain Res.* **975**, 129–134 (2003).
- Aiba, I. & Noebels, J. Spreading depolarization in the brainstem mediates sudden cardiorespiratory arrest in mouse SUDEP models. *Sci. Transl. Med.* **7**, 282ra46 (2017).
- Bahari, F. et al. Seizure-associated spreading depression is a major feature of ictal events in two animal models of chronic epilepsy. *bioRxiv* 455519 (2020).
- Fabricsius, M. et al. Association of seizures with cortical spreading depression and peri-infarct depolarizations in the acutely injured human brain. *Clin. Neurophysiol.* **119**, 1973–1984 (2008).
- Ullah, G. et al. The role of cell volume in the dynamics of seizure, spreading depression, and anoxic depolarization. *PLoS Comput. Biol.* **11**, e1004414 (2015).
- Wei, Y., Ullah, G. & Schiff, S. J. Unification of neuronal spikes, seizures, and spreading depression. *J. Neurosci.* **34**, 11733–11743 (2014).
- Maslarova, A. et al. Chronically epileptic human and rat neocortex display a similar resistance against spreading depolarization in vitro. *Stroke* **42**, 2917–2922 (2011).
- Zhao, M. et al. Spatiotemporal dynamics of perfusion and oximetry during ictal discharges in the rat neocortex. *J. Neurosci.* **29**, (2009).
- Yuzawa, I. et al. Cortical spreading depression impairs oxygen delivery and metabolism in mice. *J. Cereb. Blood Flow. Metab.* **32**, 376–386 (2012).
- Chung, D. Y. et al. Real-time non-invasive in vivo visible light detection of cortical spreading depolarizations in mice. *J. Neurosci. Methods* **309**, 143–146 (2018).
- Chung, D. Y. et al. Determinants of optogenetic cortical spreading depolarizations. *Cereb. Cortex* **29**, 1150–1161 (2019).
- Matsuura, T. & Bures, J. The minimum volume of depolarized neural tissue required for triggering cortical spreading depression in rat. *Exp. Brain Res.* **12**, 238–249 (1971).
- Rogawski, M. A. Migraine and epilepsy-shared mechanisms within the family of episodic disorders. In *Jasper's Basic Mechanisms of the Epilepsies*. 4th edn, Vol. 2012 (eds Rogawski, M. A. et al.) (Oxford University Press, USA, 2012).
- Haut, S. R., Bigal, M. E. & Lipton, R. B. Chronic disorders with episodic manifestations: focus on epilepsy and migraine. *Lancet Neurol.* **5**, 148–157 (2006).
- Ottman, R. & Lipton, R. B. Comorbidity of migraine and epilepsy. *Neurology* **44**, 2105–2110 (1994).
- Charles, A. C. & Baca, S. M. Cortical spreading depression and migraine. *Nat. Rev. Neurol.* **9**, 637–644 (2013).
- Goadsby, P. J. et al. Pathophysiology of migraine: a disorder of sensory processing. *Physiol. Rev.* **97**, 553–622 (2017).
- Riant, F. et al. PRRT2 mutations cause hemiplegic migraine. *Neurology* **79**, 2122–2124 (2012).
- Chioza, B. et al. Association between the alpha(1a) calcium channel gene CACNA1A and idiopathic generalized epilepsy. *Neurology* **56**, 1245–1246 (2001).
- Ito, M. et al. Characteristics of postictal headache in patients with partial epilepsy. *Cephalalgia* **24**, 23–28 (2004).
- Panayiotopoulos, C. P. Elementary visual hallucinations, blindness, and headache in idiopathic occipital epilepsy: differentiation from migraine. *J. Neurol. Neurosurg. Psychiatry* **66**, 536–540 (1999).
- Stead, M. et al. Microseizures and the spatiotemporal scales of human partial epilepsy. *Brain* **133**, 2789–2797 (2010).
- Schevon, C. A. et al. Microphysiology of epileptiform activity in human neocortex. *J. Clin. Neurophysiol.* **25**, 321–330 (2008).
- Worrell, G. A. et al. High-frequency oscillations in human temporal lobe: simultaneous microwire and clinical macroelectrode recordings. *Brain* **131**, 928–937 (2008).
- Litt, B. et al. Epileptic seizures may begin hours in advance of clinical onset: a report of five patients. *Neuron* **30**, 51–64 (2001).
- Merricks, E. M. et al. Single unit action potentials in humans and the effect of seizure activity. *Brain* **138**(Pt 10), 2891–2906 (2015).
- Bragin, A., Wilson, C. L. & Engel, T. J. Chronic epileptogenesis requires development of a network of pathologically interconnected neuron clusters: a hypothesis. *Epilepsia* **41**, S144–S152 (2000).
- Kudo, C. et al. The impact of anesthetics and hyperoxia on cortical spreading depression. *Exp. Neurol.* **212**, 201–206 (2008).
- Nedergaard, M. & Hansen, A. J. Spreading depression is not associated with neuronal injury in the normal brain. *Brain Res.* **449**, 395–398 (1988).
- Aiba, I. & Noebels, J. L. Spreading depolarization in the brainstem mediates sudden cardiorespiratory arrest in mouse SUDEP models. *Sci. Transl. Med.* **7**, 282ra46 (2015).
- Loonen, I. C. M. et al. Brainstem spreading depolarization and cortical dynamics during fatal seizures in Cacna1a S218L mice. *Brain* **142**, 412–425 (2019).
- Koroleva, V. I. & Bures, J. Cortical penicillin focus as a generator of repetitive spike-triggered waves of spreading depression in rats. *Exp. Brain Res.* **51**, 291–297 (1983).
- Bahari, F. et al. Spreading depression and seizure unification experimentally observed in epilepsy. *bioRxiv* 455519 (2018).
- Vinogradova, L. V., Vinogradov, V. Y. & Kuznetsova, G. D. Unilateral cortical spreading depression is an early marker of audiogenic kindling in awake rats. *Epilepsy Res.* **71**, 64–75 (2006).
- Vinogradova, L. V., Kuznetsova, G. D. & Coenen, A. M. Audiogenic seizures associated with a cortical spreading depression wave suppress spike-wave discharges in rats. *Physiol. Behav.* **86**, 554–558 (2005).
- Bragin, A., Penttonen, M. & Buzsáki, G. Termination of epileptic afterdischarge in the hippocampus. *J. Neurosci.* **17**, 2567–2579 (1997).
- Zakharov, A. et al. Segregation of seizures and spreading depolarization across cortical layers. *Epilepsia* **60**, 2386–2397 (2019).
- Kesner, R. P., O'Kelly, L. I. & Thomas, G. J. Effects of cortical spreading depression and drugs upon audiogenic seizures in rats. *J. Comp. Physiol. Psychol.* **59**, 280–282 (1965).
- Ueda, M. & Bures, J. Differential effects of cortical spreading depression on epileptic foci induced by various convulsants. *Electroencephalogr. Clin. Neurophysiol.* **43**, 666–674 (1977).
- Samotaeva, I. S. et al. Intracortical microinjections may cause spreading depression and suppress absence seizures. *Neuroscience* **230**, 50–55 (2013).
- Kelly, M. E., Battye, R. A. & McIntyre, D. C. Cortical spreading depression reversibly disrupts convulsive motor seizure expression in amygdala-kindled rats. *Neuroscience* **91**, 305–313 (1999).
- Striano, P. et al. Status epilepticus migrainosus: clinical, electrophysiologic, and imaging characteristics. *Neurology* **76**, 761 (2011). author reply 761.
- Guedes, R. C. & Cavalheiro, E. A. Blockade of spreading depression in chronic epileptic rats: reversion by diazepam. *Epilepsy Res.* **27**, 33–40 (1997).
- Koroleva, V. I., Vinogradova, L. V. & Bures, J. Reduced incidence of cortical spreading depression in the course of pentylenetetrazol kindling in rats. *Brain Res.* **608**, 107–114 (1993).
- Vinogradova, L. V., Kuznetsova, G. D. & Coenen, A. M. Unilateral cortical spreading depression induced by sound in rats. *Brain Res.* **1286**, 201–207 (2009).
- Coppola, G., Pierelli, F. & Schoenen, J. Is the cerebral cortex hyperexcitable or hyperresponsive in migraine? *Cephalalgia* **27**, 1427–1439 (2007).
- Ochs, S., Hunt, K. & Booker, H. Spreading depression using chronically implanted electrodes. *Am. J. Physiol.* **200**, 1211–1214 (1961).
- Grafstein, B. Mechanism of spreading cortical depression. *J. Neurophysiol.* **19**, 154–171 (1956).

53. Vinogradova, L. V. Initiation of spreading depression by synaptic and network hyperactivity: insights into trigger mechanisms of migraine aura. *Cephalalgia* **38**, 1177–1187 (2018).
54. Dreier, J. P. et al. Spreading convulsions, spreading depolarization and epileptogenesis in human cerebral cortex. *Brain* **135**(Pt 1), 259–275 (2012).
55. Hartings, J. A. et al. Spreading depolarisations and outcome after traumatic brain injury: a prospective observational study. *Lancet Neurol.* **10**, 1058–1064 (2011).
56. Schoknecht, K. et al. The role of spreading depolarizations and electrographic seizures in early injury progression of the rat photothrombosis stroke model. *J. Cereb. Blood Flow. Metab.* **41**, 271678X20915801 (2020).
57. Hartings, J. A., Tortella, F. C. & Rolli, M. L. AC electrocorticographic correlates of peri-infarct depolarizations during transient focal ischemia and reperfusion. *J. Cereb. Blood Flow. Metab.* **26**, 696–707 (2006).
58. Wang, H. et al. High-speed mapping of synaptic connectivity using photostimulation in Channelrhodopsin-2 transgenic mice. *Proc. Natl Acad. Sci. USA* **104**, 8143–8148 (2007).
59. Arenkiel, B. R. et al. In vivo light-induced activation of neural circuitry in transgenic mice expressing channelrhodopsin-2. *Neuron* **54**, 205–218 (2007).
60. Zhao, M. et al. Preictal and ictal neurovascular and metabolic coupling surrounding a seizure focus. *J. Neurosci.* **31**, 13292–13300 (2011).
61. Ma, Y. et al. Wide-field optical mapping of neural activity and brain haemodynamics: considerations and novel approaches. *Philos Trans R Soc Lond B.* **371**, 20150360 (2016).
62. Liou, J. Y. et al. Role of inhibitory control in modulating focal seizure spread. *Brain* **141**, 2083–2097 (2018).
63. Akdogan, I. et al. Penicillin-induced epilepsy model in rats: dose-dependant effect on hippocampal volume and neuron number. *Brain Res. Bull.* **77**, 172–177 (2008).
64. Pitkanen, A., Schwartzkroin, P. A. & Moshe, S. L. *Models of Seizures and Epilepsy*. (Elsevier, 2006).

### Acknowledgements

This work was funded by NIH (R01NS102969 to C.A., 2R01EB014641 to S.J.S.).

### Author contributions

I.T. conceived the study, designed and performed experiments and data analysis, wrote the manuscript, and drew the figure illustrations. C.A. conceived the study, designed

experiments and data analysis, performed circuit reconstruction and wrote the manuscript. D.C. contributed data analysis, experimental design, and revision of the manuscript. A.L. contributed to experimental design. I.L. contributed to revision experiments. T.Q. contributed reagents. A.M., F.S., M.E., and S.J.S. revised the manuscript.

### Competing interests

The authors declare no competing interests.

### Additional information

**Supplementary information** The online version contains supplementary material available at <https://doi.org/10.1038/s41467-021-22464-x>.

**Correspondence** and requests for materials should be addressed to C.A.

**Peer review information** *Nature Communications* thanks Jed Hartings and the other, anonymous, reviewer(s) for their contribution to the peer review of this work. Peer reviewer reports are available.

**Reprints and permission information** is available at <http://www.nature.com/reprints>

**Publisher's note** Springer Nature remains neutral with regard to jurisdictional claims in published maps and institutional affiliations.



**Open Access** This article is licensed under a Creative Commons Attribution 4.0 International License, which permits use, sharing, adaptation, distribution and reproduction in any medium or format, as long as you give appropriate credit to the original author(s) and the source, provide a link to the Creative Commons license, and indicate if changes were made. The images or other third party material in this article are included in the article's Creative Commons license, unless indicated otherwise in a credit line to the material. If material is not included in the article's Creative Commons license and your intended use is not permitted by statutory regulation or exceeds the permitted use, you will need to obtain permission directly from the copyright holder. To view a copy of this license, visit <http://creativecommons.org/licenses/by/4.0/>.

© The Author(s) 2021

## Supplementary Information for

### **SPREADING DEPRESSION AS AN INNATE ANTISEIZURE MECHANISM**

**Isra Tamim<sup>1,2</sup>, David Y. Chung<sup>1,3</sup>, Andreia Lopes de Morais<sup>1</sup>, Inge C.M. Loonen<sup>1</sup>, Tao Qin<sup>1</sup>, Amrit Misra<sup>3</sup>, Frieder Schlunk<sup>2</sup>, Matthias Endres<sup>2</sup>, Steven J. Schiff<sup>4</sup>, and Cenk Ayata<sup>1,3\*</sup>**

1 Neurovascular Research Unit, Department of Radiology, Massachusetts General Hospital, Harvard Medical School

2 Charité - Universitätsmedizin Berlin, Klinik und Hochschulambulanz für Neurologie und Centrum für Schlaganfallforschung Berlin (CSB)

3 Department of Neurology, Massachusetts General Hospital, Harvard Medical School

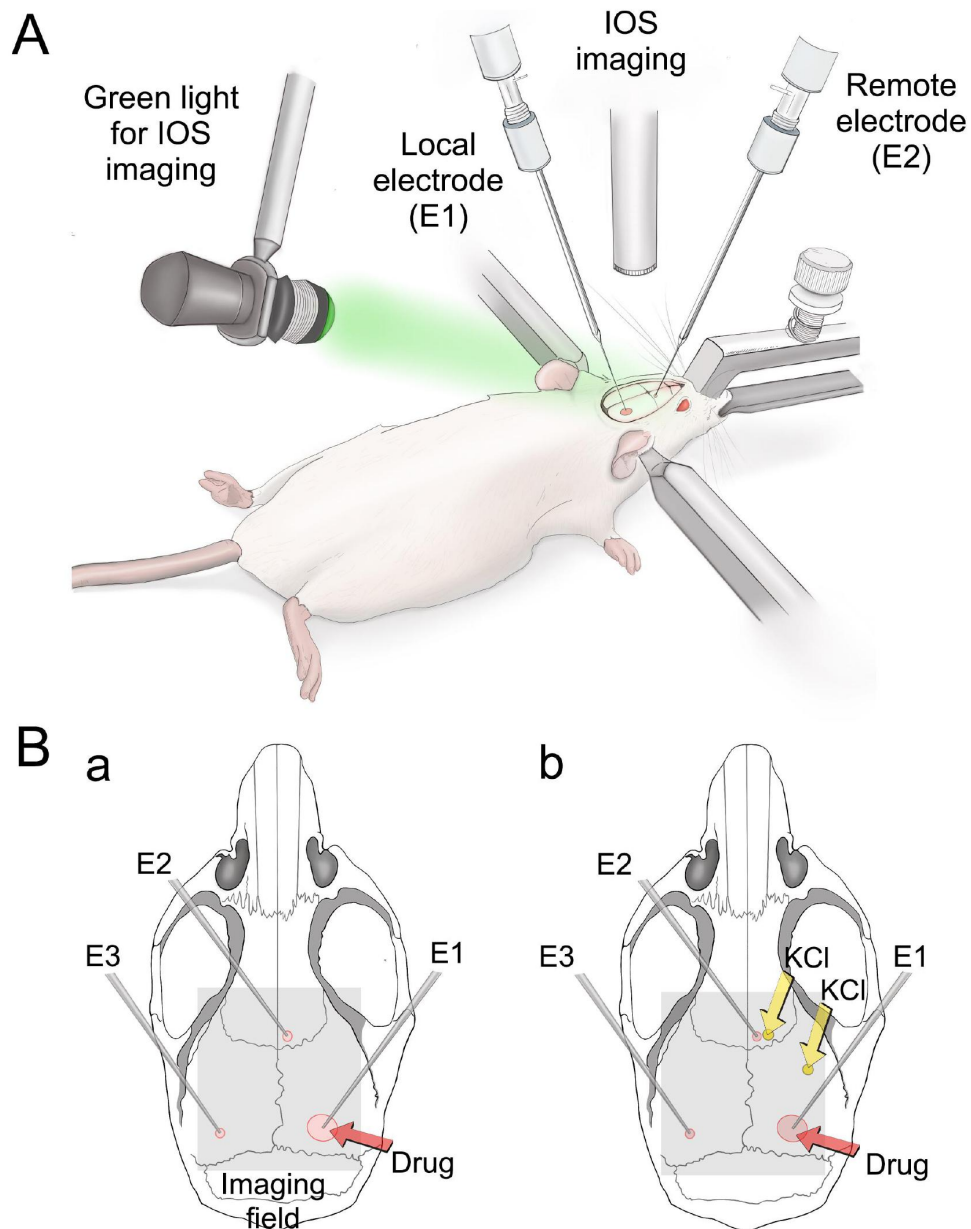
4 Center for Neural Engineering, Departments of Engineering Science and Mechanics, Neurosurgery, and Physics, The Pennsylvania State University

**Corresponding Author:**

Cenk Ayata, M.D., Ph.D.

149 13<sup>th</sup> Street, Room 6408, Charlestown, MA 02129, USA

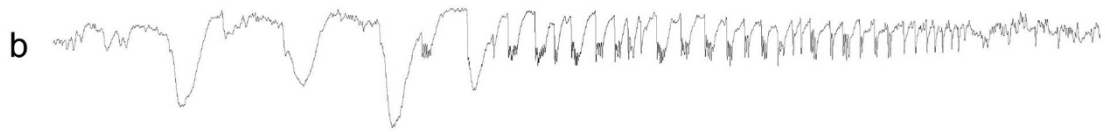
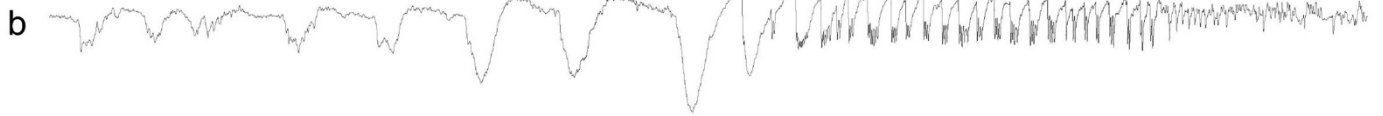
Office: (617) 726 0821; Cell: (617) 543 5442; Fax: (617) 726 2547; email: CAYATA@mgh.harvard.edu



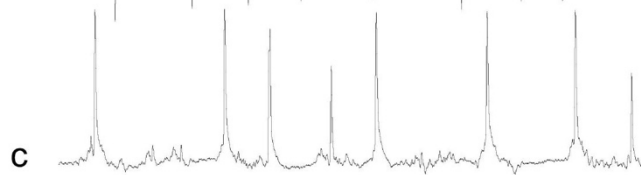
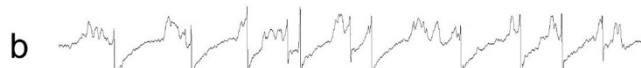
### Supplementary Figure 1. Experimental setup

(A) Basic experimental setup consisted of light source (530 nm green LED shown) to illuminate the skull, USB pen camera to image the field at 1Hz through intact skull, and 2-3 epidural glass micropipettes to record electrocorticogram (ECoG) and slow (DC) potential. (B) Seizures were generated by topical application of epileptogenic agents onto an occipital window consisting of thinned skull with a small crack to insert the epidural electrode and enhance drug diffusion (2 mm diameter, 3 mm lateral and 2 mm anterior from lambda, red arrow). Left and right panels show the most common electrode configurations (E1-E3) to capture seizure generalization and SD occurrence. E1, local electrode over the seizure focus; E2, ipsilateral remote electrode (1.5 mm lateral, 1.5 mm anterior from bregma); E3, contralateral remote electrode in homotopic to seizure focus. Grey shade shows IOS imaging field. Right panel also shows the sites of topical KCl application onto thinned skull (yellow arrows) to trigger SD. In experiments with an E2, KCl was applied between the two recording sites (lower arrow), whereas in experiments without an E2, KCl was applied onto the anterior window (upper arrow).

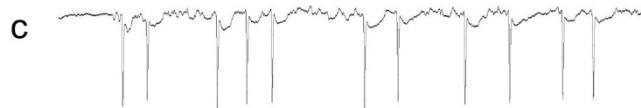
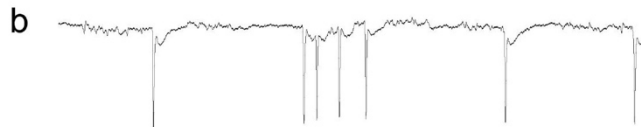
4AP



PG

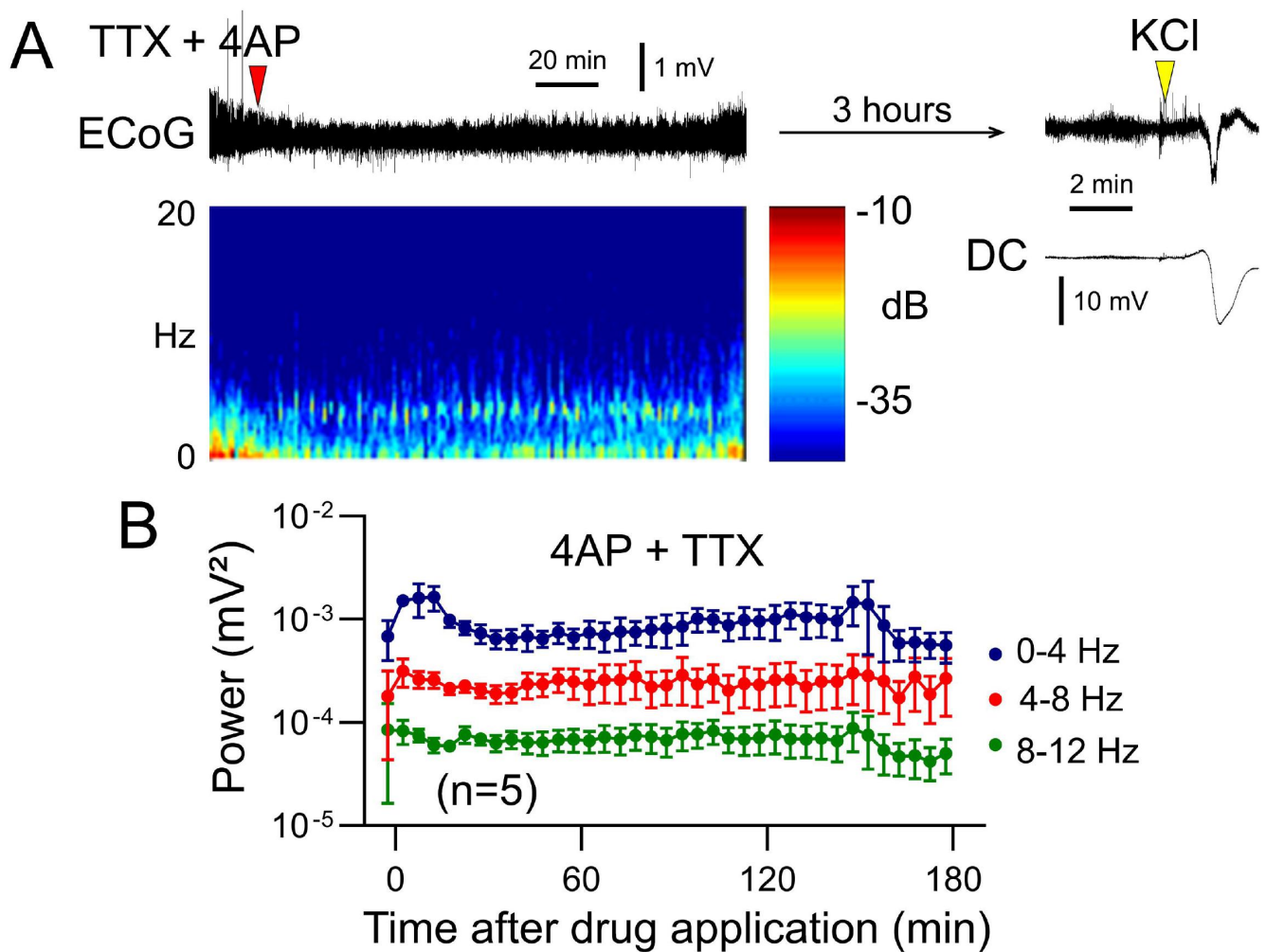


BIC



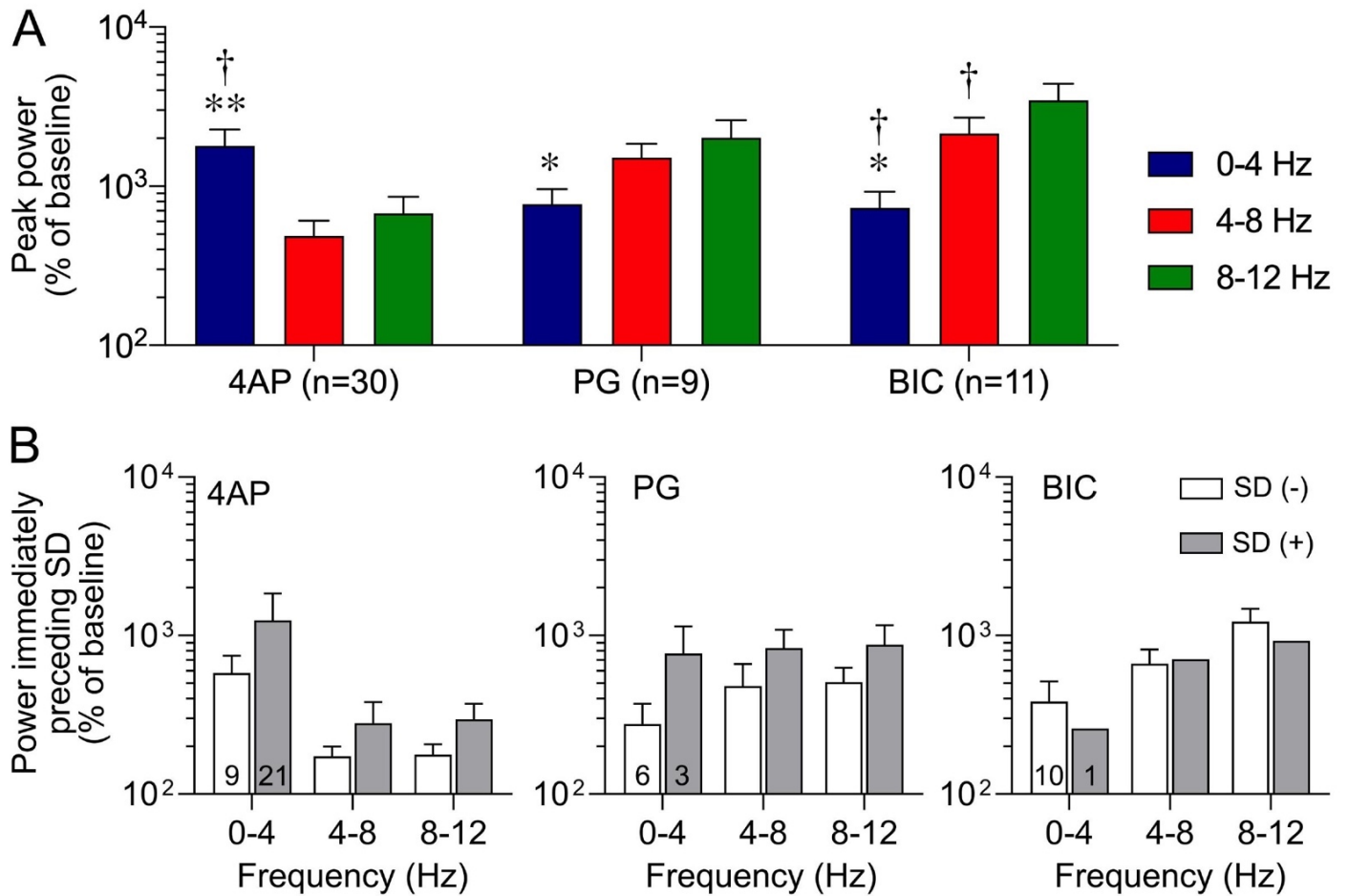
1 mV  
1 sec

Supplementary Figure 2. Seizure characteristics after topical 4AP, PG or BIC application. Electrocorticographic changes after topical 4AP, PG or BIC application shown on an expanded time scale. Source data are provided as a Source Data file.



Supplementary Figure 3. Inhibition by tetrodotoxin confirms seizures as the immediate trigger for SD.

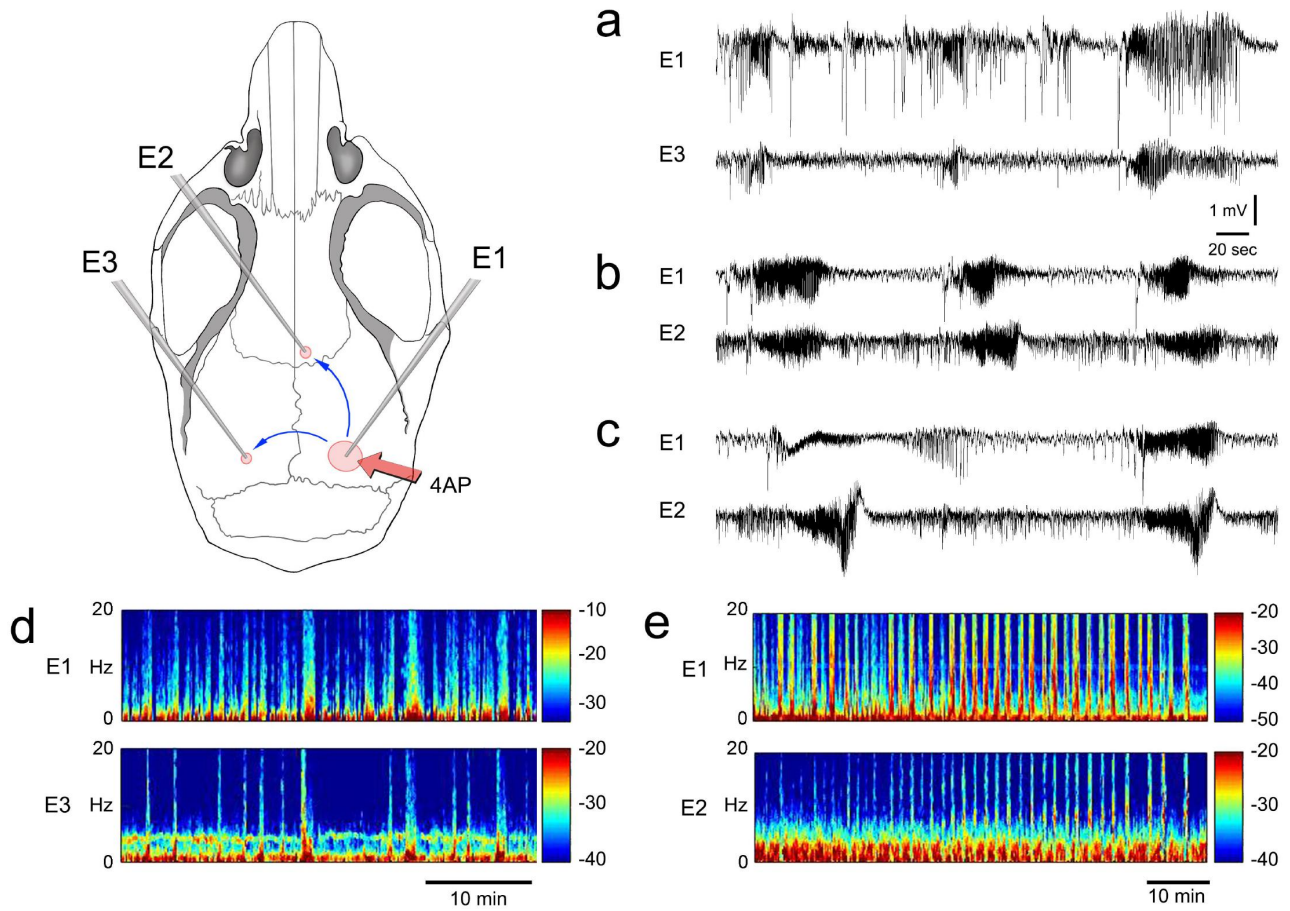
Pretreatment of cortex with TTX (30  $\mu\text{M}$ ) 30 minutes before 4AP application prevented seizures, as shown in a representative ECoG tracing and time–frequency–power spectrum (A), and the group average of ECoG power over time (B). As a result, no SD was detected in any of the experiments after TTX pretreatment. At the end of each experiment, we confirmed that TTX did not directly block SDs by inducing an SD using topical KCl application at the ipsilateral remote site and detecting it in the 4AP application site (shown in upper right). Data are mean $\pm$ SEM. Source data are provided as a Source Data file.



Supplementary Figure 4. Power density increase in the  $\delta$  frequency range predicts SD occurrence.

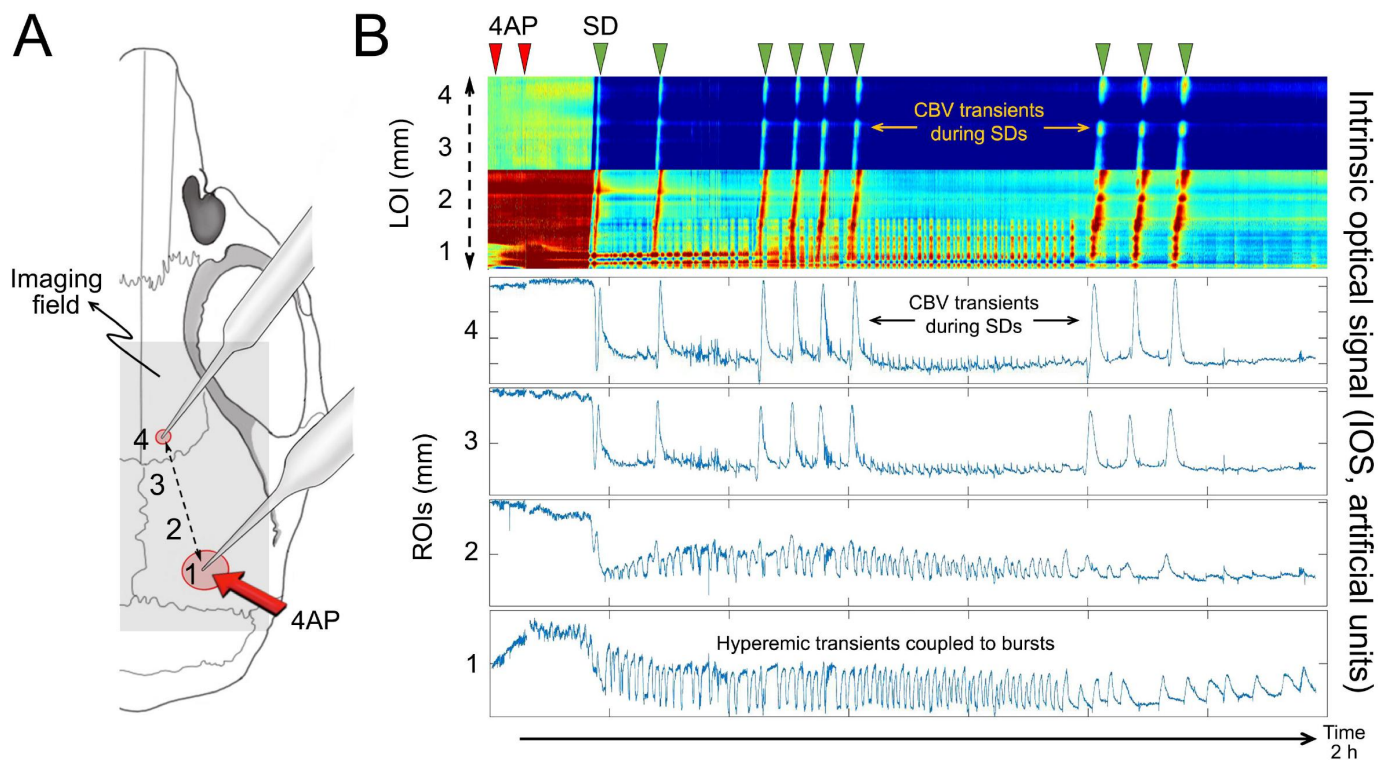
(A) Peak power change during seizures induced by three different seizure-inducing agents are shown for each frequency band. To obtain the peak change, average power was calculated using FFT in 5-minute ECoG blocks and normalized to baseline for each experiment. The highest average power increase was then taken as peak change for each animal and averaged across the entire cohort. The  $\delta$  frequency band (0-4 Hz) showed the largest power increase in 4AP-induced seizures where the highest rate of spontaneous SD occurred. \* $p < 0.05$  and \*\* $p < 0.01$  vs. 4-8 Hz; † $p < 0.05$  vs. 8-12 Hz (two-way ANOVA for repeated measures). (B) This was supported by ECoG power increase immediately before the first SD compared with time-matched power increase in animals that did not develop an SD (5-minute averages normalized to baseline). Number of animals are indicated at the bottom of each bar. Data are mean  $\pm$  SEM. Source data are provided as a Source Data file.





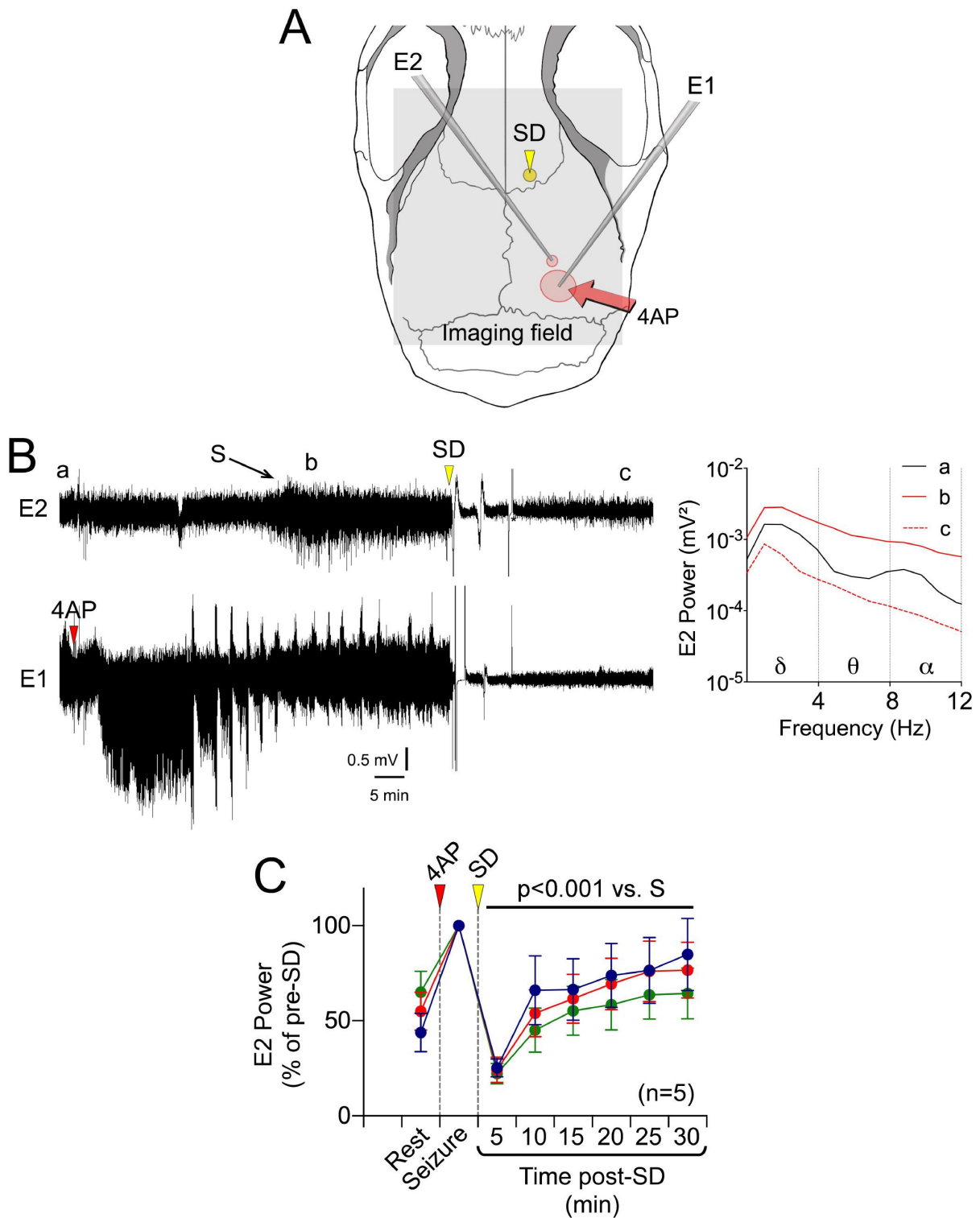
**Supplementary Figure 5. Generalization of seizures across the cortex.**

Experimental setup (upper left) to detect electrophysiological generalization of seizures (blue arrows) from the 4AP focus to the ipsilateral (E2) and contralateral (E3) remote electrodes. Representative ECoG tracings from different experiments show 4AP-induced seizure activity at the contralateral (a) and the ipsilateral (b-c) remote electrodes. Time-frequency spectra from two different experiments show synchronized power increases in contralateral (d) and ipsilateral (e) remote electrodes indicating seizure generalization. Source data are provided as a Source Data file.



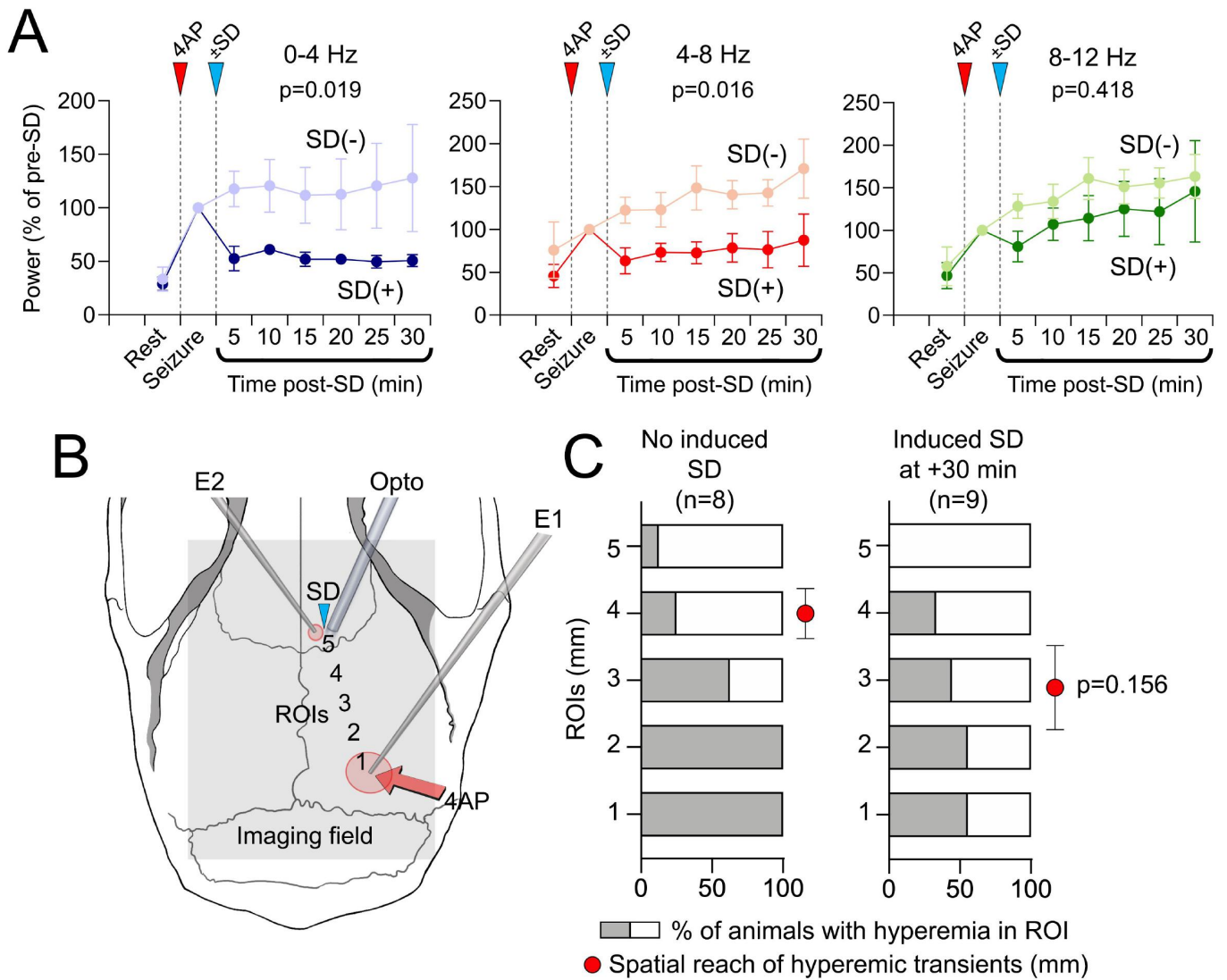
**Supplementary Figure 6. Hemodynamic changes during seizure induced SDs.**

(A) We placed a line of interest (LOI) extending from the 4AP application site anteriorly on the ipsilateral hemisphere. Four ROIs (1-4) were placed along the LOI at 1.2 mm intervals. (B) IOS intensity along the LOI and in each ROI are plotted over time. Red indicates increase and blue decrease in CBV. Recurrent SDs (green arrowheads) were associated with CBV changes typical of SDs in normal mouse cortex. The first SD triggered a triphasic response and all subsequent SDs were hyperemic, suggesting that cortex was not injured or hemodynamically compromised. The first SD penetrated ROIs 2-4 and partially affected ROI 1. Subsequent SDs did not penetrate ROI 1 (4AP application site) and had no effect on seizure-coupled hyperemic transients. Source data are provided as a Source Data file.



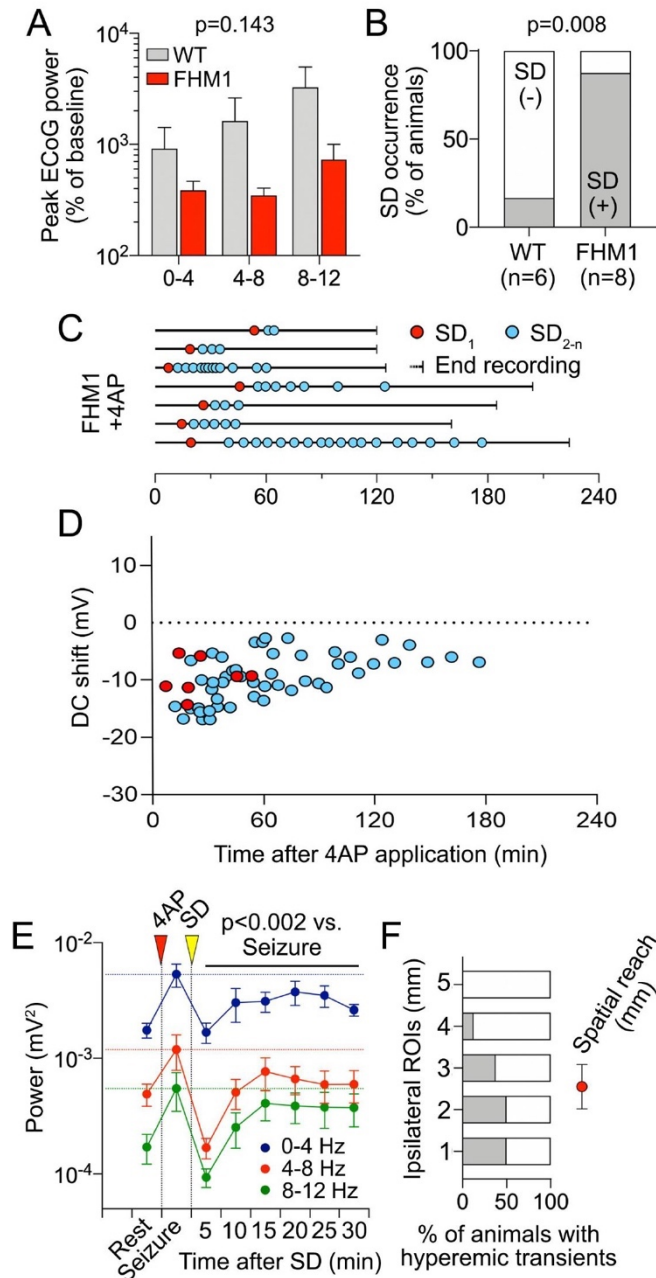
**Supplementary Figure 7. SD limits spatial spread of seizures.**

(A) Experimental setup showing two electrodes placed 1mm apart. An SD was induced via topical KCl application (yellow arrowhead) over the frontal cortex. (B) Representative ECoG tracing from E1 and E2 showing seizure starting 5 minutes after 4AP application in E1 and 35 minutes after 4AP application in E2 (S). SD was induced 20 minutes after ECoG power increased in E2, and immediately suppressed seizure activity. Power density computed using FFT at phases a-c are also shown. Recording in E1 briefly lost connection after SD induction creating an artefact. A second SD erupted 5 minutes after the first. (C) The ECoG power time course from E2 normalized to the pre-SD 5-minute average power shows the 4AP-induced increase in power from resting state (R) at this location outside the drug application site and significant reduction in seizure power after SD. ECoG power in E2 returned to baseline within 10 minutes but did not reach pre-SD seizure levels for at least 30 minutes ( $p < 0.001$  vs. pre-SD, one-way ANOVA;  $\pm$ SEM). Source data are provided as a Source Data file.



Supplementary Figure 8. Optogenetically-induced SDs are similarly antiepileptic.

(A) Averaged ECoG power time courses normalized to pre-SD (5 minutes) seizure power (S) from E1 are shown separately for each frequency band in ChR2+ mice. An optogenetic SD (blue arrowhead) induced at the remote site  $29 \pm 3$  minutes (range 19-40) after 4AP application significantly reduced seizure power (bold symbols) compared with time controls without SD (faint symbols,  $n=10$  and 8, respectively). Exact p-values are shown on each graph (two-way ANOVA with 4AP-induced seizures are shown). (B) Experimental setup showing electrode (E1-E2), optogenetic light source (opto) and ROI (1-5) placement. (C) The proportion of animals that developed hyperemic transients coupled to 4AP seizures within each of the five ROIs and the average distance to which the hyperemia reached (red circles) are shown with and without an optogenetic SD ( $p=0.156$ , t-test with Welch's correction). Source data are provided as a Source Data file.



**Supplementary Figure 9. Spontaneous SDs in familial hemiplegic migraine type 1 (FHM1) mutants and their antiepileptic effect.**

(A) Peak power change during seizures normalized to baseline ECoG in FHM1 knockin mice and their WT littermates separated into frequency bands ( $p=0.143$ , 2-way ANOVA). (B) Fraction of animals that developed spontaneous SD from the seizure focus was significantly higher in FHM1 ( $p=0.008$ ,  $\chi^2$ ). (C) Experimental timelines in FHM1 mutants that developed spontaneous SDs. Symbols represent first (SD<sub>1</sub>, red symbol) and subsequent SDs (SD<sub>2-n</sub>, blue symbol). FHM1 mutants developed a much higher frequency of SDs, which often occurred in clusters. (D) The change in DC shift amplitude of first and subsequent SDs over time in FHM1 mutant mice shows that, unlike WT mice shown in Figure 3, all but one SD penetrated the seizure focus (i.e. negative DC shift) even at late stages of the experiments. (E) Average ECoG power in the 4AP application site at rest (R), 4AP seizures 5 minutes before the first spontaneous SD (S), and every 5 minutes thereafter show that spontaneously occurring SDs exert an antiepileptic effect in FHM1 mutants ( $p=0.002$  vs. pre-SD, 2-way ANOVA for repeated measures). (F) The proportion of animals that developed hyperemic transients coupled to 4AP seizures within each of the five ROIs and the average distance to which the hyperemia reached (red circles) in FHM1 mutants. Data are mean $\pm$ SEM. Source data are provided as a Source Data file.

### Supplementary Movie 1. IOS imaging of seizure activity and recurrent SDs.

A representative experiment is shown in which seizures were induced by 4AP-application (right parietal cortex). Frame rate is 1Hz. Time after initial 4AP application is indicated in seconds. Right panel shows unprocessed reflectance images in greyscale. The hyperemic response to seizure activity appears as decreased reflectance (i.e. darker) due to increase in total hemoglobin (i.e. CBV). Left panel shows CBV in arbitrary units calculated using MATLAB. Red indicates an increase, blue a decrease in CBV. Recurrent hyperemic transients lasting less than a minute each become visible in and around the focus before first SD occurs and gradually reach farther over time. A total of 9 SDs occur over approximately 2 hours starting 15 minutes after 4AP application. These hyperemic transients were coupled to seizure bursts. Images were acquired by a camera (MU300, AmScope, Irvine, CA, USA, Aptina MT9T001 CMOS sensor, 8-bit, resolution 2048x1536) attached to the microscope after skull preparation. Exposure time ranged from 200 to 350 ms and analog gain was kept under 2. Source data are provided as a Source Data file.

### Supplementary Movie 2. Graphic depiction of SD as an endogenous antiseizure mechanism.

A unifying theory wherein SD is a fundamental endogenous antiseizure mechanism in the central nervous system. SD is triggered when intense synchronized focal neuronal network activity raises extracellular  $K^+$  above the 12 mM threshold in a minimum critical volume of tissue estimated to be  $\sim 1 \text{ mm}^3$ . SD then acts as an 'emergency brake' or 'reboot' extinguishing the seizure and propagates centimeters away from the focus to exert a broader antiseizure effect. The latter is clinically perceived as a migraine aura.

### Supplementary Table 1. Systemic physiological parameters in animals with or without a spontaneous SD during 4AP seizures.

	<b>SD (-)</b> <b>(n=10)</b>	<b>SD (+)</b> <b>(n=21)</b>
<b>pH</b>	7.34 $\pm$ 0.02	7.35 $\pm$ 0.01
<b>pCO2 [mmHg]</b>	34 $\pm$ 2.83	34 $\pm$ 1.08
<b>pO2 [mmHg]</b>	137 $\pm$ 8.56	148 $\pm$ 4.46
<b>Gluc [mg/dl]</b>	149 $\pm$ 9.7	142 $\pm$ 5.46
<b>BP [mmHg]</b>	89 $\pm$ 4.15	94 $\pm$ 1.89

Data are mean  $\pm$  SEM. Source data are provided as a Source Data file.



## **15. Curriculum Vitae**

Mein Lebenslauf wird aus datenschutzrechtlichen Gründen in der elektronischen Version meiner Arbeit nicht veröffentlicht.







## 16. Publikationsliste\*

**Tamim I**, Chung DY, Lopes A, et al. Spreading depression as an innate antiseizure mechanism. *Nature Communications*. 2021

Schlunk F, Böhm M, Boulouis G, Qin T, Arbel M, **Tamim I**, Fischer P, Bacskai BJ, Frosch MP, Endres M, Greenberg SM, Ayata C. Secondary Bleeding During Acute Experimental Intracerebral Hemorrhage. *Stroke*. 2019

Fischer P, Sugimoto K, Chung DY, **Tamim I**, Morais A, Takizawa T, Qin T, Gomez CA, Schlunk F, Endres M, Yaseen MA, Sakadzic S, Ayata C. Rapid hematoma growth triggers spreading depolarizations in experimental intracortical hemorrhage. *Journal of Cerebral Blood Flow and Metabolism*. 2020

Aykan SA, Xie H, Zheng Y, Chung DY, Kura S, Lai JH, Taylan D. Erdogan, **Tamim I**, Yagmur D, Ishikawa H, Arai K, Yaseen MA., Boas DA, Sakadzic S, Ayata C. Rho-Kinase Inhibition Improves the Outcome of Focal Subcortical White Matter Lesions. *Stroke*. 2022

## 17. Acknowledgements/Danksagung

I would like to express my deepest appreciation for the principal investigator of the *Neurovascular Research Unit* and my supervisor, Dr. Cenk Ayata. His guidance, spirit of curiosity and adventurous attitude towards research had a lasting effect on the scientist I became in his lab. Without his persistent encouragement and continuous critical review of data, this dissertation would not have been possible.

My sincere thanks also go to the Neurovascular Research Unit lab members: your work ethic and enthusiasm inspired and motivated me every day. Your guidance allowed me to establish creative, clever, and precise experimental setups that made the data of this thesis so exceptional.

Ich danke meinem Doktorvater, Prof. Matthias Endres, für sein Vertrauen in meine Fähigkeiten. Ohne seine Zustimmung und Unterstützung hätte ich nicht am Massachusetts General Hospital lernen und arbeiten und das MD/PhD-Programm der Charité nicht absolvieren können.

Dr. Frieder Schlunk danke ich für sein unermüdliches Interesse, seine Doktoranden und Doktorandinnen in ihrem beruflichen Werdegang zu beraten und für seine Bemühungen, seine Fertigkeiten und sein Wissen für uns einzusetzen. Insbesondere möchte ich ihm für die Kontaktaufnahme mit Prof. Endres und Prof. Ayata danken.

Der Studienstiftung des deutschen Volkes möchte ich für die großzügige und unkomplizierte Finanzierung meines Studiums und Forschungsaufenthalts danken.

Ich danke Anna Speth für ihre bedingungslose Unterstützung, für die Besuche in Boston und für die Aufmunterung bei jedem missglückten Experiment (und davon gab es sehr viele!).

Zu guter Letzt möchte ich meinen Eltern und Geschwistern danken, die mich immer an Stärke, Resilienz und Geduld haben wachsen lassen.

Im Chaos unserer großen Familie steckt ein Muster ewigen Rückhalts.